

**Prediction Of Worldwide Energy Resource (POWER)
--- Sustainable Buildings Methodology ---
(1.0° Latitude by 1.0° Longitude Spatial Resolution)**

(Version 1.0.3 May 27, 2015)

**Paul W. Stackhouse, Jr¹, David Westberg², James M. Hoell²,
William S. Chandler², Taiping Zhang²**

¹NASA Langley Research Center ²SSAI/NASA Langley Research Center

<u>I. Introduction</u>	1
<u>II. Sustainable Buildings Archive: Parameters & Data Sources</u>	2
<u>III. Summary Of Parameter Accuracy</u>	5
A. <u>Solar Insolation</u>	6
B. <u>Meteorology</u>	10
<u>IV. Global Insolation on a Horizontal Surface</u>	12
A. <u>Earth's Radiation budget</u>	13
B. <u>Radiative Transfer Model</u>	14
i. <u>GEWEX SRB 3.0 Radiative Transfer Model</u>	14
ii. <u>FLASHFlux Radiative Transfer Model</u>	15
C. <u>Validation:</u>	16
i. <u>Monthly 3-Hourly Mean Shortwave Insolation (All sky Conditions)</u>	17
ii. <u>Daily Mean Shortwave Insolation (All Sky Conditions)</u>	18
iii. <u>Monthly Mean Shortwave Insolation (All Sky Conditions)</u>	20
iv. <u>Daily Mean Longwave Insolation (All Sky Conditions)</u>	22
v. <u>Daily Mean Shortwave Insolation (Clear Sky Conditions)</u>	26
vi. <u>Monthly Mean Shortwave Insolation (Clear Sky Conditions)</u>	28
<u>V. Diffuse and Direct Normal Radiation on a Horizontal Surface</u>	30
A. <u>POWER Method</u>	30
B. <u>Validation</u>	32
i. <u>Monthly Mean Diffuse (All Sky Conditions)</u>	32
ii. <u>Monthly Mean Direct Normal (All Sky Conditions)</u>	33
iii. <u>Monthly Mean Diffuse (Clear Sky Conditions)</u>	34
iv. <u>Monthly Mean Direct Normal (Clear Sky Conditions)</u>	35
<u>VI. Insolation on a Tilted Surface</u>	36
A. <u>Overview of RETScreen Method</u>	36
B. <u>Validation: Monthly Mean Insolation (All Sky Conditions)</u>	39
i. <u>GEWEX SRB 3.0 vs RETScreen</u>	40
ii. <u>GEWEX SRB 3.0 vs Direct Measurements of Tilt Insolation</u>	40
iii. <u>GEWEX SRB 3.0 vs BSRN Based Tilt Insolation</u>	41
<u>VII. Meteorological Parameters</u>	43
A. <u>Assessment of Assimilation Modeled Temperatures</u>	43
B. <u>Relative Humidity</u>	48
C. <u>Dew/Frost Point Temperatures</u>	50
D. <u>Precipitation</u>	51
E. <u>Wind Speed Parameters</u>	55
F. <u>Heating/Cooling Degree Days</u>	60
G. <u>Surface Pressure</u>	61
<u>VIII. References</u>	64

Appendix A: <u>Downscaling Assimilation Modeled Temperatures</u>	67
<u>Downscaling Methodology</u>	70
<u>Global Downscaling</u>	72
<u>Regional Downscaling</u>	74
<u>Heating/Cooling Degree Days</u>	78

I. Introduction

NASA, through its' Earth science research program has long supported satellite systems and research providing data important to the study of climate and climate processes. These data include long-term estimates of meteorological quantities and surface solar energy fluxes. These satellite and modeled based products have also been shown to be accurate enough to provide reliable solar and meteorological resource data over regions where surface measurements are sparse or nonexistent, and offer two unique features – the data is global and, in general, contiguous in time. These two important characteristics, however, tend to generate very large data files/archives which can be intimidating for users, particularly those with little experience or resources to explore these large data sets. Moreover, the data products contained in the various NASA archives are often in formats that present challenges to new users. NASA's Applied Sciences Program (<http://appliedsciences.nasa.gov/about.php>) was established to foster the use of Earth science research results for near-term applications and benefits. The Prediction Of Worldwide Energy Resource (POWER) project is one of the activities funded by the Applied Science Program.

The POWER project was initiated in 2003 as an outgrowth of the Surface meteorology and Solar Energy (SSE - https://eosweb.larc.nasa.gov/project/sse/sse_table) project. The SSE project has as its focus the development of parameters related to the solar based energy industry. The current POWER project encompasses the SSE project with the objective to improve subsequent releases of SSE, and to create new datasets with applicability to the architectural (e.g. Sustainable buildings) and agricultural (e.g. Agro-climatology) industries. The POWER web interface (<http://power.larc.nasa.gov>) currently provides a portal to the SSE data archive, tailored for the renewable energy industry, as well as to the Sustainable Buildings Archive with parameters tailored for the sustainable buildings community, and the Agro-climatology Archive with parameters for the agricultural industry. In general, the underlying data behind the parameters used by each of these industries is the same – global solar radiation, or insolation, and meteorology, including surface and air temperatures, moisture, and winds.

The purpose of this document is to describe the underlying data contained in Buildings Archive, and to provide additional information relative to the various industry specific parameters, their limitations, and estimated accuracies. The intent is to provide information that will enable new and/or long time users to make decisions concerning the suitability of the Sustainable Buildings data for their project in a particular region of the globe. This document is focused primarily on the Sustainable Buildings parameters, although the underlying solar and meteorological data for all three POWER archives (SSE, Sustainable Buildings, and Agro-climatology) are the derived from common data sources.

Companion documents describe the data and parameters in the POWER/SSE and POWER/Agro-climatology sections of the POWER data portal.

[\(Return to Content\)](#)

II. Sustainable Buildings Archive: Parameters & Data Sources:

The parameters contained in the Sustainable Buildings Archive are based primarily upon solar radiation derived from satellite observations and meteorological data from assimilation models. The various parameters have been selected and developed through close collaboration with industry and government partners in the buildings community, and a web-based portal provides access to industry-friendly parameters.

The archive contains:

- (1) Monthly averaged primary and derived solar and cloud related parameters over a 24 year period from January 1984 through December 2007;
- (2) Monthly averaged temperature related parameters spanning a 25 year period from January 1983 – 2007;
- (3) Daily solar insolation data are available for the time period July 1, 1983 to within seven days of present time; and
- (4) Daily values of the minimum, maximum and averaged temperatures are available from January 1, 1983 to within 3 days of current time.

All parameters are available globally on a 1-degree latitude, longitude grid. Time series data can be accessed through the POWER web portal for any user specified latitude, longitude grid.

Parameters in the Sustainable Buildings Archive have been developed from various data sources as follows:

(1) Solar parameters from release 3 of the NASA/GEWEX Surface Radiation Budget (GEWEX SRB 3.0 - <http://gewex-srb.larc.nasa.gov/> & https://eosweb.larc.nasa.gov/project/srb/srb_table) project for the time period July 1, 1983 – December 31, 2007;

(2) Solar parameters from NASA's Fast Longwave And Shortwave Radiative Fluxes (FLASHFlux - <http://flashflux.larc.nasa.gov/>) project for the time period from January 1, 2008 to within a week of real time;

(3) Meteorological parameters from NASA's Global Model and Assimilation Office (GMAO - <http://gmao.gsfc.nasa.gov/>), Goddard Earth Observing System model version 4 (GEOS-4) for the time period from January 1, 1983 – December 31, 2007; and from GEOS-5 for the time period from January 1, 2008 to within several days of real time.

(4) Monthly averaged 2.5° precipitation values re-gridded to 1° were obtained from the Global Precipitation Climate Project (GPCP - <http://precip.gsfc.nasa.gov/>) from January 1983 – December, 2007.

(5) Daily averaged 1° resolution precipitation values were obtained from the Global Precipitation Climate Project (GPCP - <http://precip.gsfc.nasa.gov/>) currently from January 1987 - August 2009.

(6) Monthly averaged wind data is based upon the NASA/GMAO GEOS version 1 (GEOS-1) for the time period July 1983 – June 1993.

(7) Daily mean wind speeds over the time period January 1, 1983 – December 31, 2007 are from GEOS-4 and over the time period January 1, 2008 to within several days of current time are from GEOS-5.

Table II-1 gives a more detailed overview of the monthly and daily averaged parameters, the respective temporal coverage, and various programs from which the underlying solar and meteorological data are obtained.

Table II-1
SUSTAINABLE BUILDINGS ARCHIVE:
PARAMETERS, TEMPORAL COVERAGE & DATA SOURCES

MONTHLY MEAN SOLAR INSOLATION:

(January 1984 – December 2007 → GEWEX SRB 3.0)

- All-sky Insolation (Average, Min, Max)
- Diffuse horizontal radiation (Average, Min, Max)
- Direct normal radiation (Average, Min, Max)
- All-sky Insolation at available GMT times
- Clear sky insolation
- Clear sky diffuse
- Clear sky direct normal
- Radiation on tilted surfaces

MONTHLY MEAN ILLUMINANCE:

(January 1984 – December 2007 → GEWEX SRB 3.0)

- Illuminance on tilted surfaces at available GMT times
- Illuminance on tilted surfaces over a 24 hour period

MONTHLY CLOUDS:

(January 1984 – December 2007 → GEWEX SRB 3.0)

- Daylight cloud amount
- Cloud amount at available GMT times
- Frequency of cloud amount at available GMT times

PARAMETERS FOR SIZING BATTERY OR OTHER ENERGY-STORAGE SYSTEMS

(January 1984 – December 2007 → GEWEX SRB 3.0)

- Minimum available insolation as % of average values over consecutive-day period
- Horizontal surface deficits below expected values over consecutive-day period
- Equivalent number of NO-SUN days over consecutive-day period

PARAMETERS FOR SIZING SURPLUS-PRODUCT STORAGE SYSTEMS:

(January 1984 – December 2007 → GEWEX SRB 3.0)

- Available surplus as % of average values over consecutive-day period

Table II-1 (cont'd)
SUSTAINABLE BUILDINGS ARCHIVE:
PARAMETERS, TEMPORAL COVERAGE & DATA SOURCES

MONTHLY MEAN TEMPERATURES:
(January 1983 – December 2007 → GEOS-4)

- Air Temperature at 2 m
- Daily Temperature Range at 2 m
- Dew Point Temperature at 2 m
- Cooling Degree Days above 18° C
- Heating Degree Days below 18° C
- Arctic Heating Degree Days below 10° C
- Arctic Heating Degree Days below 0° C
- Specific Humidity
- Earth Skin Temperature
- Daily Mean Earth Temperature (Min, Max, Amplitude)
- Frost Days
- Air Temperature at 2 m for available GMT times

Table II-1. (cont'd). THE POWER - SUSTAINABLE BUILDINGS ARCHIVE:
PARAMETERS, TEMPORAL COVERAGE & DATA SOURCES

MONTHLY AVERAGED PSYCHROMETRIC CHART FOR THE CONTINENTAL UNITED STATES:
(January 1, 1983 through December 31, 2007 → GEOS-4)

MONTHLY MEAN WIND:
(July 1983 – June 1993 → GEOS-1)

- Wind Speed at 50 m (Average, Min, Max)
- Percent of time for ranges of Wind Speed at 50 m
- Wind Speed at 50 m for available GMT times
- Wind Speed at 50, 100, 150, and 300 m
- Wind Speed for several vegetation and surface types
- Wind Direction at 50 m
- Wind Direction at 50 m for available GMT times

MONTHLY MEAN PRECIPITATION:
(January 1, 1981 – August 2009 → GPCP 2.5-degree monthly re-gridded to 1-degree)

DAILY INSOLATION:
(July 1, 1983 - December 31, 2007 → GEWEX SRB 3.0;
January 1, 2008 - Near present → FLASHFlux)

- Shortwave Insolation on Horizontal Surface
- Downward Longwave Radiative Flux
- Top-of-atmosphere Insolation
- Insolation Clearness Index
- Clear Sky Insolation
- Clear Sky Insolation Clearness Index

Table II-1 (concl'd)
SUSTAINABLE BUILDINGS ARCHIVE:
PARAMETERS, TEMPORAL COVERAGE & DATA SOURCES

DAILY METEOROLOGICAL:

(January 1, 1983 - December 31, 2007 → GEOS-4;
 January 1, 2008 - Near present → GEOS-5)

- Surface Air Pressure
- Average Air Temperature at 2 m
- Minimum Air Temperature at 2 m
- Maximum Air Temperature at 2 m
- Specific Humidity at 2 m
- Relative Humidity at 2 m
- Dew/Frost Point Temperature at 2 m
- Earth Skin Temperature

DAILY PRECIPITATION:

(January 1, 1987 - August 31, 2009 → GPCP 1-degree daily)

DAILY WIND SPEED AT 10M:

(January 1, 1983 - December 31, 2007 → GEOS-4;
 January 1, 2008 - Near present → GEOS-5)

3-HOURLY TEMPERATURE, HUMIDITY, AND WIND SPEED

(January 1, 1983 - December 31, 2008 → GEOS-4)

- Surface Air Pressure Air Temperature at 2 m
- Specific Humidity at 2 m
- Relative Humidity at 2 m
- Dew Point Temperature at 2 m
- Wind Speed at 10 m

Note that the time series of daily surface insolation is comprised of values from the GEWEX SRB project (July 1983 – December 31 2007) and the FLASHFlux project (January 1, 2008 – near real time); and daily temperature data is comprised of results from the GEOS-4 assimilation model (January 1, 1993 – December 31, 2007) and the GEOS-5 assimilation model (January 1, 2008 to within several days of current time.) Accordingly, care should be taken when assessing climate trends that encompass the pre- and post-January 1, 2008 data.

[\(Return to Content\)](#)

III. Summary Of Parameter Accuracy: This section provides a summary of the estimated uncertainty associated with the data underlying the solar and metrological parameters available through the POWER/Buildings archive. The uncertainty estimates are based upon comparisons with ground measurements. A more detailed description of the parameters and the procedures used to estimate their uncertainties is given in the subsequent sections of this document. Additional validation results have been reported by White, et al. (2008 and 2011) and by Bai, et al (2010).

III-A Solar Insolation: Quality ground-measured data are generally considered more accurate than satellite-derived values. However, measurement uncertainties from calibration drift, operational uncertainties, or data gaps are often unknown or unreported for many ground site data sets. In 1989, the World Climate Research Program estimated that most routine-operation solar-radiation ground sites had "end-to-end" uncertainties from 6 to 12%. Specialized high quality research sites such as those in the Baseline Surface Radiation Network (BSRN) are estimated to be more accurate by a factor of two. Note that the time series of daily surface insolation is comprised of values from the GEWEX SRB project (July 1983 – December 31 2007) and the FLASHFlux project (January 1, 2008 – near real time); and daily temperature data is comprised of results from the GEOS-4 assimilation model (January 1, 1993 – December 31, 2007) and the GEOS-5 assimilation model (January 1, 2008 to within several days of current time.) Accordingly, care should be taken when assessing climate trends that encompass the pre- and post-January 1, 2008 data.

NASA/GEWEX SRB 3.0 Solar Insolation; Table III-A.1a summarizes the results of comparing the total or global NASA/GEWEX SRB 3.0 solar shortwave insolation on a horizontal surface to observations from the BSRN (see Figure IV-C.1 for location of BSRN stations) for the time period January 1, 1992, the beginning of the BSRN observations, through December 31, 2007.

Table III-A.1a: Comparisons of shortwave solar insolation from NASA/GEWEX SRB 3.0 versus BSRN (Figure IV-C.1) insolation on a horizontal surface for the time period January 1, 1992 - December 31, 2007 (3-hourly, daily, and monthly mean – all sky and clear sky).

Parameter	Region: All BSRN Sites	Bias (%)	RMSE (%)
3-Hrly Monthly Mean SW All Sky Insolation (Figure IV-3)	Global	-2.45	14.96
	60° Poleward	-8.91	38.08
	60° Equatorward	-1.87	12.54
Daily Mean SW All Sky Insolation (Figure IV-4a)	Global	-1.84	20.47
	60° Poleward	-6.94	41.59
	60° Equatorward	-1.14	17.66
Monthly Mean SW All Sky Insolation (Figure IV-5a)	Global	-3.03	13.63
	60° Poleward	-8.90	32.99
	60° Equatorward	-2.18	10.26
Daily Mean SW Clear Sky Insolation (Figure IV-7a)	Global	-0.84	7.04
Monthly Mean SW Clear Sky Insolation (Figure IV-8a)	Global	-2.35	3.66

Table III-A.1b summarizes the results of comparing diffused and direct NASA/GEWEX SRB 3.0 shortwave solar insolation derived from the NASA/GEWEX SRB horizontal insolation to BSRN observations of the corresponding solar components for the time period January 1, 1992, the beginning of the BSRN observations, through December 31, 2007.

Table III-A.1b: Comparison of NASA/GEWEX SRB 3.0 versus BSRN ([Figure IV-C.1](#)) monthly mean diffuse and direct normal shortwave insolation on a horizontal surface for the time period January 1, 1992 - December 31, 2007 (all sky and clear sky).

Parameter	Region: All BSRN Sites	Bias (%)	RMSE (%)
Monthly Mean SW Diffuse Radiation All Sky (Figure V-1a)	Global 60° Poleward 60° Equatorward	-9.19 -15.4 -7.91	24.27 38.57 20.81
Monthly Mean SW Direct Normal Radiation All sky (Figure V-2a)	Global 60° Poleward 60° Equatorward	11.08 24.77 8.69	32.83 71.51 23.59
Monthly Mean Diffuse Radiation Clear Sky (Figure V-3a)	Global	3.55	14.29
Monthly Mean Direct Normal Radiation Clear sky (Figure V-4a)	Global	1.35	3.85

Table III-A.1c summarizes the results of comparing shortwave solar insolation on a south facing tilted surface derived from the NASA/GEWEX SRB 3.0 horizontal insolation to the corresponding insolation derived from BSRN observations for the time period January 1, 1992, the beginning of the BSRN observations, through December 31, 2007.

Table III-A.1c: Comparison of NASA/GEWEX SRB 3.0 versus BSRN ([Figure IV-C.1](#)) monthly mean shortwave insolation on a tilted Surface for the time period January 1, 1992 - December 31, 2007.

Parameter	Region: All BSRN Sites	Bias (%)	RMSE (%)
Monthly Mean All Sky SW Insolation (Figure VI.2a)	Global	2.92	13.70

Table III-A.1d summarizes the results of comparing the daily mean NASA/GEWEX SRB longwave insolation to that from BSRN observation for the time period January 1992 – December 2008.

Table III-A.1d: Comparison of longwave solar insolation from NASA/GEWEX SRB 3.0 versus BSRN (Figure IV-C.1) daily mean insolation on a horizontal surface for the time period January 1, 1992 - December 31, 2007.

Parameter	Region: All BSRN Sites	Bias (%)	RMSE (%)
Daily Mean	Global	0.16	7.0
All Sky LW Insolation (Figure IV-6a)	60° Poleward	1.27	13.44
	60° Equatorward	-0.03	5.73

NASA/FLASHFlux Solar Insolation; Table III-1e summarizes the results of comparing the total or global shortwave solar insolation on a horizontal surface from the NASA/FLASHFlux project to observations from the BSRN for the time period January 1, 2008 through July 2011.

Table III-A.1e: Comparison of solar insolation from FLASHFlux Project versus BSRN (Figure IV-C.1) shortwave insolation on a horizontal surface for the time period January 1, 2008 – July, 2011 (monthly and daily mean).

Parameter	Region: All BSRN Sites	Bias (%)	RMSE (%)
Daily Mean	Global	-2.12	18.33
All Sky SW	60° Poleward	-12.36	35.41
Insolation (Figure IV-4b)	60° Equatorward	-0.85	15.36
Monthly Mean	Global	-4.46	14.48
All Sky SW	60° Poleward	-15.19	30.69
Insolation (Figure IV-5b)	60° Equatorward	-2.44	9.96
Daily Mean	Global	-3.59	5.76
Clear Sky SW	60° Poleward	1.29	15.93
Insolation (Figure IV-7b)	60° Equatorward	-3.82	5.49
Monthly Mean	Global	-5.28	5.80
Clear Sky SW Insolation (Figure IV-8b)			

Table III-A.1f summarizes the results of comparing the daily mean FLASHFlux longwave insolation to that from BSRN observation for the time period January 1, 2008 through December 31, 2010.

Table III-A.1f: Comparison of longwave (LW) solar insolation from FLASHFlux versus BSRN (Figure IV-C.1) insolation on a horizontal surface for the time period January 1, 2008 - December 31, 2010 (daily mean)

Parameter	Region: All BSRN Sites	Bias (%)	RMSE (%)
Daily Mean LW	Global	-0.35	6.20
All Sky Insolation	60° Poleward	4.16	12.14
(Figure IV-6b)	60° Equatorward	-1.09	12.07

[\(Return to Content\)](#)

III.B Meteorology This section provides a summary of the estimated uncertainty associated with the meteorological data underlying the derived parameters available through the POWER/Buildings archive. As with the solar validations, the uncertainty estimates are based upon comparisons with ground measurements. A more detailed description of the parameters and the procedures used to estimate their uncertainties is given in the subsequent sections of this document.

Table III-B.1a summarizes the results of comparing GEOS-4 meteorological parameters to ground observations reported in the National Center for Environmental Information (NCEI – formally National Climatic Data Center) global summary of the day (GSOD) files.

Within the Sustainable Buildings archive a user can download in tabular format, the 25 year monthly mean GEOS-4 temperatures at a given ground site as unadjusted values or as unadjusted plus downscaled values (e.g. lapse rate and offset adjusted) based upon the elevation of the ground site. (See Appendix A for a description of the downscaling methodology.) Table III-B.1b and Table III-B.1c give, respectively, the globally monthly averaged Mean Bias Error (MBE) and Root Mean Square Error (RMSE) for unadjusted and downscaled 2007 GEOS-4 temperatures relative to NCEI temperatures.

Table III-B.1a: Linear least squares regression analysis of daily temperature estimates from GEOS-4 assimilation model versus corresponding values reported in the NCEI GSOD files for the time period January 1983 through December 31, 2006. Appendix A describes a method for downscaling Tmax, Tmin, and Tave temperatures from the Global Model and Assimilation Office GEOS-4 model. The statistics associated the GEOS-4 temperatures in this table have not been downscaled (i.e. unadjusted). The Table. 2b gives the statistics associated with the application of the downscaling methodology described in Appendix A.

Parameter	Slope	Intercept	R ²	RMSE	Bias
Tmax (°C) (Table VII A.1)	0.96	-1.16	0.91	3.95	-1.82
Tmin (°C) (Table VII A.1)	0.99	0.32	0.91	3.46	0.26
Tavg (°C) (Table VII A.1)	1.00	-0.57	0.94	2.75	-0.56
Tdew (°C)	0.96	-0.80	0.95	2.46	-1.07
RH (%)	0.79	12.72	0.56	9.40	-1.92
Heating Degree Days (degree days) (Table VII B.1)	1.02	12.47	0.93	77.20	17.28
Cooling Degree Days (degree days) (Table VII B.1)	0.86	2.36	0.92	28.90	-5.65
Atmospheric Pressure (hPa)	0.89	102.16	0.74	27.33	-10.20

Table III-B.1b. Globally and monthly averaged MBE and RMSE values associated with unadjusted 2007 GEOS-4 temperatures relative to 2007 NCEI GSOD temperatures.

	JAN	FEB	MAR	APR	MAY	JUN	JUL	AUG	SEP	OCT	NOV	DEC	YR
Tmax MBE	-2.00	-2.11	-2.00	-1.64	-1.13	-1.15	-0.84	-1.27	-1.49	-1.85	-1.73	-1.90	-1.89
Tmax RMSE	4.04	4.00	4.01	3.75	3.73	3.64	3.57	3.64	3.66	3.72	3.71	4.02	3.79
Tmin MBE	-0.24	-0.49	-0.23	0.19	0.56	0.49	0.66	0.61	0.81	0.76	0.50	-0.41	0.27
Tmin RMSE	4.13	4.02	3.70	3.32	3.25	3.09	3.10	3.13	3.30	3.50	3.84	4.26	3.55
Tave MBE	-1.0	-1.15	-0.88	-0.54	-0.03	-0.06	-0.13	-0.18	-0.15	-0.43	-0.59	-1.08	-0.50
Tave RMSE	3.20	3.18	2.92	2.62	2.66	2.54	2.55	2.50	2.51	2.56	2.91	3.41	2.80

Table III-B.1c. Globally averaged monthly MBE and RMSE associated with downscaled 2007 temperatures relative to 2007 NCEI GSOD temperatures. The GEOS-4 temperatures were downscaled using the globally and monthly averaged λ and β values given in Table A-4.

	JAN	FEB	MAR	APR	MAY	JUN	JUL	AUG	SEP	OCT	NOV	DEC	YR
Tmax MBE	0.04	-0.07	-0.04	-0.06	0.00	-0.32	-0.08	-0.30	-0.32	-0.29	0.14	0.04	-0.10
Tmax RMSE	3.35	3.11	3.17	2.97	3.18	3.16	3.18	3.13	3.02	2.98	3.06	3.40	3.14
Tmin MBE	1.06	0.85	0.87	0.74	0.74	0.52	0.59	0.45	0.57	0.69	0.92	0.56	0.71
Tmin RMSE	4.11	3.87	3.54	3.13	2.99	2.83	2.86	2.87	3.01	3.26	3.71	4.12	3.36
Tave MBE	0.52	0.33	0.48	0.28	0.27	-0.04	0.04	-0.11	0.13	0.14	0.41	0.25	0.22
Tave RMSE	2.94	2.69	2.44	2.11	2.22	2.18	2.24	2.16	2.12	2.20	2.61	3.06	2.41

Table III-B.2a summarizes the comparison statistics for wind speeds. The monthly averaged wind speeds have been carried over from the Goddard GEOS-4 assimilation model because newer data sets do not provide enough information about vegetation/surface types to permit an updated validation of the resulting wind data. The RETScreen Weather Database (RETScreen 2005) was used to test uncertainties in the GEOS-1 wind speeds.

Table III-B.2a: Estimated uncertainty for yearly averaged GEOS-1 wind speeds for the time period July 1983 through June 1993

Parameter	Method	Bias	RMSE
Wind Speed at 10 meters for terrain similar to airports (m/s)	RETScreen Weather Database (documented 10-m height airport sites)	-0.2	1.3
	RETScreen Weather Database (unknown-height airport sites)	-0.0	1.3

Table III-B.2b summarizes the comparison statistics associated with comparing wind speeds reported in the NCEI GSOD files with estimates from the GEOS-4 and -5 assimilation models.

Parameter	Slope	Intercept	R ²	RMSE	Bias
GEOS-4 Wind Speed at 10 meters (m/s) (Jan. 1, 2007 – Dec. 31, 2007)	0.55	1.62	0.42	1.76	0.011
GEOS-5 Wind Speed at 10 meters (m/s) (Jan. 1, 2009 – Dec. 31, 209)	0.65	1.62	0.46	1.83	0.38

Table III-B.3 summarizes the regression statistics associated with scatter plots of the GPCP mean daily precipitation and the monthly mean precipitation computed from the GPCP daily mean values versus daily and monthly means values from ground observation reported in the NCEI GSOD files.

Parameter	Slope	Intercept	R ²	RMSE	Bias
Daily 1-DD GPCP precipitation (mm)	0.42	1.78	0.22	7.02	0.68
Monthly Average of Daily GPCP (mm)	0.60	1.43	0.46	1.72	0.68

[\(Return to Content\)](#)

IV. Global Insolation on a Horizontal Surface:

The monthly and daily mean solar radiation and cloud parameters for the time period July 1983 – December 2007 are obtained directly or derived from parameters available from the NASA/Global Energy and Water Cycle Experiment - Surface Radiation Budget Project Release 3.0 archive (NASA/GEWEX SRB 3.0; see <http://gewex-srb.larc.nasa.gov/> & https://eosweb.larc.nasa.gov/project/srb/srb_table). Daily Solar radiation for the time period from January 1, 2008 to within a week of real time is obtained from NASA's Fast Longwave And SHortwave Radiative Fluxes (FLASHFlux; see <http://flashflux.larc.nasa.gov/>) project.

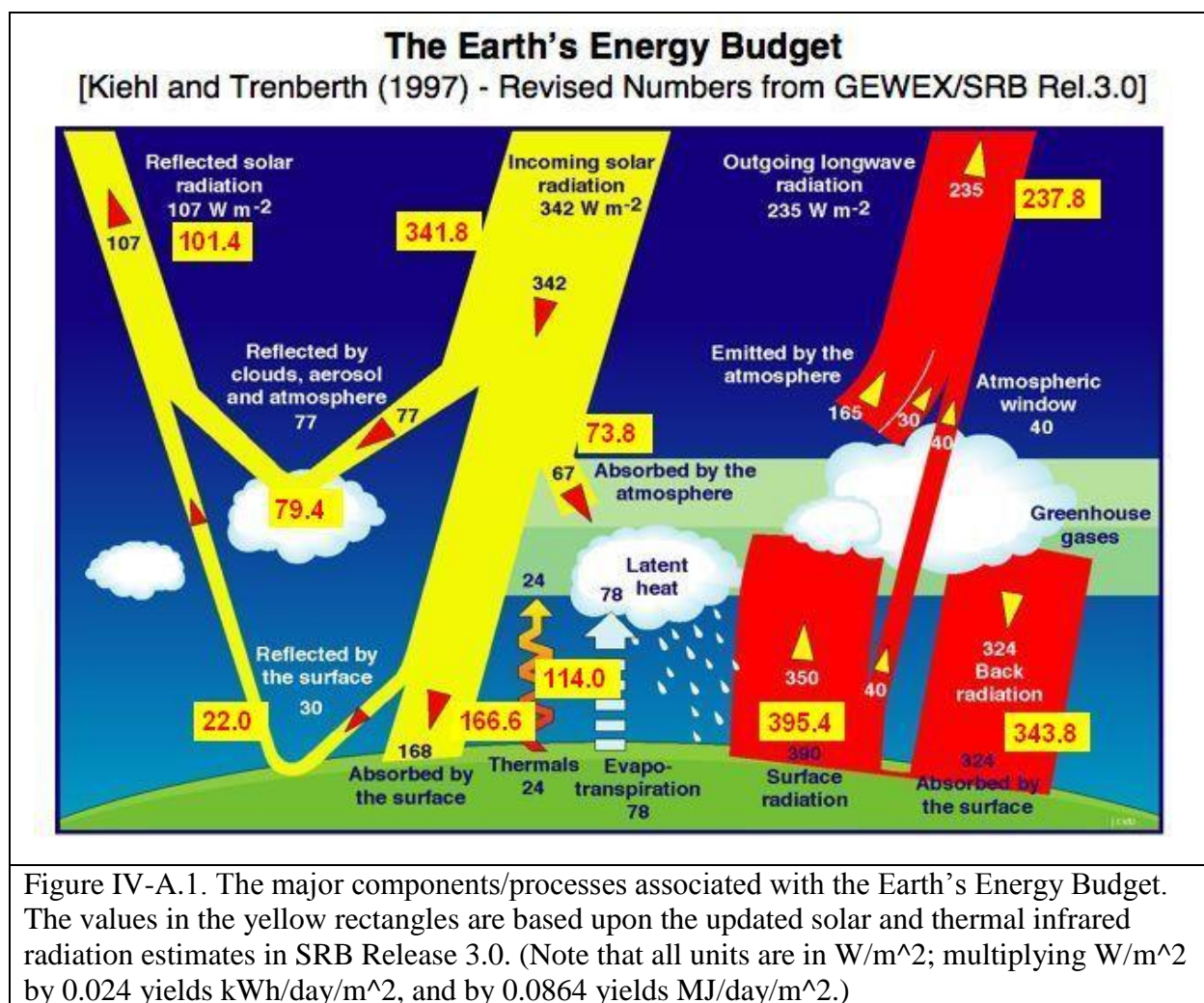
The NASA/GEWEX SRB Project focuses on providing estimates of the Earth's Top-of-atmosphere (TOA) and surface radiative energy flux components in support of NASA's effort to

quantify components of the Earth's radiation budget, while the focus of the FLASHFlux project is to provide solar data within one week of satellite observations.

While it is not the intent or purpose of this document to provide a detailed description of the methodology for inferring solar data from satellite observations, a brief synopsis is provided in the following sections.

[\(Return to Content\)](#)

A. Earth's Radiation budget: A central focus of the NASA's satellite programs is to quantify the process associated with the Earth's energy budget. Figure IV-A,1 illustrates the major components/processes associated with the Earth's Energy Budget including updated radiative flux components estimated from SRB Release 3.0 in the yellow boxes.



These values are based on a 24 year (July 1983 – Dec. 2007) annual global averaged radiative fluxes with year-to-year annual average variability of $\pm 4 \text{ W m}^{-2}$ in the solar wavelengths and

+/- 2 W m⁻² in the thermal infrared (longwave) flux estimates. The absolute uncertainty of these components is still the subject of active research. For instances, the most recent satellite based measurements of the incoming solar radiation disagree with previous measurements and indicate this value should be closer 340.3 W m⁻² providing another source of uncertainty. Other uncertainties involving the calibration of satellite radiances, atmospheric properties of clouds, aerosols and gaseous constituents, surface spectral albedos are all the subject of research within the GEWEX SRB project.

[\(Return to Content\)](#)

IV-B Radiative Transfer Model:

B.i GEWEX SRB Radiative Transfer Model: The process of inferring the surface solar radiation, or insolation, from satellite observations employs the modified method of Pinker and Laszlo (1992). This method involves the use of a radiative transfer model, along with water vapor column amounts from the GEOS-4 product and ozone column amounts from satellite measurements. Three satellite visible radiances are used: the instantaneous clear sky radiance, the instantaneous cloudy sky radiance, and the clear sky composite radiance, which is a representation of a recent dark background value. The observed satellite radiances are converted into broadband shortwave TOA albedos, using Angular Distribution Models from the Earth Radiation Budget Experiment (Smith et al., 1986). The spectral shape of the surface albedo is fixed by surface type. The radiative transfer model (through the use of lookup tables) is then used to find the absolute value of the surface albedo which produces a TOA upward flux which matches the TOA flux from the conversion of the clear-sky composite radiance. For this step, a first guess of the aerosol amount is used. The aerosol used for this purpose was derived from six years (2000-2005) of daily output from the MATCH chemical transport model (Rasch *et al.*, 1997). A climatology of aerosol optical depth was developed for each of the twelve months by collecting the daily data for each grid cell, and finding the mode of the frequency distribution. The mode was used rather than the average so as to provide a typical background value of the aerosol, rather than an average which includes much higher episodic outbreak values. The surface albedo now being fixed, the aerosol optical depth is chosen within the radiative transfer model to produce a TOA flux which matches the TOA Flux from the conversion of the instantaneous clear sky radiance. Similarly the cloud optical depth is chosen to match the TOA flux implied from the instantaneous cloudy sky radiance. With all parameters now fixed, the model outputs a range of parameters including surface and TOA fluxes. All NASA/GEWEX SRB 3.0 parameters are output on a 1⁰ by 1⁰ global grid at 3-hourly temporal resolution for each day of the month.

Primary inputs to the model include: visible and infrared radiances, and cloud and surface properties inferred from International Satellite Cloud Climatology Project (ISCCP) pixel-level (DX) data (Rossow and Schiffer, 1999; data sets and additional information can be found at https://eosweb.larc.nasa.gov/project/isccp/isccp_table); temperature and moisture profiles from GEOS-4 reanalysis product obtained from the NASA Global Modeling and Assimilation Office (GMAO; Bloom et al., 2005); and column ozone amounts constituted from Total Ozone Mapping Spectrometer (TOMS) and TIROS Operational Vertical Sounder (TOVS) archives, and

Stratospheric Monitoring-group's Ozone Blended Analysis (SMOBA), an assimilation product from NOAA's Climate Prediction Center.

To facilitate access to the GEWEX SRB 3.0 data products, the POWER project extracts the fundamental parameters (i.e. solar) from the SRB archive and metrological from the GEOS-4 & 5.1 and GPCP archives. The data products listed in Table III are available through the respective archives although in some instances the product may be bundled with a number of other parameters and generally are large global spatial files (i.e. 1 per day) rather than temporal files.

[\(Return to Content\)](#)

B.ii. FLASHFlux Radiative Transfer Model: The Fast Longwave and SHortwave Flux (FLASHFlux) project is based upon the algorithms developed for analysis and data collected by the Clouds and the Earth's Radiant Energy System (CERES - <http://ceres.larc.nasa.gov/>) project. CERES is currently producing world-class climate data products derived from measurements taken aboard NASA's Terra and Aqua spacecrafts. While of exceptional fidelity, CERES data products require a extensive calibration checks and validation to assure quality and verify accuracy and precision. The result is that CERES data are typically released more than six months after acquisition of the initial measurements. For climate studies, such delays are of little consequence especially considering the improved quality of the released data products. There are, however, many uses for the CERES data products on a near real-time basis such as those referred to within the POWER project. To meet those needs, FLASHFlux has greatly speeded up the processing by using the earliest stream of data coming from CERES instruments and using fast radiation algorithms to produce results within one week of satellite observations. This results in the loss of climate-quality accuracy due to bypassing of some calibration checks, and some gaps in the earliest stream of satellite data.

For speedy retrieval of surface insolation, FLASHFlux uses the SW Model B that is also used in CERES processing. This model is named the Langley Parameterized SW Algorithm (LPSA) and described in detail in Gupta et al. (2001). It consists of physical parameterizations which account for the attenuation of solar radiation in simple terms separately for clear atmosphere and clouds. Surface insolation, F_{sd} , is computed as

$$F_{sd} = F_{toa} T_a T_c ,$$

where F_{toa} is the corresponding TOA insolation, T_a is the transmittance of the clear atmosphere, and T_c is the transmittance of the clouds. Both FLASHFlux and CERES rely on similar input data sets from the meteorological products and MODIS. However, it is important to note that even though the FLASHFlux endeavor intends to incorporate the latest input data sets and improvements into its algorithms, there are no plans to reprocess the FLASHFlux data products once these modifications are in place. Thus, in contrast to the CERES data products, the FLASHFlux data products are **not** to be considered of climate quality. Users seeking climate quality should instead use the CERES data products. In the following section estimates of the accuracy of the GEWEX SRB 3.0 and FLASHFlux solar data are provided.

[\(Return to Content\)](#)

IV.C. Validation: The solar data in the GEWEX SRB 3.0 (July 1983 – December 2007) and FLASHFlux (January 2008 – near real time) data have been tested/validated against research quality observations from the Baseline Surface Radiation Network (BSRN; Ohmura *et al.*, 1998). Figure IV-C.1 shows the location of ground stations within the BSRN networks/archives. Scatter plots showing the total (i.e. diffuse plus direct) surface insolation observed at the BSRN ground sites versus insolation values from the SRB release 3.0 archive are shown in Figures IV-C.2a for the monthly averaged 3-hourly values, in Figure IV-C.3a for daily mean values, and in Figure IV-4a for monthly averaged values. The scatter plots shown in Figures IV-C.5a and 5b are for the SRB and FLASHFlux longwave insolation. Each of the SRB plots (i.e. –a charts) covers the time period January 1, 1992, the earliest that data from BSRN is available, through December 31, 2007. The corresponding scatter plots (i.e. companion –b charts) for the FLASHFLUX data are for the time period January 2008 through December 2010..

We note here that 3-hourly SRB values are the initial values estimated through the retrieval process described above and are used to calculate the daily total insolation and the monthly averages. The 3-hourly values are available through the Atmospheric Science Data Center (ASDC/SRB – https://eosweb.larc.nasa.gov/project/srb/srb_table). Global spatial files of the daily and monthly insolation values are also available from ASDC/SRB.

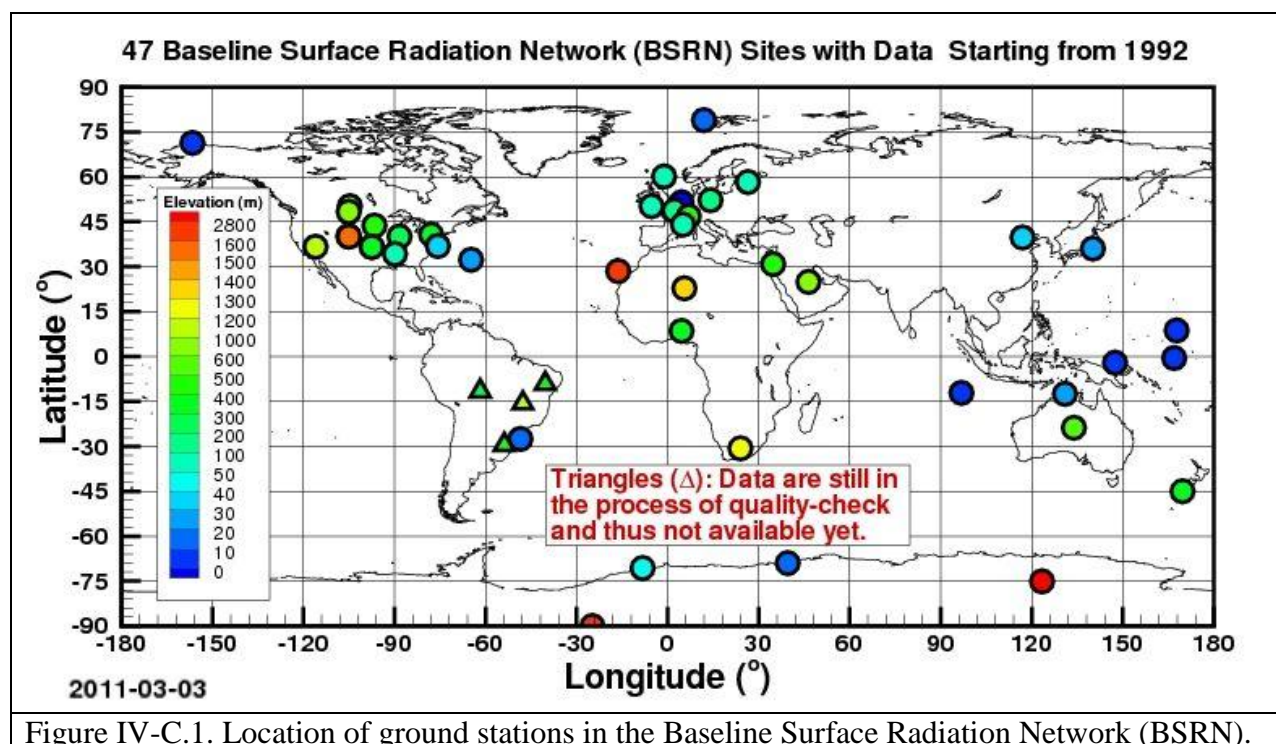


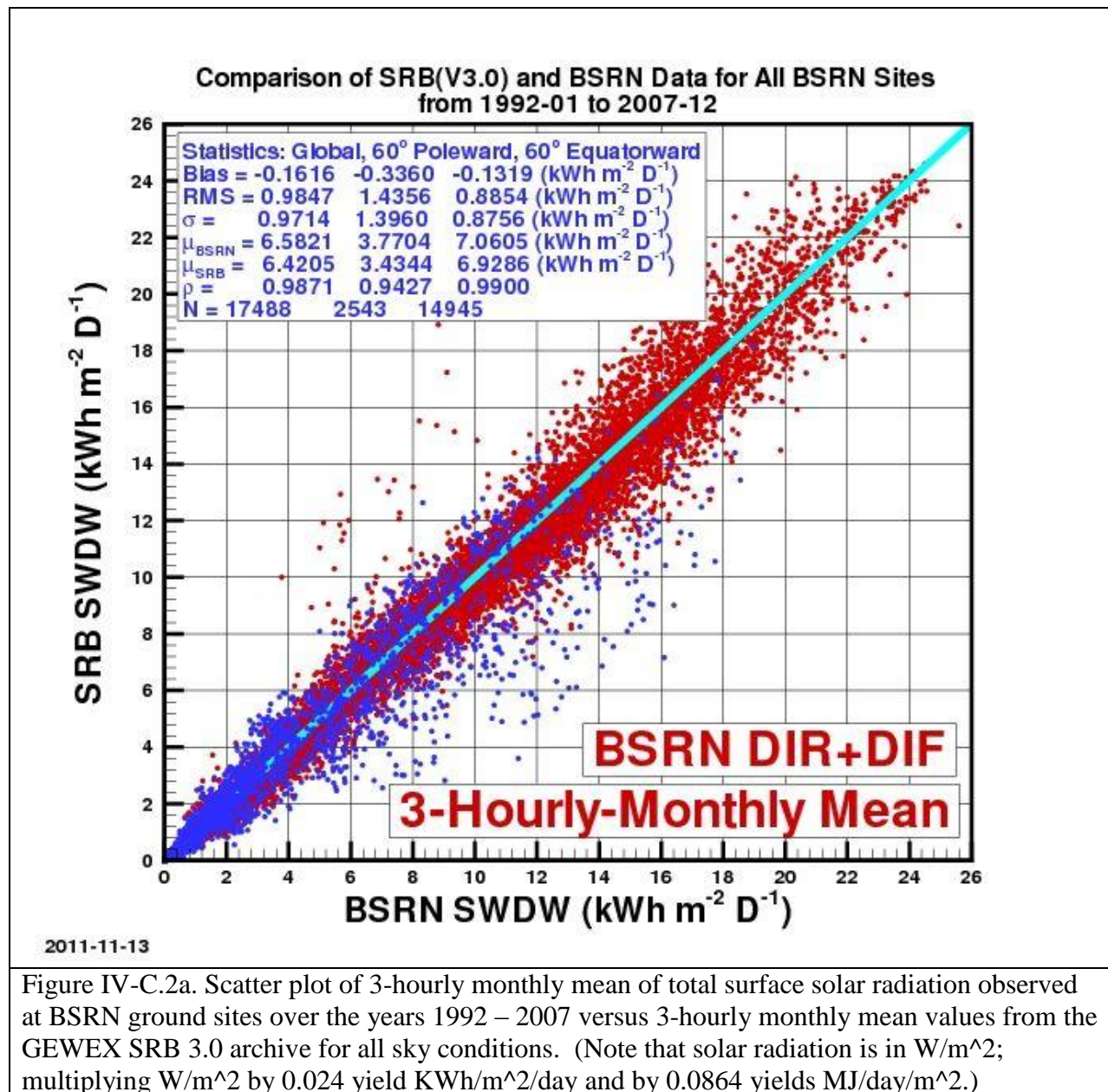
Figure IV-C.1. Location of ground stations in the Baseline Surface Radiation Network (BSRN).

Correlation and accuracy parameters for each scatter plots (Figures IV-C.2 – IV-C.5) are given in the legend box in each figure. Note that the correlation and accuracy parameters are given for all sites (e.g. Global), for the BSRN sites in regions above 60° latitude, north and south (i.e. 60° poleward), and for BSRN sites between 60° north and 60° south (i.e. 60° equatorward). The Bias is the difference between the mean (μ) of the respective solar radiation values for SRB and

BSRN. The RMS is the root mean square difference between the respective SRB and BSRN values. The correlation coefficient between the SRB and BSRN values is given by ρ , the variance in the SRB values is given by σ , and N is number of SRB:BSRN pairs for each latitude region.

[\(Return to Content\)](#)

IV.C.i Monthly 3-Hourly Mean Shortwave Insolation (All sky Conditions)



[\(Return to Content\)](#)

IV.C.ii. Daily Mean Shortwave Insolation (All sky Conditions)

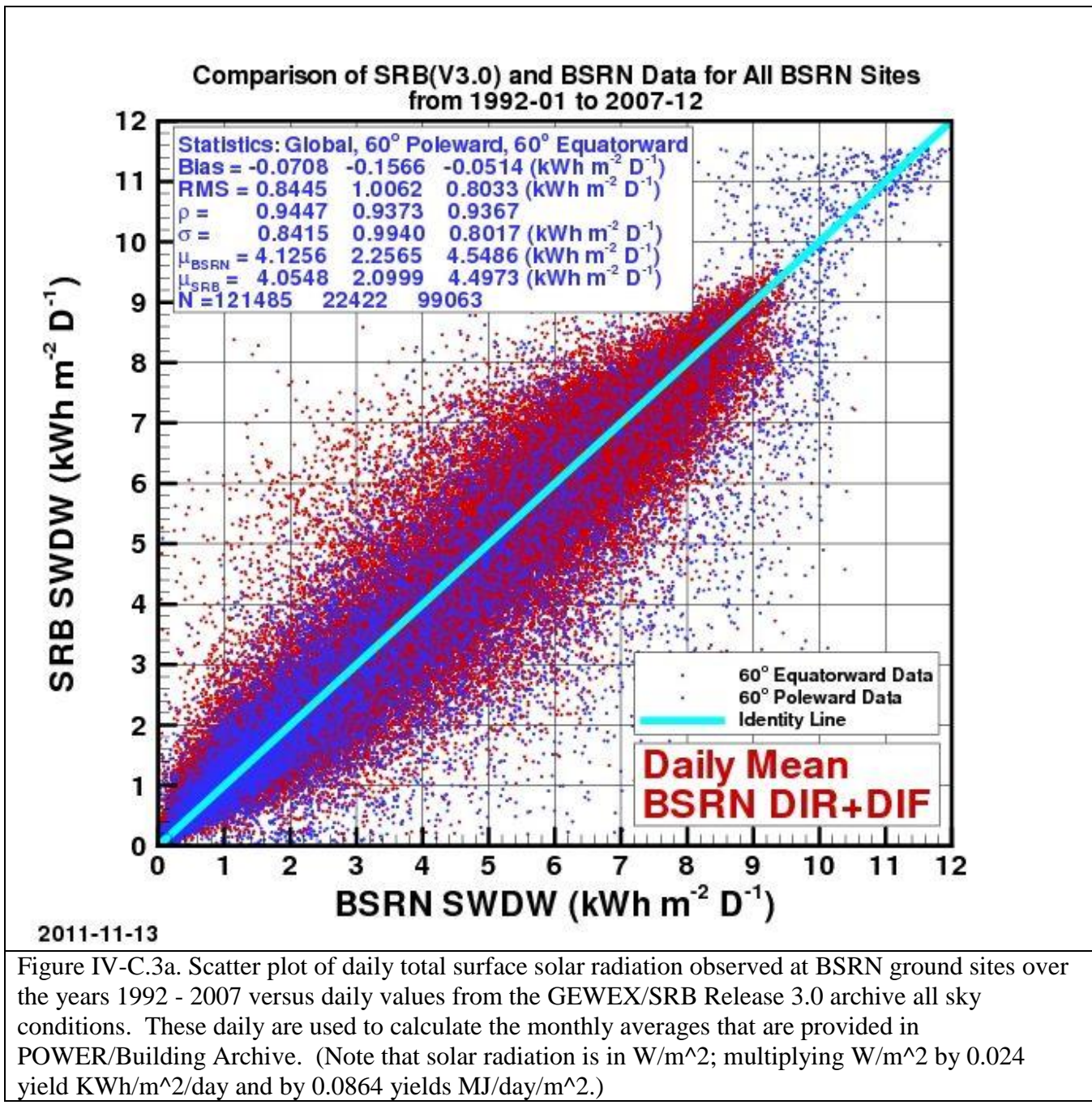


Figure IV-C.3a. Scatter plot of daily total surface solar radiation observed at BSRN ground sites over the years 1992 - 2007 versus daily values from the GEWEX/SRB Release 3.0 archive all sky conditions. These daily are used to calculate the monthly averages that are provided in POWER/Building Archive. (Note that solar radiation is in W/m²; multiplying W/m² by 0.024 yield kWh/m²/day and by 0.0864 yields MJ/day/m².)

[\(Return to Content\)](#)

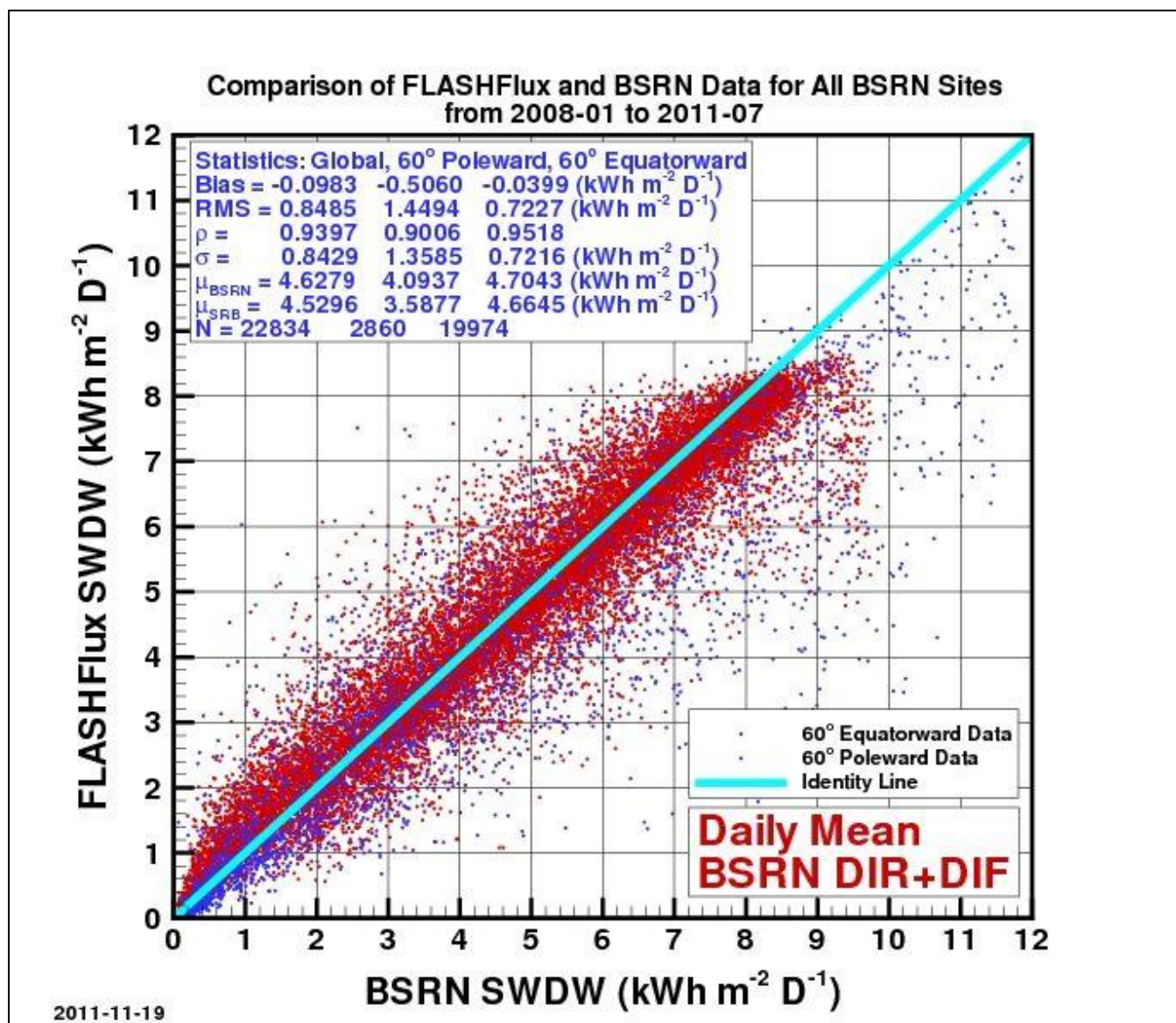
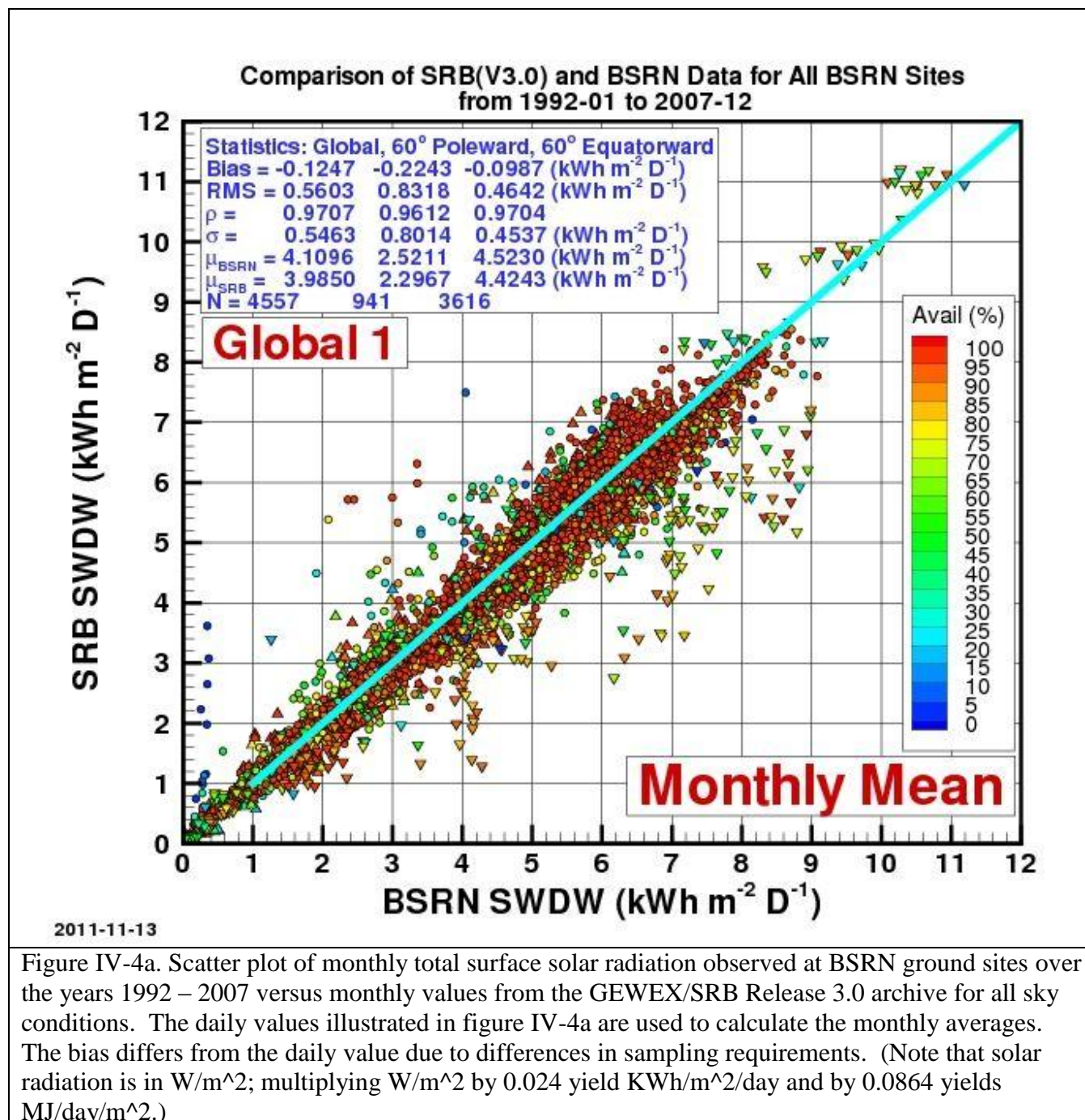


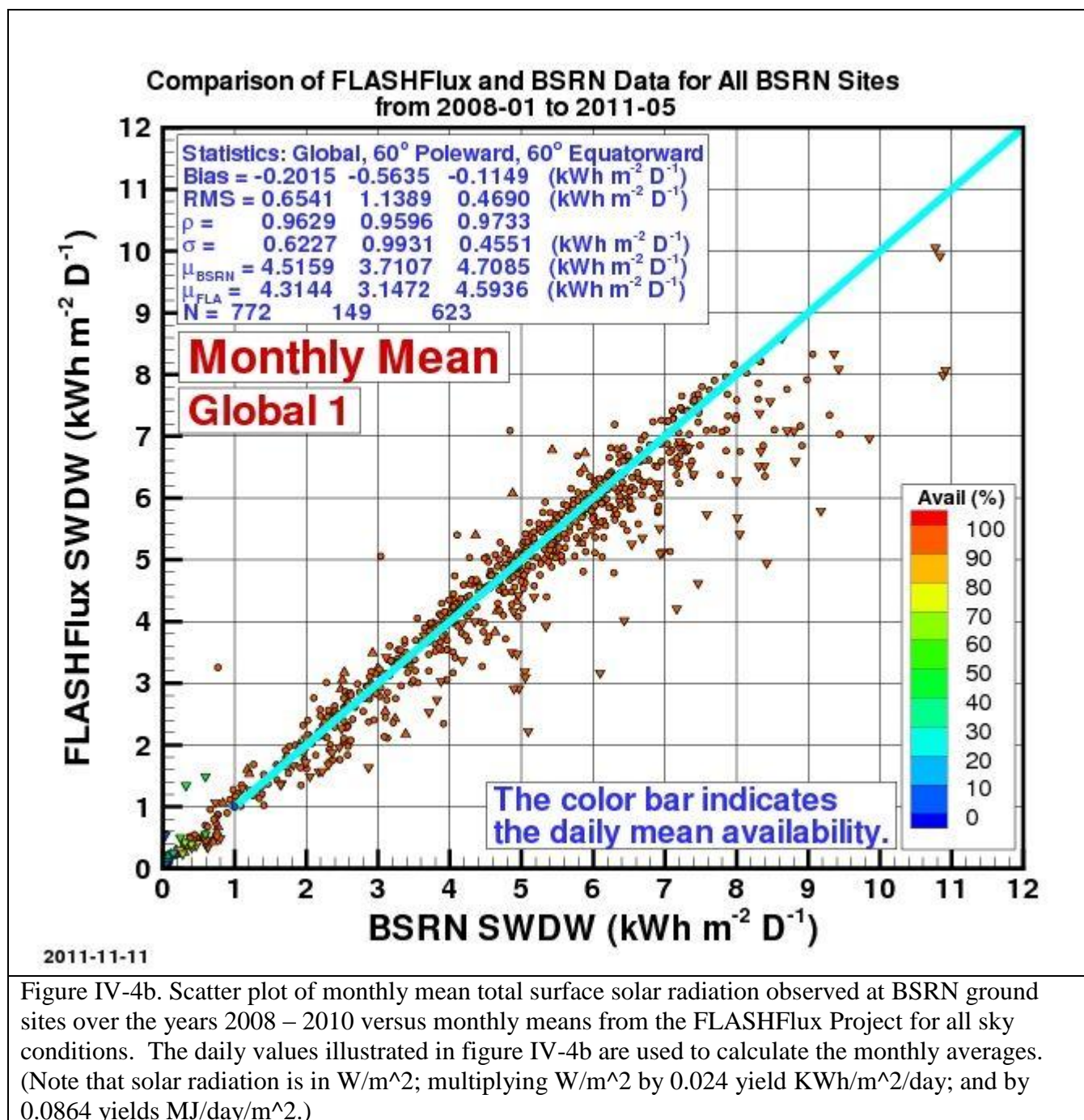
Figure IV-3b. Scatter plot of daily total surface solar shortwave radiation observed at BSRN ground sites over the years 2008 - 2010 versus daily values from the FLASHFlux archive. (Note that solar radiation is in MJ/day/m²; multiplying MJ/day/m² by 0.2778 yield kWh/m²/day and by 11.574 yields w/m².)

[\(Return to Content\)](#)

IV.C.iii. Monthly Mean Shortwave Insolation (All sky Conditions)



[\(Return to Content\)](#)



[\(Return to Content\)](#)

IV.C.iv. Daily Mean Longwave Insolation (All sky Conditions)

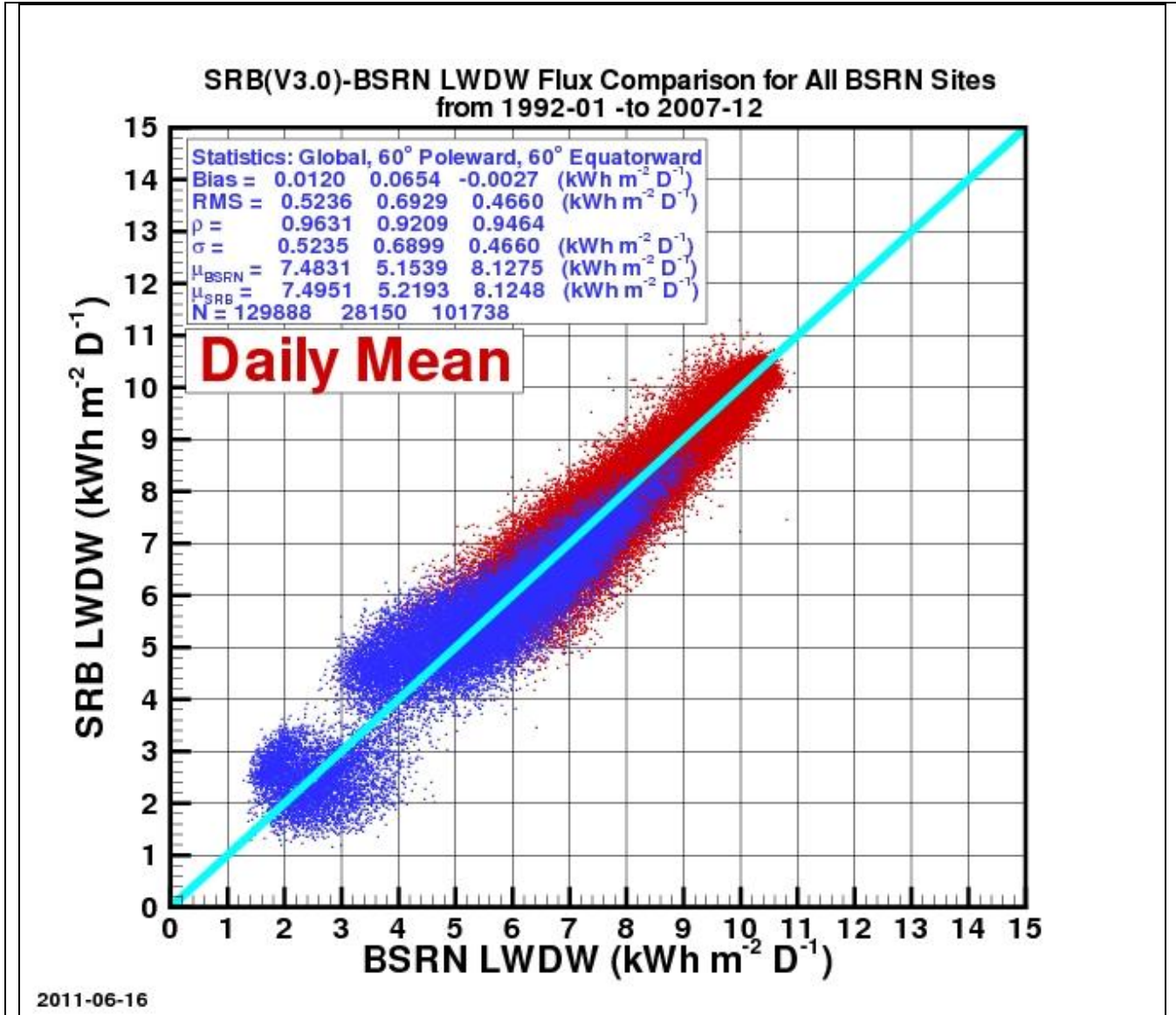
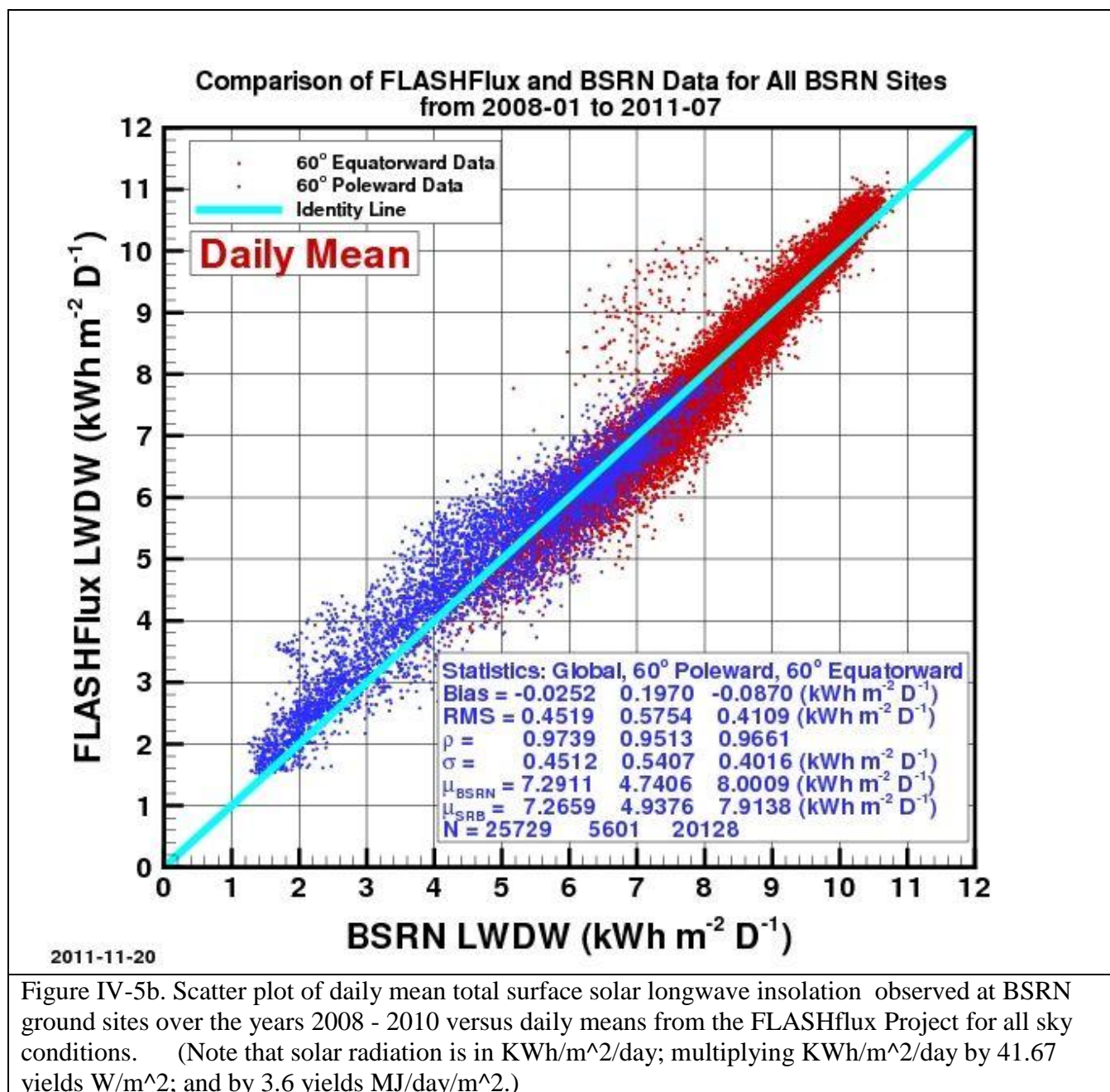


Figure IV-5a. Scatter plot of daily mean total surface solar longwave insolation observed at BSRN ground sites over the years 1992 - 2007 versus daily means from the SRB Project for all sky conditions. (Note that solar radiation is in KWh/m²/day; multiplying KWh/m²/day by 41.67 yields W/m²; and by 3.6 yields MJ/day/m².)

[\(Return to Content\)](#)



[\(Return to Content\)](#)

As noted above the monthly and yearly climatological averages of the insolation over the years January 1984 – December 2007 are one set of parameters available through the POWER Building Archive. Table IV-C.1 gives the estimated accuracies of the monthly climatological averages based upon comparisons with the BSRN observations.

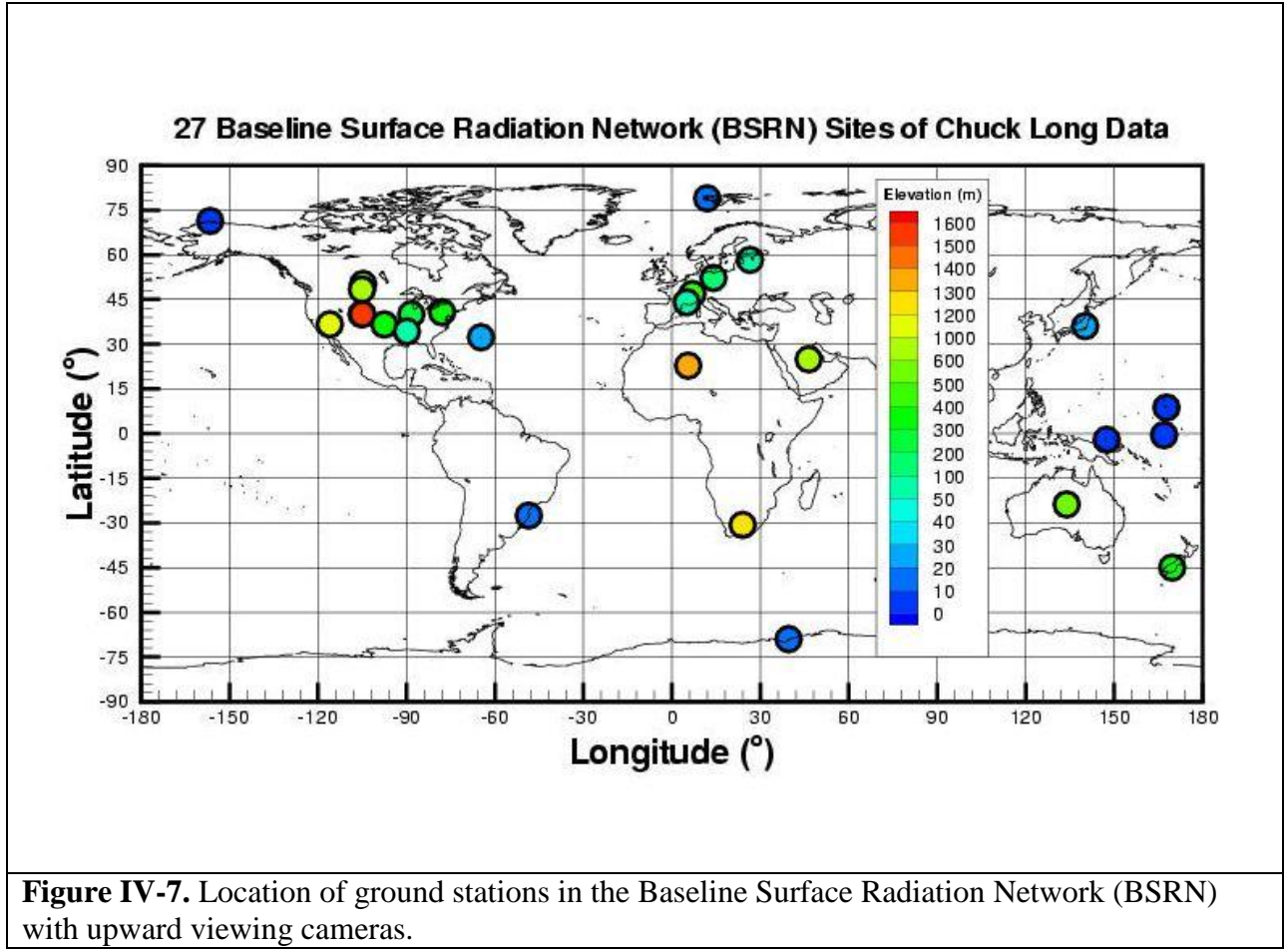
Table IV-C.1. Statistics of SRB (V3.0)-BSRN daily mean shortwave downward flux comparison from 1992-01 to 2007-12.

Month	Bias (kWh/ m ² da)	RMS (kWh/ m ² da)	ρ	M (kWh/ m ² da)	Bias (%)	RMS (%)	N
01	-0.096	0.8664	0.9449	3.1296	-3.09	27.68	9657
02	-0.0912	0.8232	0.9175	3.4536	-2.67	23.86	8781
03	-0.1152	0.8208	0.9207	3.9912	-2.87	20.59	10045
04	-0.0768	0.8064	0.9420	4.5144	-1.72	17.84	9947
05	-0.0648	0.8352	0.9489	5.0112	-1.29	16.67	10354
06	-0.0336	0.8952	0.9486	5.1408	-0.63	17.44	10217
07	0	0.84	0.9499	5.1264	0.01	16.38	10751
08	-0.036	0.7944	0.9428	4.7016	-0.78	16.88	10579
09	-0.0384	0.744	0.9351	4.248	-0.91	17.54	10149
10	-0.0768	0.8376	0.9171	3.6504	-2.09	22.92	10544
11	-0.1032	0.912	0.9273	3.1992	-3.21	28.52	10170
12	-0.1272	0.9384	0.9455	3.1368	-4.05	29.89	10291
Overall	-0.072	0.8448	0.9447	4.1256	-1.72	20.47	121485

* As of 2011-06-16.

[\(Return to Content\)](#)

IV.C.iv. Clear Sky Total: The clear sky total insolation is obtained from the GEWEX SRB Release 3.0 archive. (https://eosweb.larc.nasa.gov/project/srb/srb_table). In Figure IV-7 the monthly averaged total insolation on a horizontal is compared to ground observations from the BSRN network (Figure IV-6) for “clear” sky conditions. For these comparisons it was necessary to ensure that the ground observations and the satellite derived solar radiation values are for equivalent clear sky conditions. Fortunately, observational data from a number of BSRN ground sites (see Figure IV-6) and the satellite observational data provide information related to cloud cover for each observational period. Recall in Section III and in Table III-2, it was noted that cloud parameters from the NASA ISCCP were used to infer the solar radiation in the GEWEX SRB 3.0 archive. Parameters within the ISCCP data provide a measure of the clearness for each satellite observation use in the SRB-inversion algorithms. Similarly, observations from upward viewing cameras at the 27 BSRN sites shown in Figure IV-6 provided a measure of cloud cover for each ground observational period. The comparison data shown in Figures IV-7 used the ground cameras and the ISCCP data to matched clearness conditions. In particular, the comparison shown below use clearness criteria defined such that clouds in the field of view of the upward viewing camera and the field of view from the ISCCP satellites must both be less than 10%.



[\(Return to Content\)](#)

IV.C.iv Daily Mean Shortwave Insolation (Clear Sky Conditions)

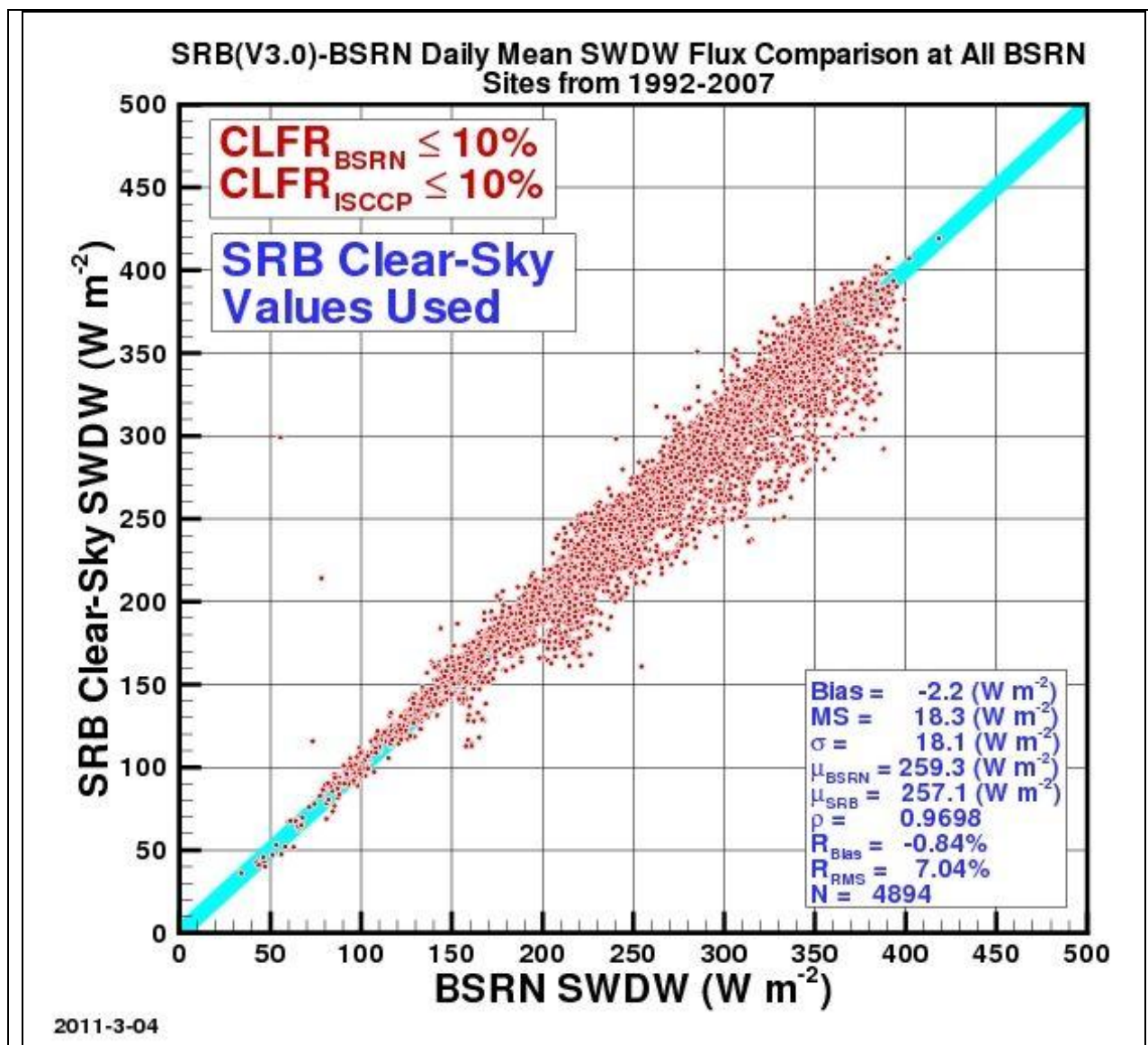


Figure IV-8a. Scatter plot of the daily total clear sky radiation derived from observations at BSRN ground sites vs. daily total values from GEWEX SRB 3.0. Clear sky conditions are for less than 10% cloud cover in field-of-view of both the upward viewing ground and downward viewing satellite cameras. The Bias is the difference between the mean (μ) of the respective solar radiation values for SRB and BSRN. RMS is the root mean square difference between the respective SRB and BSRN values. The correlation coefficient between the SRB and BSRN values is given by ρ , the variance in the SRB values is given by σ , and N is number of SRB:BSRN month pairs for each latitude region. (Note that solar radiation is in W/m^2 ; multiplying W/m^2 by 0.024 yield $\text{KWh/m}^2/\text{day}$ and by 0.0864 yields MJ/day/m^2 .)

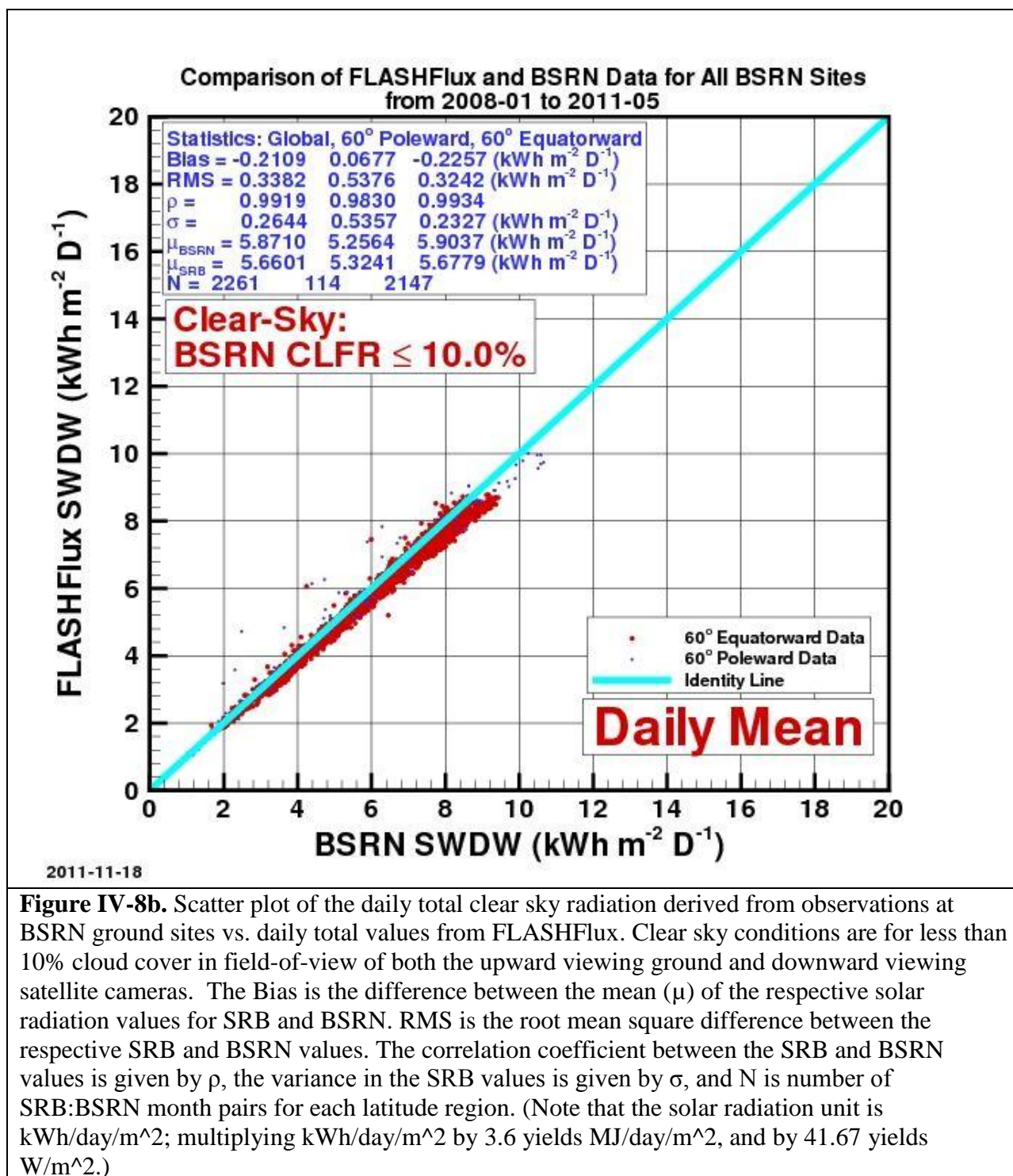


Figure IV-8b. Scatter plot of the daily total clear sky radiation derived from observations at BSRN ground sites vs. daily total values from FLASHFlux. Clear sky conditions are for less than 10% cloud cover in field-of-view of both the upward viewing ground and downward viewing satellite cameras. The Bias is the difference between the mean (μ) of the respective solar radiation values for SRB and BSRN. RMS is the root mean square difference between the respective SRB and BSRN values. The correlation coefficient between the SRB and BSRN values is given by ρ , the variance in the SRB values is given by σ , and N is number of SRB:BSRN month pairs for each latitude region. (Note that the solar radiation unit is kWh/day/m²; multiplying kWh/day/m² by 3.6 yields MJ/day/m², and by 41.67 yields W/m².)

[\(Return to Content\)](#)

IV.C.iv Monthly Mean Shortwave Insolation (Clear Sky Conditions)

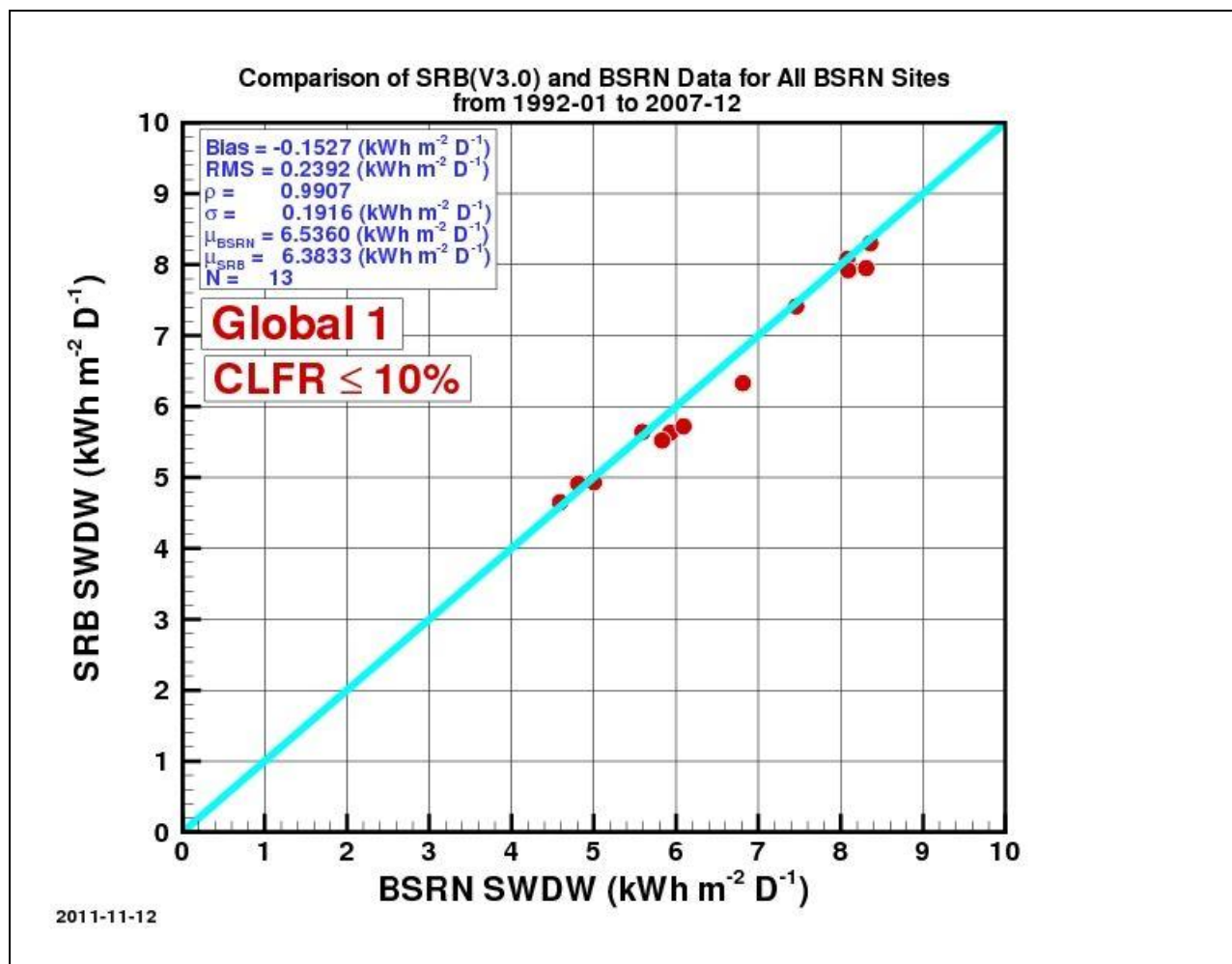
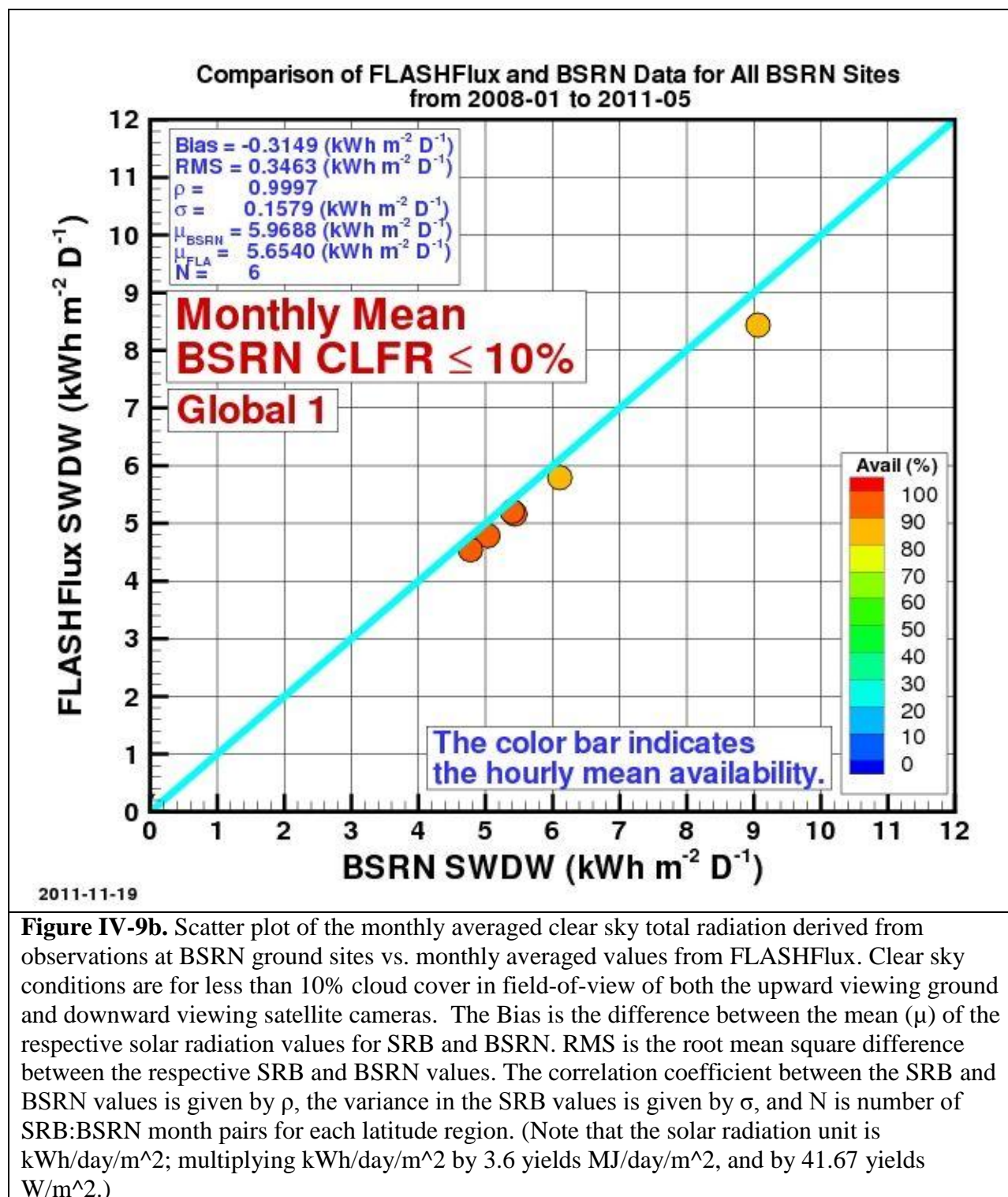


Figure IV-9a. Scatter plot of the monthly averaged clear sky total radiation derived from observations at BSRN ground sites vs. monthly averaged values from GEWEX SRB 3.0. Clear sky conditions are for less than 10% cloud cover in field-of-view of both the upward viewing ground and downward viewing satellite cameras. The Bias is the difference between the mean (μ) of the respective solar radiation values for SRB and BSRN. RMS is the root mean square difference between the respective SRB and BSRN values. The correlation coefficient between the SRB and BSRN values is given by ρ , the variance in the SRB values is given by σ , and N is number of SRB:BSRN month pairs for each latitude region. (Note that solar radiation is in W/m^2 ; multiplying W/m^2 by 0.024 yield $\text{KWh/m}^2/\text{day}$ and by 0.0864 yields MJ/day/m^2 .)



V. Diffuse and Direct Normal Radiation on a Horizontal Surface:

The all sky (i.e. all cloud conditions) total global solar radiation from the SRB archive discussed in Section VI is the sum of diffuse and direct normal radiation. However, estimates of all sky horizontal diffuse, $(H^{All})_{Diff}$, and direct normal radiation, $(H^{All})_{DNR}$ are often needed parameters for the design of hardware such as solar panels, solar concentrator size, day lighting, as well as agricultural and hydrology applications. From an observational perspective, $(H^{All})_{Diff}$ at the surface of the earth is that radiation remaining with $(H^{All})_{DNR}$ from the sun's beam blocked by a shadow band or tracking disk. $(H^{All})_{Diff}$ is typically measured using a sun tracking pyrliometer with a shadow band or disk to block the direct normal radiation from the sun. Similarly, from an observational perspective, $(H^{All})_{DNR}$ is the amount of solar radiation from the direction of the sun, and is typically measured using a pyrliometer tracking the sun through out the day.

[\(Return to Content\)](#)

V.A. POWER Method: Measurements of $(H^{All})_{Diff}$ and $(H^{All})_{DNR}$ are difficult to make and consequently are generally only available at high quality observational sites such as those in the BSRN network or the . In order to use the global estimates of the total surface solar radiation, H^{All} from SRB Release 3.0 to provide estimates of $(H^{All})_{Diff}$ and $(H^{All})_{DNR}$, a set of polynomial equations have been developed relating the ratio of $[(H^{All})_{Diff}]/[H^{All}]$ to the clearness index $KT = [H^{All}]/[H^{TOA}]$ using ground based observations from the BSRN network. These relationships were developed by employing observations from the BSRN network to extend the methods employed by RETScreen (RETScreen, 2005) to estimate $(H^{All})_{DNR}$.

In this section we outline the techniques for estimating the $[(H^{All})_{Diff}]$ and $[(H^{All})_{DNR}]$ from the solar insolation values available in SRB Release 3.0. In the following section results of comparative studies with ground site observations are presented, which serve to validate the resulting $[(H^{All})_{Diff}]$ and $[(H^{All})_{DNR}]$ and provide a measure of the overall accuracy of our global results.

All Sky Monthly Averaged Diffuse Radiation $[(H^{All})_{Diff}]$: As just noted, measurements of $(H^{All})_{Diff}$, $(H^{All})_{DNR}$, and H^{All} are made at the ground stations in the BSRN network. These observational data were used to develop the set of polynomial equations given below relating the ratio $[(H^{All})_{Diff}]/[H^{All}]$ to the clearness index $KT = [H^{All}]/[H^{TOA}]$. We note that the top of atmosphere solar radiation, H^{TOA} , is known from satellite observations.

For latitudes between 0 and 45 degrees North and South:

$$[(H^{All})_{Diff}]/[H^{All}] = 0.96268 - 1.45200*KT + 0.27365*KT^2 + (0.04279*KT^3 + 0.000246*SSHA + 0.001189*NHSA)$$

For latitudes between 45 and 90 degrees North and South:

If SSHA = 0 - 81.4 deg:

$$[(H^{All})_{Diff}]/[H^{All}] = 1.441 - (3.6839*KT) + (6.4927*KT^2) - (4.147*KT^3) + (0.0008*SSHA) - (0.008175*NHSA)$$

If SSHA = 81.4 - 100 deg:

$$[(H^{All})_{Diff}]/[H^{All}] = 1.6821 - (2.5866 * KT) + (2.373 * KT^2) - (0.5294 * KT^3) - (0.00277 * SSHA) - (0.004233 * NHSA)$$

If SSHA = 100 - 125 deg:

$$[(H^{All})_{Diff}]/[H^{All}] = 0.3498 + (3.8035 * KT) - (11.765 * KT^2) + (9.1748 * KT^3) + (0.001575 * SSHA) - (0.002837 * NHSA)$$

If SSHA = 125 - 150 deg:

$$[(H^{All})_{Diff}]/[H^{All}] = 1.6586 - (4.412 * KT) + (5.8 * KT^2) - (3.1223 * KT^3) + (0.000144 * SSHA) - (0.000829 * NHSA)$$

If SSHA = 150 - 180 deg:

$$[(H^{All})_{Diff}]/[H^{All}] = 0.6563 - (2.893 * KT) + (4.594 * KT^2) - (3.23 * KT^3) + (0.004 * SSHA) - (0.0023 * NHSA)$$

where:

$$KT = [H^{All}]/[H^{TOA}]$$

SSHA = sunset hour angle in degrees

NHSA = noon solar angle from the horizon in degrees

The above set of polynomial equations relate the ratio of monthly averaged horizontal diffuse radiation for all sky conditions to the monthly averaged total solar radiation for all sky conditions $\{ [(H^{All})_{Diff}]/[H^{All}] \}$ to the clearness index $KT = [H^{All}]/[H^{TOA}]$.

All Sky Monthly Averaged Direct Normal Radiation:

$$[(H^{All})_{DNR}] = ([H^{All}] - [(H^{All})_{Diff}]) / \text{COS}(\text{THMT})$$

where:

THMT is the solar zenith angle at the mid-time between sunrise and solar noon (Gupta, et al. 2001) for the “monthly average day” (Klein 1977).

$$\text{COS}(\text{THMT}) = f + g [(g - f) / 2g]^{1/2}$$

H^{All} = Total of direct beam solar radiation and diffuse atmospheric radiation falling on a horizontal surface at the earth's surface

$(H^{All})_{Diff}$ = diffuse atmospheric radiation falling on a horizontal surface at the earth's surface

$$f = \sin(\text{latitude}) \sin(\text{solar declination})$$

$$g = \cos(\text{latitude}) \cos(\text{solar declination})$$

If the Sunset Hour Angle = 180 degrees, then $\text{COS}(\text{THMT}) = f$.

[\(Return to Content\)](#)

V.B. Validation: Figures V-1a and V-1b show respectively scatter plots for the monthly mean diffuse and monthly mean direct normal radiation for all sky conditions computed from measured values at the BSRN sites (designated as BSRN SWDF and BSRN SWDN) versus the corresponding GEWEX SRB 3.0 values (designated as SRB SWDF and SRB SWDN) derived from the expression discussed above. Figures V-2a and V-2b show similar scatter plots for clear sky conditions.

V.B i. Monthly Mean Diffuse (All Sky Conditions)

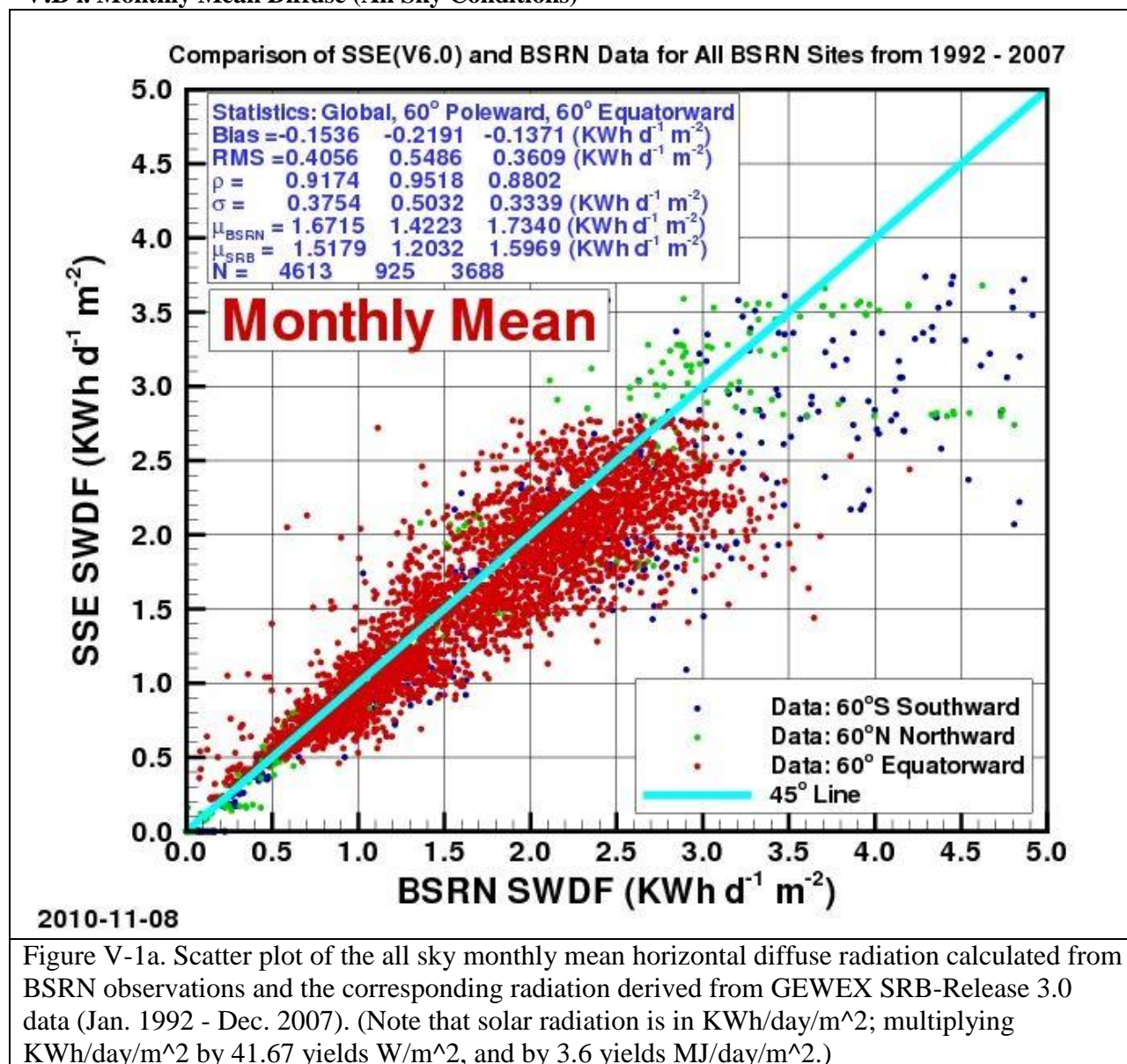


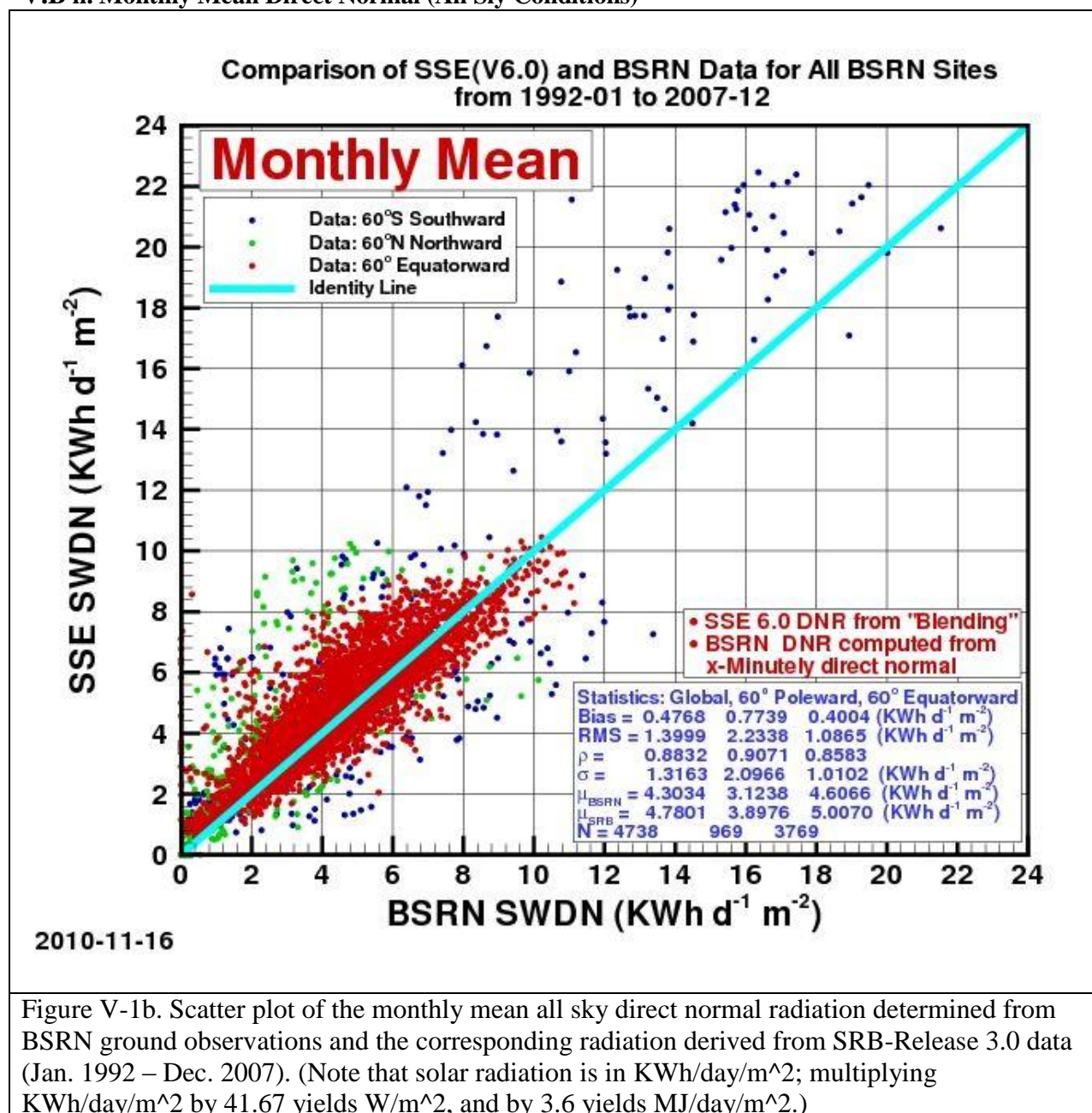
Figure V-1a. Scatter plot of the all sky monthly mean horizontal diffuse radiation calculated from BSRN observations and the corresponding radiation derived from GEWEX SRB-Release 3.0 data (Jan. 1992 - Dec. 2007). (Note that solar radiation is in KWh/day/m²; multiplying KWh/day/m² by 41.67 yields W/m², and by 3.6 yields MJ/day/m².)

Correlation and accuracy parameters are given in the legend boxes. Note that for the all sky condition the correlation and accuracy parameters are given for all sites (e.g. Global), for the BSRN sites regions above 60° latitude, north and south, (i.e. 60° poleward) and for BSRN sites

below 60° latitude, north and south (60° equatorward). However, because of the scarcity of clear sky values only the global region is used for the statistics in Figures V-2a and V-2b. The Bias is the difference between the mean (μ) of the respective solar radiation values for SRB and BSRN. RMS is the root mean square difference between the respective SRB and BSRN values. The correlation coefficient between the SRB and BSRN values is given by ρ , the variance in the SRB values is given by σ , and N is number of SRB:BSRN pairs for each latitude region.

[\(Return to Content\)](#)

V.B ii. Monthly Mean Direct Normal (All Sky Conditions)



[\(Return to Content\)](#)

V.B iii. Monthly Mean Diffuse (Clear Sky Conditions)

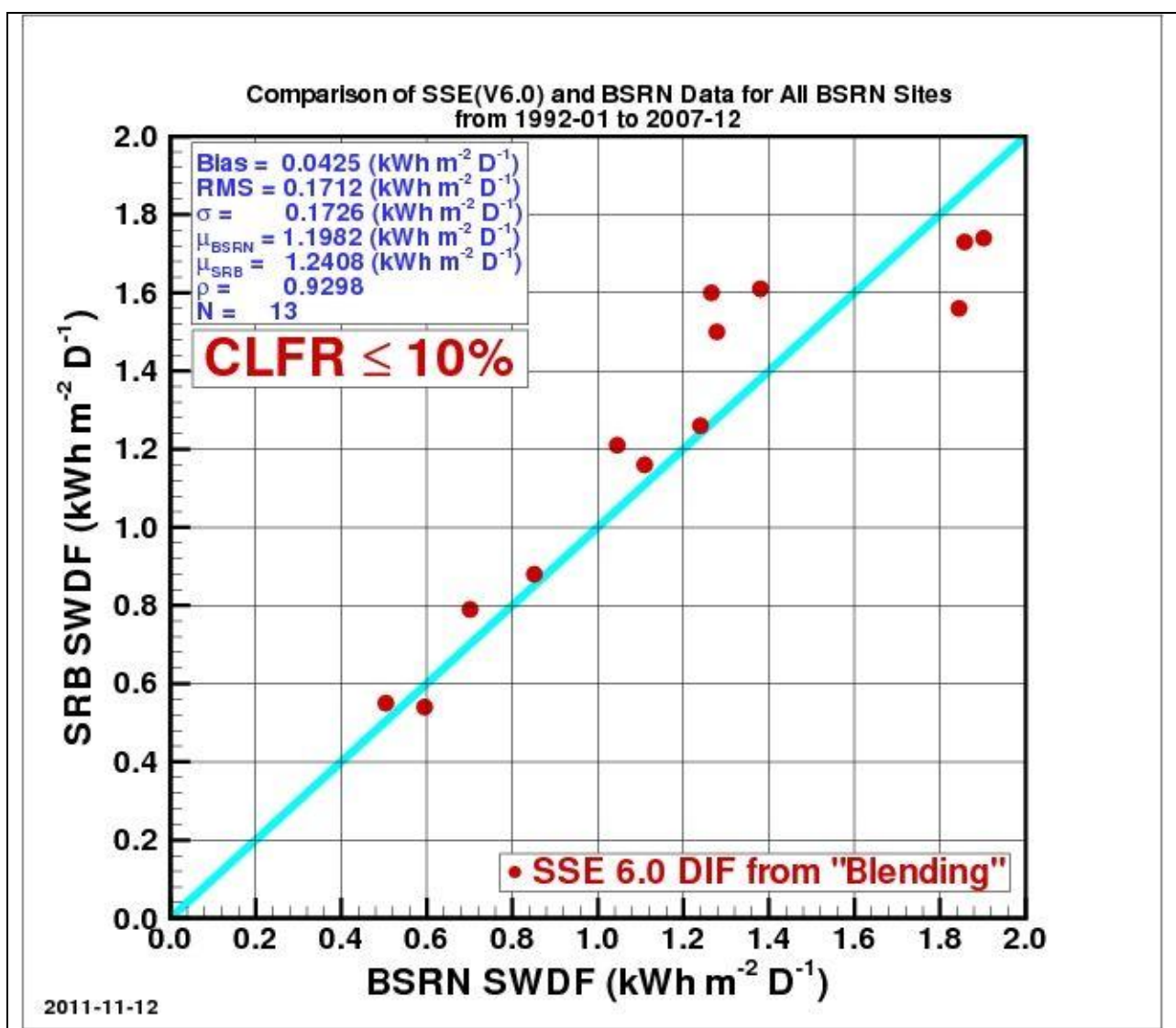


Figure V-2a. Scatter plot of the monthly mean clear sky diffuse radiation on a horizontal surface determined from BSRN ground observations and the corresponding radiation derived from SRB-Release 3.0 data (Jan. 1992 – Dec. 2007). (Note that solar radiation is in KWh/day/m²; multiplying KWh/day/m² by 41.67 yields W/m², and by 3.6 yields MJ/day/m².)

[\(Return to Content\)](#)

V.B iv. Monthly Mean Direct Normal (Clear Sky Conditions)

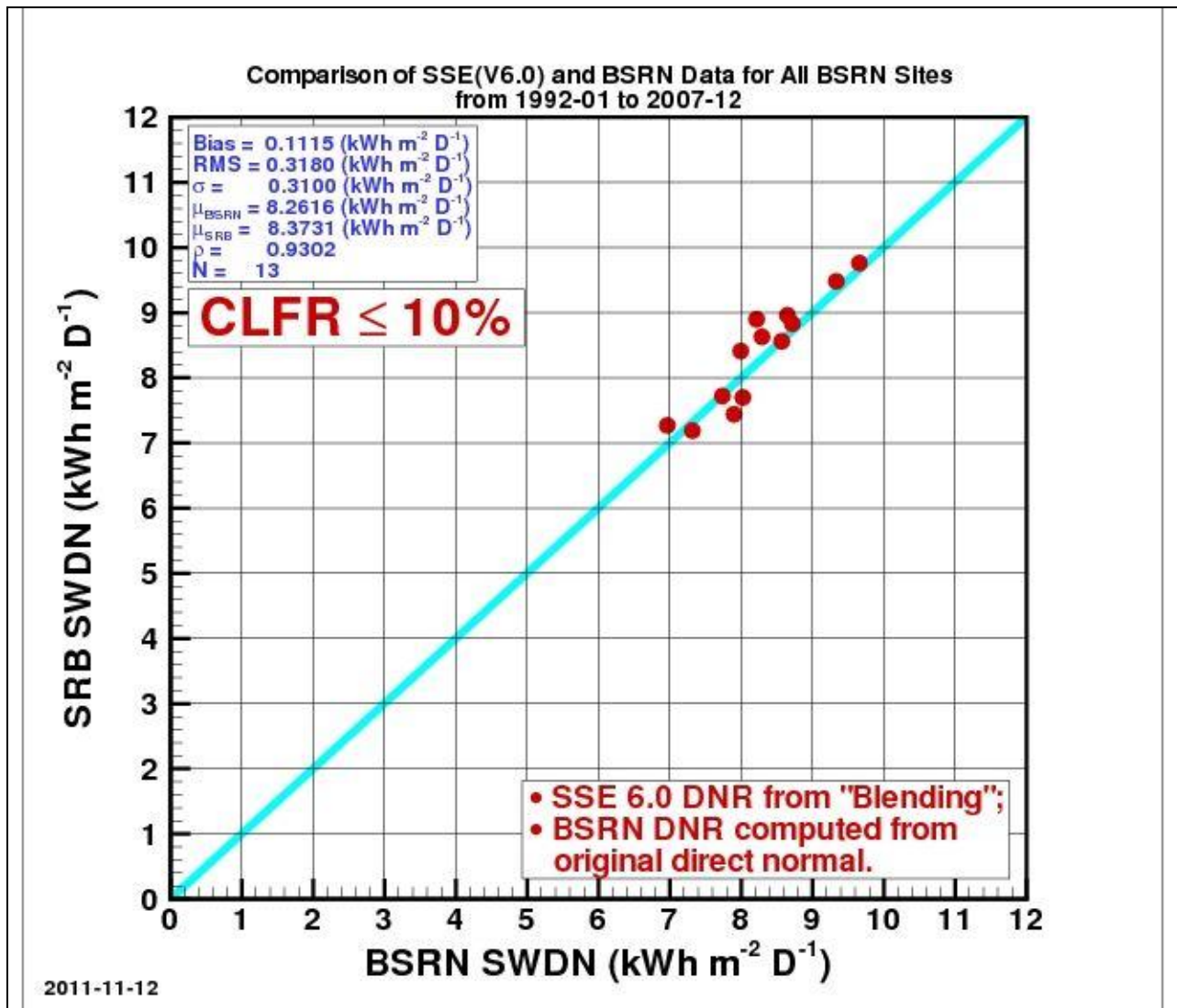


Figure V-2b. Scatter plot of the monthly mean clear sky direct normal radiation on a horizontal surface determined from BSRN ground observations and the corresponding monthly mean clear sky direct normal radiation derived from SRB-Release 3.0 data (Jan. 1992 – Dec. 2007). (Note that solar radiation is in KWh/day/m²; multiplying KWh/day/m² by 41.67 yields W/m², and by 3.6 yields MJ/day/m².)

[\(Return to Content\)](#)

VI. Insolation On a Tilted Surface

The calculation of the insolation impinging on a tilted surface basically follows the method employed by RETScreen (RETScreen 2005). The major difference is that the diffuse radiation is derived from the equations described in Section V above which contain slight modifications on the RETScreen approach.

VI.A. Overview of RETScreen Method: In this section we briefly outline the RETScreen method. The RETScreen method uses the “monthly average day” hourly calculation procedures where the equations developed by Collares-Pereira and Rabl (1979) and Liu and Jordan (1960) are used respectively for the “monthly average day” hourly insolation and the “monthly average day” hourly diffuse radiation.

Hourly Total and Diffuse Insolation on a Horizontal Surface: We first describe the method of estimating the hourly horizontal surface insolation (H_h) and horizontal diffuse (H_{dh}) for daylight hours between 30 minutes after sunrise to 30 minutes before sunset during the “monthly average day”. The “monthly average day” is the day in the month whose declination is closest to the average declination for that month (Klein 1977). Table VI.1 lists the date and average declination for each month.

Table VI.1. List of the day in the month whose solar declination is closest to the average declination for that month					
Month	Date in month	Declination	Month	Date in month	Declination
January	17	-20.9	July	17	21.2
February	16	-13.0	August	16	13.5
March	16	-2.4	September	15	2.2
April	15	9.4	October	15	-9.6
May	15	18.8	November	14	-18.9
June	11	23.1	December	10	-23.0

$$H_h = r_t H$$

$$H_{dh} = r_d H_d$$

where:

H is the monthly average horizontal surface insolation from the SRB 3.0 data set.

H_d is the monthly average horizontal diffuse from the method described in section V.

$$r_t = (\pi/24) * (A + B \cos \omega) * [(\cos \omega - \cos \omega_s) / (\sin \omega_s - \omega_s \cos \omega_s)]$$

(Collares-Pereira and Rabl; 1979)

$$r_d = (\pi/24) * [(\cos \omega - \cos \omega_s) / (\sin \omega_s - \omega_s \cos \omega_s)] \quad (\text{Liu and Jordan; 1960})$$

where:

$$A = 0.409 + 0.5016 \sin[\omega_s - (\pi/3)]$$

$$B = 0.6609 - 0.4767 \sin[\omega_s - (\pi/3)]$$

where:

ω = solar hour angle for each daylight hour relative to solar noon between sunrise plus 30 minutes and sunset minus 30 minutes. The sun is displaced 15° from the local meridian for each hour from local solar noon.

ω_s = sunset hour angle

$\omega_s = \cos^{-1}[-\tan(\text{solar declination}) * \tan(\text{latitude})]$, (+ = west relative to solar noon)

where:

solar declination = $23.45 * \sin[6.303 * \{(284 + n)/365\}]$

n = day number of year, 1 = January 1

Hourly total radiation on a tilted surface: Next, we describe the method of estimating hourly total radiation on a tilted surface (H_{th}) as outlined in the RETScreen tilted surface method. The equation, in general terms, is:

H_{th} = solar beam component + sky diffuse component + surface/sky reflectance component

The solution is as follows:

$\cos\theta_{zh} = \cos(\text{latitude}) \cos(\text{solar declination}) \cos\omega + \sin(\text{latitude}) \sin(\text{solar declination})$

$\cos\theta_h = \cos\theta_{zh} \cos\beta_h + (1 - \cos\theta_{zh}) (1 - \cos\beta_h) (\cos(\gamma_{sh} - \gamma_h))$

where:

β_h = hourly slope of the PV array relative to a horizontal surface. β_h is constant for fixed panels or panels in a vertical-axis tracking system. $\beta_h = \theta_z$ for panels in a two-axis tracking system. Values for other types of tracking systems are given in Braun and Mitchell (1983).

$\gamma_{sh} = \sin^{-1} [(\sin\omega \cos(\text{solar declination}))/\sin\theta_{zh}]$

= hourly solar azimuth angle; angle between the line of sight of the Sun into the horizontal surface and the local meridian. Azimuth is zero facing the equator, positive west, and negative east.

γ_h = hourly surface azimuth of the tilted surface; angle between the projection of the normal to the surface into the horizontal surface and the local meridian. Azimuth is zero facing the equator, positive west, and negative east. γ_h is constant for fixed surfaces. $\gamma_h = \gamma_{sh}$ for both vertical- and two-axis tracking systems. See Braun and Mitchell (1983) for other types of tracking systems.

$H_{th} = (H_h - H_{dh})(\cos\theta_h/\cos\theta_{zh}) + H_{dh} [(1+\cos\beta_h)/2] + H_h * \rho_s [(1-\cos\beta_h)/2]$

where:

ρ_s = surface reflectance or albedo is assumed to be 0.2 if temperature is above 0°C or 0.7 if temperature is below -5°C . Linear interpolation is used for temperatures between these values.

Finally, the monthly average tilted surface insolation (H_t) is estimated by summing hourly values of H_{th} over the “monthly average day”. It was recognized that such a procedure would be less accurate than using quality “day-by-day” site measurements, but RETScreen validation studies indicate that the “monthly average day” hourly calculation procedures give tilted surface results ranging within 3.9% to 8.9% of “day-by-day” hourly methods.

It should be emphasized that the optimum tilt angle of a tilted solar panel at a given latitude and longitude is not simply based on solar geometry and the site latitude. The solar geometry relative to the Sun slowly changes over the period of a month because of the tilted axis of the Earth. There is also a small change in the distance from the Sun to Earth over the month because of the elliptical Earth orbit around the Sun. The distance variation may cause a change in the trend of the weather at the latitude/longitude location of the tilted solar panel. The weather trend over the month may be toward either clearer or more cloudy skies over that month for that particular year. Cloudy- diffuse or clear-sky direct normal radiation may vary from year to year. As a result, the hourly calculations of tilted solar panel performance for a monthly-average day are made for all 1-degree cells over the globe for a 22-year period. Both the tilt angles and insolation values should be considered as average values over that 22-year period.

Table VI.2 illustrates the tilted radiation that is provide for a user selected latitude = 45.9N and a latitude = 116.21W. The monthly averaged total (i.e. diffuse + direct normal) solar insolation incident on a surface at the selected coordinates is provide for a horizontal panel (tilt angle = 0°), and at angles relative to the horizontal equal to the latitude, and latitude $\pm 15^\circ$ and for the surface facing south (S) , north (N), east (E) , and West (W) [e.g. Total 30° (S)].

Monthly Averaged Radiation Incident On Tilted Surfaces (kWh/m²/day)

Lat 45.9 Lon -116.21	Jan	Feb	Mar	Apr	May	Jun	Jul	Aug	Sep	Oct	Nov	Dec	Annual Average
Total 0°	1.53	2.43	3.63	4.71	5.55	6.57	7.08	6.15	4.56	2.87	1.63	1.30	4.00
Total 30° (S)	3.31	4.28	5.29	5.70	5.96	6.58	7.27	7.03	6.18	4.72	3.32	2.85	5.21
Total 30° (E)	1.65	2.44	3.63	4.64	5.31	6.36	6.88	5.95	4.45	2.81	1.73	1.30	3.93
Total 30° (N)	0.33	0.44	1.47	2.99	4.28	5.62	5.86	4.28	2.25	0.67	0.33	0.29	2.40
Total 30° (W)	1.65	2.44	3.63	4.64	5.31	6.36	6.88	5.95	4.45	2.81	1.73	1.30	3.93
Total 45° (S)	3.91	4.83	5.66	5.68	5.63	6.05	6.75	6.84	6.44	5.23	3.88	3.38	5.36
Total 45° (E)	1.69	2.40	3.54	4.47	4.99	6.02	6.53	5.67	4.28	2.73	1.75	1.31	3.78
Total 45° (N)	0.37	0.47	0.62	1.85	3.26	4.63	4.72	2.95	0.88	0.50	0.37	0.32	1.74
Total 45° (W)	1.69	2.40	3.54	4.47	4.99	6.02	6.53	5.67	4.28	2.73	1.75	1.31	3.78
Total 60° (S)	4.27	5.07	5.68	5.36	5.04	5.27	5.93	6.30	6.31	5.41	4.20	3.70	5.21
Total 60° (E)	1.67	2.31	3.38	4.20	4.58	5.55	6.03	5.28	4.02	2.60	1.72	1.27	3.55
Total 60° (N)	0.40	0.53	0.72	1.01	2.06	3.38	3.31	1.58	0.78	0.57	0.41	0.34	1.26
Total 60° (W)	1.67	2.31	3.38	4.20	4.58	5.55	6.03	5.28	4.02	2.60	1.72	1.27	3.55
Total 90° (S)	4.16	4.62	4.68	3.78	3.07	2.97	3.44	4.15	4.91	4.77	4.02	3.63	4.02
Total 90° (E)	1.46	1.91	2.76	2.92	2.56	2.81	3.07	3.59	3.19	2.10	1.49	1.06	2.41
Total 90° (N)	0.44	0.61	0.86	0.97	1.13	1.27	1.34	1.22	0.98	0.68	0.45	0.37	0.86
Total 90° (W)	1.46	1.91	2.76	2.92	2.56	2.81	3.07	3.59	3.19	2.10	1.49	1.06	2.41

Table VI.2 Example of the insolation of a surface at the user selected latitude, longitude coordinates. The total insolation (i.e. diffuse + direct normal) is given as climatological monthly averages for a horizontal surface (i.e. Total 0°) and for surfaces tilted at angles equal to the latitude $\pm 15^\circ$ relative to the horizontal and for surfaces facing south (S), east (E), north (N), and west (W).

[\(Return to Content\)](#)

VI.B Validation of Monthly Mean Insolation on a Tilted Surface: In this section results from three approaches for validation of the monthly mean insolation on a tilted surface are presented. The first involves comparison of the insolation on a tilted surface derived from the GEWEX/SRB 3.0 and FLASHFlux insolation and RETScreen formulation. The remaining two approaches provide more definitive validation statistics in that the surface insolation on a tilted surface is compared to measured tilted surface insolation values and to values that were derived from measurements of the diffuse and direct normal components of solar flux on tilted surfaces at BSRN sites.

[\(Return to Content\)](#)

VI.B i. GEWEX SRB 3.0 vs RETScreen. Table VI-3 summarizes the agreement between the POWER and RETScreen formulation in terms of the Bias and RMSE between the two methods, and the parameters (i.e. slope, intercept, and R^2) characterizing the linear least square fit to the RETScreen values (x-axis) to GEWEX SRB 3.0 values (y-axis) when both the RETScreen and POWER methods have the same horizontal insolation as inputs.

Table IV-3. Summary results from a comparison of the insolation on a tilted surface as estimated using the RETScreen and POWER methods. Both approaches start with the GEWEX SRB 3.0 monthly averaged insolation on a horizontal surface.

Location	Lat x Long	Tilt Angle	Titled-Bias	Titled-RMSE	Titled-Slope	Titled-In'cept	Titled-R2	
Ottawa Int'l Airport, Ontario, Canada	45.3N x 75.7W	45	0.47	0.56	1.17	-1.19	0.94	
Berverlodge, Alberta, CN	55.2N x 119.4W	40	0.30	0.36	1.09	-0.65	0.99	
Castlegar AP, British Cl, CN	49.3N x 117.6W	49	0.35	0.45	1.24	-1.43	0.99	
Totonto Int'l AP, Ontario, CN	43.7N x 79.6W	43	0.06	0.09	1.02	-0.12	1.00	
Burmington, AL	33.6N x 86.8W	48	0.06	0.07	1.05	-0.29	1.00	
Dodge City, KS	37.8N x 100.0W	37	0.04	0.07	1.01	-0.11	0.99	
Covington, KY	39.1N x 84.7W	39	0.03	0.05	1.00	-0.03	1.00	
San Francisco, CA	37.6N x 122.4W	37	0.03	0.05	1.00	-0.01	1.00	
San Jose, Costa Rica	10.0N x 84.2W	25	-0.09	0.24	0.79	1.08	0.93	
<hr/>								
Boulogne Sur Seine, France	50.7N x 1.6E	35	0.15	0.18	1.06	-0.36	1.00	
Riyadh (Saud-AFB), Saudi Arabia	24.7N x 46.7E	39	0.09	0.11	1.07	-0.51	0.99	
Tabuk (Saud-AFB), Saudi Arabia	28.4N x 36.6E	43	0.07	0.09	1.09	-0.59	0.97	
Bisha (Civ/Mil), Saudi Arabia	20.0N x 42.6E	35	-0.16	0.45	0.53	2.99	0.26	
Beer-Sheva/Teyman, Israel	31.2N x 34.8E	46	0.05	0.09	0.98	0.07	0.99	
Jerusalem/Atarot, Israel	31.5N x 35.2E	46	0.10	0.12	0.99	-0.05	0.99	
Naha (Civ/JASDF), Japan	26.2N x 127.7E	41	0.07	0.08	1.00	-0.08	1.00	
<hr/>								
Brasila, Brasil	15.8S x 47.9W	30	-0.09	0.24	0.83	1.02	0.94	
Antofagasta, Chile	23.4S x 70.5W	38	0.08	0.10	1.01	-0.13	1.00	
Arica/Chacallute, Chile	18.4S x 70.5W	33	-0.20	0.49	1.14	-0.50	0.90	
<hr/>								
Windhoek/Eros (SAAF), Namibia	22.6S x 17.1E	37	-0.05	0.32	0.89	0.74	0.74	
Pretoria (Met), S. Africa	25.7S x 28.2E	40	0.06	0.09	1.02	-0.19	0.98	
Pietersburg (SAAF), S. Africa	23.9S x 29.5E	38	0.07	0.09	0.99	-0.03	0.98	
Johannesburg, S. Africa	26.1S x 28.2E	41	0.04	0.07	1.06	-0.38	0.99	
Canberra, Australlia	35.3S x 149.2E	35	0.04	0.06	0.99	0.00	1.00	
			AVE =	0.06	0.19	1.00	-0.03	0.94
			STD =	0.15	0.16	0.14	0.86	0.15

Recall that the major difference between the two methods involves the determination of the diffuse radiation, and note that the results from the two methods are in good agreement.

[\(Return to Content\)](#)

VI.B.ii GEWEX SRB 3.0 vs Direct Measurements of Tilt Insolation. Figure VI.1 show the time series of the monthly mean solar insolation derived from measurements and the corresponding values from GEWEX SRB 3.0. Figure VI.1a gives the measured and GEWEX SRB 3.0 solar insolation on a horizontal surface and Figure VI.b gives the measured and GEWEX SRB 3.0 values on a South facing surface tilted at 45° . The measured values were

taken from the University of Oregon Solar Radiation Monitoring Laboratory archive (<http://solardat.uoregon.edu/index.html>) for Chaney, WA. For comparison the RETScreen values have also been included. We note that the monthly averages have been computed from GEWEX SRB 3.0 data over the 1992 – 2005 time period.

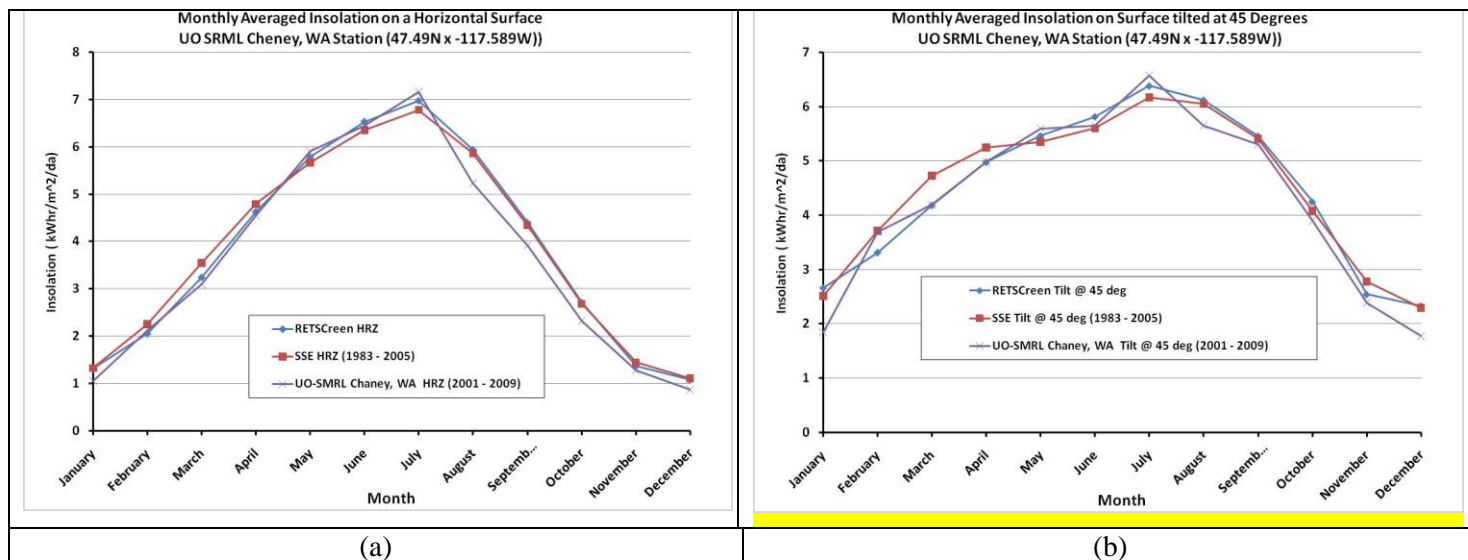


Figure VI.1 Monthly time series of solar insolation measure on a horizontal (a) and tilted (b) surface at the University of Oregon Solar Radiation Monitoring Laboratory Chaney, WA station, and corresponding insolation from RETScreen and BEWEX SRB 3.0. (Note that solar radiation is in KWh/day/m²; multiplying KWh/day/m² by 41.67 yields W/m², and by 3.6 yields MJ/day/m².)

[\(Return to Content\)](#)

VI.B.iii. GEWEX SRB 3.0 vs BSRN Based Tilt Insolation. Solar insolation measurements at the most of the ground sites in the BSRN include the diffuse and direct normal components as well as a direct measurement of the global, or total, insolation on a horizontal surface. These measurements are typically made with at 1-, 2-, 3- or 5-minute intervals throughout the day. The diffuse and direct normal measurements, coupled with the solar zenith angle, provide the necessary components to estimate solar insolation on a tilted surface as outlined below.

For any given BSRN site, consider a 3-D coordinate system with the origin at the BSRN site, X-axis pointing eastward, Y-axis northward, and Z-axis upward. For any given instant corresponding to a BSRN record, the unit vector pointing to the Sun is $\{\sin(Z)\cos[(\pi/2)-A]\mathbf{i}, \sin(Z)\sin[(\pi/2)-A]\mathbf{j}, \cos(Z)\mathbf{k}\}$, and the unit vector along the normal of the titled surface is $[0\mathbf{i}, -\sin(T)\mathbf{j}, \cos(T)\mathbf{k}]$ for Northern Hemisphere, and $[0\mathbf{i}, \sin(T)\mathbf{j}, \cos(T)\mathbf{k}]$ for Southern Hemisphere, where Z is the solar zenith angle, A is the azimuth angle of the Sun, and T is the tilt angle of the titled surface. And the direct flux on the titled surface is the direct normal flux times the dot product of the aforementioned two unit vectors which is $-\sin(Z)\cos(A)\sin(T)+\cos(Z)\cos(T)$ for Northern Hemisphere and $\sin(Z)\cos(A)\sin(T)+\cos(Z)\cos(T)$ for Southern Hemisphere. If the dot product of the two unit vectors is less than zero, which means the Sun is behind the titled surface, the direct flux on the titled surface is set to zero. After this conversion, the 3-hourly, daily and monthly means of the direct component on the titled surface can then be derived, and the diffuse

component can be similarly derived. The sum of the direct and diffuse components is the total flux on the tilted surface.

Figure VI.2 is a scatter plot of the climatological monthly mean insolation on a tilted surface derived from the BSRN measurements of the diffuse and direct normal components versus the corresponding GEWEX SRB 3.0 tilt radiation values.

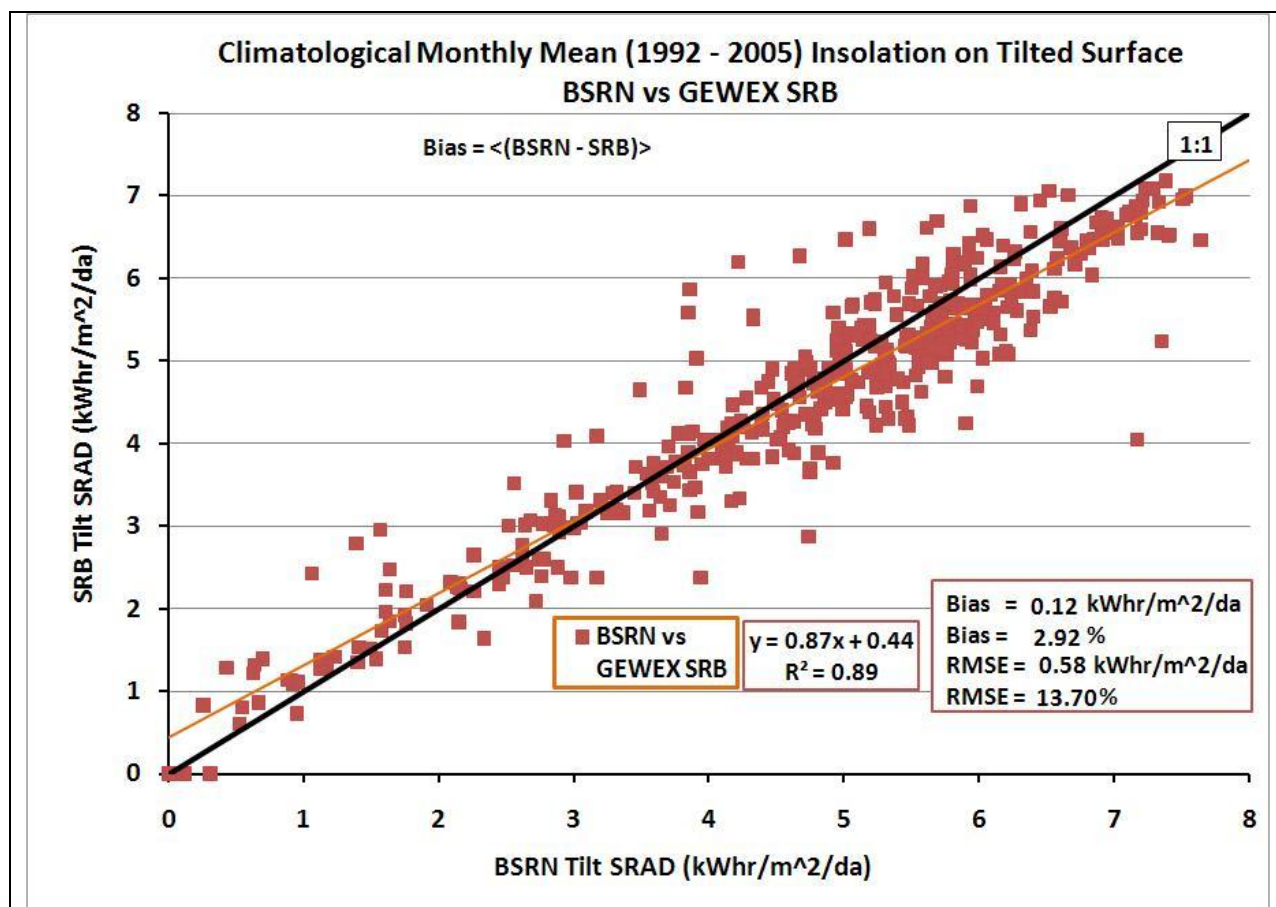


Figure VI.2a Scatter plot of the climatological monthly mean insolation on a tilted surface derived from the BSRN measurements of the diffuse and direct normal components versus the corresponding GEWEX-SRB 3.0 tilt radiation values for all sky conditions. (Note that solar radiation is in kWh/day/m²; multiplying kWh/day/m² by 41.67 yields W/m², and by 3.6 yields MJ/day/m².)

[\(Return to Content\)](#)

VII. Meteorological Parameters

Table II-1 lists the meteorological parameters provided through the Sustainable Buildings archive, their temporal coverage and source. The global distribution of meteorological parameters in the POWER/Sustainable Buildings archive are obtained from NASA's Global Model and Assimilation Office (GMAO), Goddard Earth Observing System global assimilation models version 4 (GEOS-4: <http://gmao.gsfc.nasa.gov/systems/geos4/>) and version-5 (GEOS-5: <http://gmao.gsfc.nasa.gov/products/>). The relative humidity is a calculated parameter based upon pressure, temperature and specific humidity, all parameters obtained from the assimilation models. Dew/frost point temperatures are calculated values based upon the relative humidity and air temperature which is obtained from the assimilation model. Precipitation is obtained from the Global Precipitation Climate Project. Monthly mean winds are from the GOES-2 assimilation model, and daily winds are from the GEOS-4 assimilation model over the time period January 1, 1983 – December 31, 2007 and from the GEOS-5 model over the time period January 1, 2008 – to within several days of current time. In this section the results associated with testing /validating each parameter against ground site observation is discussed.

[\(Return to Content\)](#)

VII.A. Assessment of Assimilation Modeled Temperatures: As noted above all meteorological parameters, except precipitation, are based directly or indirectly (i.e. calculated) on the GMAO assimilation models. The meteorological parameters emerging from the GMAO assimilation models are estimated via “An atmospheric analysis performed within a data assimilation context [that] seeks to combine in some “optimal” fashion the information from irregularly distributed atmospheric observations with a model state obtained from a forecast initialized from a previous analysis.” (Bloom, et al., 2005). The model seeks to assimilate and optimize observational data and model estimates of atmospheric variables. Types of observations used in the analysis include (1) land surface observations of surface pressure; (2) ocean surface observations of sea level pressure and winds; (3) sea level winds inferred from backscatter returns from space-borne radars; (4) conventional upper-air data from rawinsondes (e.g., height, temperature, wind and moisture); (5) additional sources of upper-air data include drop sondes, pilot balloons, and aircraft winds; and (6) remotely sensed information from satellites (e.g., height and moisture profiles, total perceptible water, and single level cloud motion vector winds obtained from geostationary satellite images). Emerging from the analysis are 3-hourly global estimates of the vertical distribution of a range of atmospheric parameters. The assimilation model products are bi-linearly interpolated to a 1^0 by 1^0 grid. Table II-1 lists the basic meteorological parameters from the GMAO models (as well as other data sources) provided through the Sustainable Buildings archive along

In addition to the analysis reported by the NASA's Global Model and Assimilation Office (GMAO) (Bloom, et al. 2005), the POWER project initiated a study focused on determining the accuracy of the GEOS-4 meteorological parameters in terms of the applications within the POWER project. In particular, the GEOS-4 temperatures (minimum, maximum and daily averaged air and dew point), relative humidity, and surface pressure have been explicitly compared to global data obtained from the National Center for Environmental Information (NCEI – formally National Climatic Data Center- <http://www.ncdc.noaa.gov/oa/ncdc.html>) global “Summary of the Day” (GSOD) files, and to observations from other high quality

networks such as the Surface Radiation (SURFRAD - <http://www.srrb.noaa.gov/surfrad/index.html>), Atmospheric Radiation Measurement (ARM - <http://www.arm.gov/>), as well as observations from automated weather data networks such as the High Plains Regional Climate Center (HPRCC - <http://www.hprcc.unl.edu/index.php>).

In this section we will focus primarily on the analysis of the GEOS-4 daily maximum and minimum temperatures, and the daily mean temperature using observations reported in the NCEI - GSOD files, with only summary comments regarding results from the other observational networks noted above. The GEOS-4 re-analysis model outputs meteorological parameters at 3-hourly increments (e.g. 0, 3, 6, 9, 12, 15, 18, and 21 Z) on a global 1- deg by 1.25-deg grid at 50 pressure levels. The 1-deg by 1.25-deg grid is bi-linearly interpolated to a 1-deg by 1-deg grid to match the GEWEX/SRB 3.0 solar radiation values. The local daily maximum (Tmax) and minimum (Tmin) temperature, and the local daily mean (Tave) temperature at 2 meters above the surface were obtained from the GEOS-4 3-hourly data. The Sustainable Buildings GEOS-4 meteorological data spans the time period from January 1, 1983 - through December 2007; comparative analysis discussed here is based upon observational data from January 1, 1983 through December 31, 2006.

The observational data reported in the NCEI GSOD files are hourly observations from globally distributed ground stations with observations typically beginning at 0Z. For the analysis reported herein, the daily Tmin, Tmax and Tave were derived from the hourly observations filtered by an “85%” selection criteria applied to the observations reported for each station. Namely, only data from NCEI stations reporting 85% or greater of the possible 1-hourly observations per day and 85% or greater of the possible days per month were used to determine the daily Tmin, Tmax, and Tave included in comparisons with the GEOS-4 derived data. Figure VII-A.1 illustrates the global distribution of the surface stations remaining in the NCEI data files for 1983 and 2004 after applying our 85% selection criteria. Note that the number of stations more than doubled from 1983 (e.g. 1104 stations) to 2004 (e.g. 2704 stations), and that majority of the stations are located in the northern hemisphere.

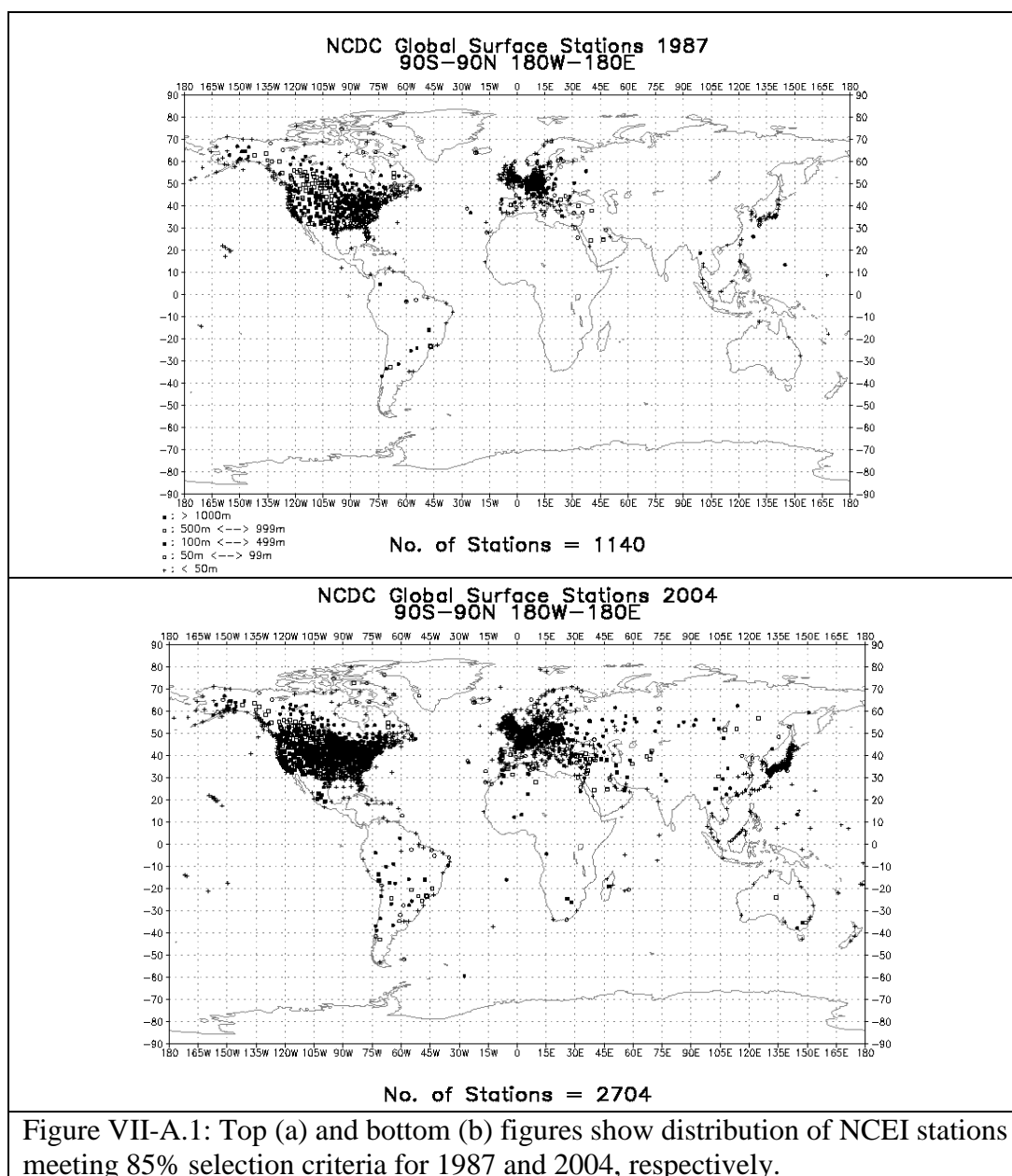
Unless specifically noted otherwise, all GEOS-4 air temperatures represent the average value on a 1° x 1° latitude, longitude grid cell at an elevation of 2 m above the earth’s surface and NCEI values are ground observations at an elevation of 2 meters above the earth’s surface. Scatter plots of Tave, Tmax, and Tmin derived from ground observations in the NCEI files versus GEOS-4 values for the years 1987 and 2004 are shown in Figure VII-A.2. These plots illustrate the agreement typically observed for all the years 1983 through 2006. In the upper left corner of each figure are the parameters for the linear least squares regression fit to these data, along with the mean Bias and RMSE between the GEOS-4 and NCEI observations. The mean Bias and RMSE are given as:

$$\text{Bias} = \sum_j \{ \sum_i \{ [(T_i^j)_{\text{GEOS4}} - (T_i^j)_{\text{NCEI}}] \} \} / N$$

$$\text{RMSE} = \{ \sum_j \{ \sum_i \{ [(T_i^j)_{\text{GEOS4}} - (T_i^j)_{\text{NCEI}}]^2 / N \} \} \}^{1/2},$$

where, \sum_i is summation over all days meeting the 85% selection criteria, \sum_j indicates the sum over all stations, $(T_i^j)_{\text{NCEI}}$ is the temperature on day i for station j , and $(T_i^j)_{\text{GEOS4}}$ is the GEOS-4

temperature corresponding to the overlapping GEOS-4 1-degree cell for day i and station j , and N is the number of matching pairs of NCEI and GEOS-4 values.



For the year 1987, 1139 stations passed our 85% selection criteria yielding 415,645 matching pairs on NCEI/GEOS-4 values; for 2004, 2697 stations passed yielding 987,451 matching pairs of NCEI/GEOS-4 temperature values. The color bar along the right side of the scatter plot provides a measure of the distribution of the NCEI/GEOS-4 temperature pairs. For example, in Figure VII-A.2, each data point shown in dark blue represents a 1-degree cell with 1 to 765 matching temperature pairs, and all of the 1-degree cells shown in dark blue contain 15.15% of the total number of ground site points. Likewise, the darkest orange color represents 1-degree

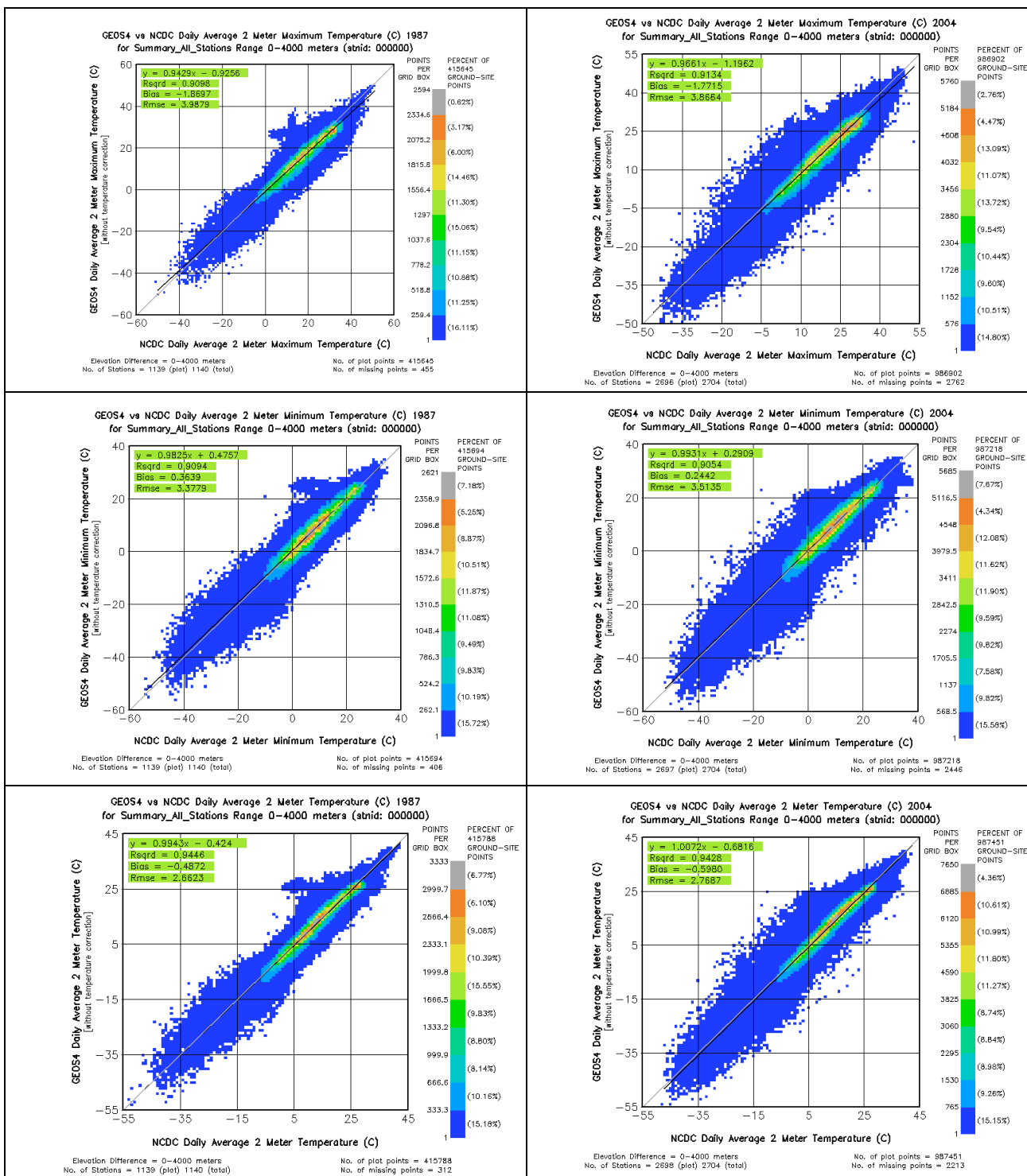


Figure VII-A.2. Top (a), middle (b) and bottom (c) figures show the scatter plot of ground site observations versus GEOS-4 values of Tmax, Tmin, and Tave for the years 1987 and 2004. The color bar in each figure indicates the number and percentage of ground stations that are included within each color range.

cells for which there are from 6120 to 6885 matching temperature pairs, and taken as a group all of the 1-degree cells represented by orange contain 10.61% of the total number of matching ground site points. Thus, for the data shown in Figure VII-A.2a, approximately 85% of matching temperature pairs (i.e. excluding the data represented by the dark blue color) is “tightly” grouped along the 1:1 correlation line.

In general, the scatter plots shown in Figure VII-A.2, and indeed for all the years from 1983 through 2006, exhibit good agreements between the GEOS-4 data and ground observations. Notice however that for both the 1987 and 2004 data, on a global basis, the GEOS-4 Tmax values are cooler than the ground values (e.g. bias = -1.9 C in 1987 and -1.8 C in 2004); the GEOS-4 Tmin values are warmer (e.g. bias = 0.4° C in 1987 and 0.2° C in 2004); and that GEOS-4 Tave values are cooler (e.g. bias = -0.5° C in 1987, and -0.6° C in 2004. Similar trends in the respective yearly averaged biases between GEOS-4 and NCEI observations were noted for each year from 1983 – 2006 (see Table VII-A.1 below). The ensemble average for the years 1983 – 2006 yields a GEOS-4 Tmax which is 1.82° C cooler than observed at NCEI ground Sites, a Tmin about 0.27° C warmer, and a Tave about 0.55° C cooler. Similar trends are also observed for measurements from other meteorological networks. For example, using the US National Weather Service Cooperative Observer Program (COOP) observations, White, et al (2008) found the mean values of GEOS-4 Tmax, Tmin, and Tave to be respectively 2.4° C cooler, Tmin 1.1° C warmer, and 0.7° C cooler than the COOP values.

Table VII-A.1 Global year-by-year comparison of daily Tmax, Tmin, and Tave: NCEI GSOD values vs GEOS-4 temperatures

Year	Tmax					Tmin					Tave				
	Slope	Intercept (C)	R^2	RMSE (C)	Bias (C)	Slope	Intercept (C)	R^2	RMSE (C)	Bias (C)	Slope	Intercept (C)	R^2	RMSE (C)	Bias (C)
2006	0.97	-1.28	0.92	3.88	-1.72	1.00	0.09	0.90	3.59	0.11	1.02	-0.79	0.94	2.82	-0.59
2005	0.97	-1.40	0.92	4.00	-1.92	0.99	0.20	0.91	3.57	0.16	1.01	-0.81	0.95	2.81	-0.67
2004	0.97	-1.20	0.91	3.86	-1.78	0.99	0.28	0.91	3.50	0.24	1.01	-0.69	0.94	2.76	-0.60
2003	0.95	-0.91	0.91	3.96	-1.74	0.99	0.46	0.91	3.49	0.38	1.00	-0.47	0.94	2.82	-0.53
2002	0.94	-0.88	0.91	4.06	-1.94	0.98	0.47	0.90	3.55	0.30	0.98	-0.48	0.94	2.85	-0.66
2001	0.97	-1.69	0.92	4.00	-2.20	1.00	0.10	0.90	3.62	0.11	1.01	-0.97	0.95	2.78	-0.81
2000	0.97	-1.17	0.91	3.84	-1.67	1.00	0.25	0.91	3.50	0.27	1.01	-0.65	0.94	2.77	-0.52
1999	0.97	-1.25	0.91	3.80	-1.78	0.99	0.47	0.91	3.37	0.39	1.00	-0.60	0.95	2.63	-0.54
1998	0.98	-1.29	0.92	3.67	-1.71	0.99	0.11	0.91	3.27	0.07	1.01	-0.81	0.94	2.62	-0.68
1997	0.97	-1.20	0.92	3.64	-1.66	0.99	-0.01	0.91	3.30	-0.05	1.00	-0.72	0.95	2.67	-0.68
1996	0.95	-0.71	0.91	3.67	-1.56	0.98	0.27	0.91	3.31	0.15	0.99	-0.46	0.94	2.66	-0.55
1995	0.97	-1.44	0.92	3.93	-1.91	1.00	0.32	0.92	3.44	0.29	1.01	-0.69	0.95	2.69	-0.60
1994	0.98	-1.58	0.92	4.08	-1.93	1.00	-0.01	0.91	3.55	-0.04	1.01	-0.82	0.95	2.85	-0.71
1993	0.96	-1.22	0.92	3.93	-1.80	0.99	0.22	0.92	3.40	0.16	1.00	-0.51	0.95	2.68	-0.52
1992	0.95	-0.92	0.91	3.90	-1.70	0.98	0.43	0.90	3.46	0.33	1.00	-0.43	0.94	2.67	-0.43
1991	0.95	-1.05	0.91	4.14	-1.89	0.99	0.35	0.91	3.45	0.27	1.00	-0.45	0.94	2.80	-0.49
1990	0.95	-1.12	0.90	4.18	-1.94	0.99	0.40	0.91	3.49	0.35	1.00	-0.44	0.94	2.79	-0.49
1989	0.96	-1.18	0.91	4.15	-1.91	0.99	0.48	0.92	3.50	0.42	0.99	-0.40	0.95	2.79	-0.46
1988	0.95	-1.11	0.91	4.03	-1.90	0.99	0.55	0.91	3.38	0.47	1.00	-0.38	0.95	2.63	-0.42
1987	0.94	-0.93	0.91	3.99	-1.87	0.98	0.48	0.91	3.38	0.36	0.99	-0.42	0.94	2.66	-0.49
1986	0.95	-1.02	0.91	4.05	-1.88	0.98	0.52	0.91	3.37	0.39	0.99	-0.35	0.94	2.70	-0.45
1985	0.96	-1.11	0.92	4.03	-1.84	0.99	0.38	0.92	3.58	0.32	0.99	-0.44	0.95	2.83	-0.49
1984	0.96	-1.07	0.91	4.00	-1.79	1.00	0.44	0.91	3.46	0.41	1.00	-0.45	0.94	2.79	-0.47
1983	0.96	-1.19	0.91	4.02	-1.78	0.99	0.41	0.91	3.44	0.34	1.00	-0.49	0.94	2.82	-0.52
Average	0.96	-1.16	0.91	3.95	-1.82	0.99	0.32	0.91	3.46	0.26	1.00	-0.57	0.94	2.75	-0.56
STDEV	0.01	0.22	0.01	0.15	0.13	0.01	0.17	0.01	0.10	0.14	0.01	0.17	0.00	0.08	0.10

The average of the least square fit along with the average RMSE and Bias values given in Table VII-A.1 are taken as representative of the agreement expected between GEOS-4 temperatures and ground site measurements.

Further analysis, described in Appendix A, shows that one factor contributing to the temperature biases between the assimilation model estimates and ground site observations is the difference in the elevation of the reanalysis grid cell and the ground site. Appendix A describes a

downscaling methodology based upon a statistical calibration of the assimilation temperatures relative to ground site observations. The resulting downscaling parameters (i.e. lapse rate and offset values) can be regionally and/or seasonally used to downscale the model temperatures yielding estimates of local temperatures with reduced biases relative to ground site observations.

Application of the downscaling procedure described in Appendix A is currently implemented in the Sustainable Buildings Archive to provide adjusted 25–year monthly mean Tmax, Tmin, and Tave temperatures based upon a user's input of the ground site elevation. As an example of downscaling, Table A.5 and Table A.6 in Appendix A give, respectively, the global monthly averaged Mean Bias Error (MBE) and Root Mean Square Error (RMSE) for unadjusted and downscaled 2007 GEOS-4 temperatures relative to NCEI temperatures.

Assessment of GEOS-5 Temperatures: An initial assessment of the GEOS-5 temperatures follows the methodology described above for the GEOS-4 temperatures. Results from the assessment, which included 4,172 globally distributed ground stations reporting observations in the NCEI GSOD files for the year 2009, are given in Table VII-A.2.

Table VII-A.3. Summary of statistics for a global comparison of the uncorrected GEOS-5 daily temperatures to ground observations reported by 4172 stations in the NCEI GSOD files during 2009

Parameter	Bias	RMSE	Slope	Intercept	R ²	Daily Values
Tave	-0.98	3.15	0.96	-0.74	0.92	1,214,462
Tmax	-1.07	3.62	0.97	-0.58	0.93	1,518,601
Tmin	0.84	3.68	0.97	1.05	0.91	1,519,039

[\(Return to Content\)](#)

VII. B. Relative Humidity: The relative humidity (RH) values in the POWER archives are calculated from pressure (P_a in kPa), dry bulb temperature (T_a in °C), and mixing ratio (e.g. specific humidity, q in kg/kg), parameters that are available in the NASA's MERRA assimilation model. The following is a summary of the expressions used to calculate RH. The units are indicated in square brackets.

From Iribarne and Godson (1981) a fundamental definition of the Relative Humidity (Eq. 83, pg 75):

$$(VII.B.1) \quad RH = (e_a/e_{sat}) \times 100\%$$

where

e_a = the water vapor pressure and

e_{sat} the saturation water vapor pressure at the ambient temperature T_a .

The 100% has been added to cast RH in terms of percent.

Since water vapor and dry air (a mixture of inert gases) can be treated as ideal gases, it can be shown that (Iribarne and Godson, pg 74, Eq. 76; Note that the symbol, r , use in Eq. 76 for the mixing ratio has been replaced by “ w ” and the factor of “10” has been added to convert the units to hPa.)

$$(VII.B.2) \quad e_a = (10 \times P_a \times w) / (\epsilon + w) \quad [\text{hPa}]$$

where w is the mixing ratio define as the ratio of mass of water to dry air and

$$(VII.B.3) \quad \epsilon = \frac{R'}{R_v} = \frac{287.05}{461.5} \simeq 0.622$$

where R' and R_v are the dry and water vapor gas constants respectively (note that there is no exact consensus for the gas constants past 3 significant digits, therefore the value of the ratio is kept to 3 significant digits). The mixing ratio is related to specific humidity by the relation (Jupp 2003, pg.37):

$$(VII.B.4) \quad w = q / (1-q) \quad [\text{kg/kg}]$$

Combining (VII.B.2) and (VII.B.4) leads to the following expression for e in terms of q :

$$(VII.B.5) \quad e_a = q \times 10 \times P_a / [\epsilon + q \times (1 - \epsilon)] \quad [\text{hPa}]$$

An eighth-order polynomial fit (Flatau, et. al. 1992) to measurements of vapor pressure over ice and over water provides an expression to calculate the saturated water vapor pressure over ice and over water. The eight-order fit for e_{satw} is given by

$$(VII.B.6) \quad e_{\text{wsat}} = A_{1w} + A_{2w} \times (T_a) + \dots + A_{(n-1)w} \times (T_a)^n$$

and

$$(VII.B.7) \quad e_{\text{isat}} = A_{1i} + A_{2i} \times (T_a) + \dots + A_{(n-1)i} \times (T_a)^n \quad ,$$

Where

e_{wsat} = saturated vapor pressure over water in [hPa = mb]

e_{isat} = saturated vapor pressure over ice [hPa=mb]

T_a is the ambient dry bulb temperature in °C.

Table VII.B.1 gives the coefficients for e_{sat} over water and over ice and the temperature range over which the coefficient are applicable.

Table VII.B.1. Coefficients of the eight-order polynomial fit (Taken from Flatau, et. al. 1992 Table 4.) to measurements of saturated vapor pressure measurements,	
Coefficients for e_{sat} over water valid over the temperature range $-85\text{ }^{\circ}\text{C}$ to $+70\text{ }^{\circ}\text{C}$	Coefficients for e_{sat} over ice valid over the temperature range $-90\text{ }^{\circ}\text{C}$ to $0\text{ }^{\circ}\text{C}$
A1w = 6.11583699	A1i = 6.09868993
A2w = 0.444606896	A2i = 0.499320233
A3w = 0.143177157E-1	A3i = 0.184672631E-1
A4w = 0.264224321E-3	A4i = 0.402737184E-3
A5w = 0.299291081E-5	A5i = 0.565392987E-5
A6w = 0.203154182E-7	A6i = 0.521693933E-7
A7w = 0.702620698E-10	A7i = 0.307839583E-9
A8w = 0.379534310E-13	A8i = 0.105758160E-11
A9w = -0.321582393E-15	A9i = 0.161444444E-14

Note that only the relative humidity over water is calculated and provided in the POWER/Sustainable Buildings Archive consistent with the values reported by the National Weather Service..

GEOS-4 Relative Humidity: Table VII-B.2 Summarizes the comparison statistics for the relative humidity based upon GEOS-4 q, P, T values vs. ground observations reported in the 2007 NCEI GSOD files.

(Note that for the comparison statistics in Tables VII-B.1 and –B.2 the RH was calculated using a different approximation for calculating RH, however the percentage differences in the RH values was typically less the 10%.)

Table VII-B.2. Summary of statistics for a global comparison of the daily mean relative humidity based upon GEOS-4 q, P, T values to ground observations reported in the NCEI GSOD files during 2007.					
Bias	RMSE	Slope	Intercept	R ²	Daily Values
-1.89	12.67	0.76	1.62	0.55	1,214,462

GEOS-5 Relative Humidity: Table VII-B.3 Summarizes the comparison statistics for the relative humidity values based upon GEOS-5 q, P, and T vs. ground observations reported in the 2009 NCEI GSOD files.

Table VII-B.3. Summary of statistics for a global comparison of the daily mean relative humidity based upon GEOS-5 q, P, T values to ground observations reported in the NCEI GSOD files during 2009.					
Bias	RMSE	Slope	Intercept	R ²	Daily Values
-0.95	11.79	0.81	0.24	0.61	1,428,047

[\(Return to Content\)](#)

VII. C. Dew/Frost Point Temperatures: The daily dew and frost point temperatures are calculated from the relative humidity and temperature. Note that as per <http://www.ofcm.gov/fmh-1/pdf/J-CH10.pdf> section 10.5.1 of the “Federal Meteorological handbook NO. 1 – Surface Weather observations and Reports, September 2005”, the “Dew point shall be calculated with respect to water at all temperatures.” Accordingly, the nomenclature that will be used herein is to designate dew/frost point temperatures based upon the RH over water as Tdpt. The Tdpt is calculated using the expression (2003, Encyclopedia of Agricultural, Food, and Biological Engineering, Page 189, Edited by Dennis R. Heldman; Online ISBN 0-8247-0937-3).

$$(VII.C.1) \quad Tdpt = T_a - \left[(14.55 + 0.114 \times T_a) \times RH_1 + ((2.5 + 0.007 \times T_a) \times RH_1)^3 + ((15.9 + 0.117 \times T_a) \times RH_1^{14}) \right]$$

Where

T_a = Ambient air temperature

and

$$RH_1 = 1.0 - RH/100.$$

The RH value over water is calculated, as described in Section VII.B.

The following tables give the statistics associated with comparing the dew/frost point temperatures based upon GEOS-4 RH and T_a values (Table VII-C.1) and GEOS-5 RH and T_a values (Table VII-C.2).

(Note that for the comparison statistics in Tables VII-C.1 and –C.2 the RH was calculated using a different approximation for calculating RH, however the differences in the dew point temperatures ranging from approximately -50C to 40C was less than 1C.)

Table VII-C.1. Summary of statistics for a global comparison of the GEOS-4 daily mean dew point to ground observations reported by 3410 station in the NCEI GSOD files during 2007.

Bias	RMSE	Slope	Intercept	R ²	Daily Values
-0.98	3.15	0.96	-0.74	0.92	1,214,462

Table VII-C.2. Summary of statistics for a global comparison of the GEOS-5 daily mean dew point to ground observations reported by 4172 stations the NCEI GSOD files during 2009.

Bias	RMSE	Slope	Intercept	R ²	Daily Values
-0.43	3.03	0.95	-0.16	0.92	1,428,047

[\(Return to Content\)](#)

VII-D. Precipitation: The precipitation data in POWER/Building archive has been obtained from version 2.1 Global Precipitation Climate Project (GPCP – 1DD) Satellite-Gauge Product <http://precip.gsfc.nasa.gov>). Version 2.1, is a global 1°x1° daily accumulation based upon combination of observations from multiple platforms described at http://precip.gsfc.nasa.gov/gpcp_v2.1_comb_new.html and synopsized below as:

Version 2.1 Global Precipitation Climate Project Satellite-Gauge Product

1. Special Sensor/Microwave Imager (SSM/I; 0.5°x0.5° by orbit, GPROF algorithm) provides fractional occurrence of precipitation, and
2. GPCP Version 2 Satellite-Gauge (SG) combination (2.5°x2.5° monthly) data provides monthly accumulation of precipitation as a “scaling constraint” that is applied to the algorithms use to estimate precipitation values from :
 - a. geosynchronous-orbit IR (geo-IR) T_b histograms (1°x1° grid in the band 40°N-40°S, 3-hourly),
 - b. low-orbit IR (leo-IR) GOES Precipitation Index (GPI; same time/space grid as geo-IR),
 - c. TIROS Operational Vertical Sounder (TOVS; 1°x1° on daily nodes, Susskind algorithm), and
 - d. Atmospheric Infrared Sounder (AIRS; 1°x1° on daily nodes, Susskind algorithm).

In general, precipitation often tends to be a rather localized and short duration event. Consequently, accurately capturing the amount of precipitation, even in terms of mean daily amounts, from satellite observation is challenging. The GPCP -1DD data were used as the base precipitation source since it is derived from inputs from multiple platforms and therefore was deemed to have a better chance of capturing daily rainfall events.

The 1-degree POWER estimates of precipitation are based upon replicating GPCP values for the POWER cell that overlaps GPCP cells and averaging GPCP values when the POWER cell overlaps two or more GPCP cells.

It is noted that the Tropical Rainfall Measurement Mission (TRMM - <http://trmm.gsfc.nasa.gov/>) is another potential source for precipitation data, however it's polar orbit combined with a ¼ - degree resolution limits the daily coverage that can be provided for a given location. Moreover the global coverage afforded by TRMM is nominally from 40N to 40S latitude. Currently the TRMM data is not included as part of the POWER/Building precipitation data product.

Numerous validation studies of the GPCP data products have been published (Adler, et. al. 2003; McPhee and Margulis , 2005; references cited in these publications), however, analysis/validation of the GPCP 1-degree daily products have, in general, been based upon methodologies that temporally and/or spatially average the precipitation data. In the remainder

of this section, validations based upon comparisons of the daily 1-degree precipitation values obtained from the POWER/Building archive to corresponding ground sites observation within the same 1-degree cell are discussed.

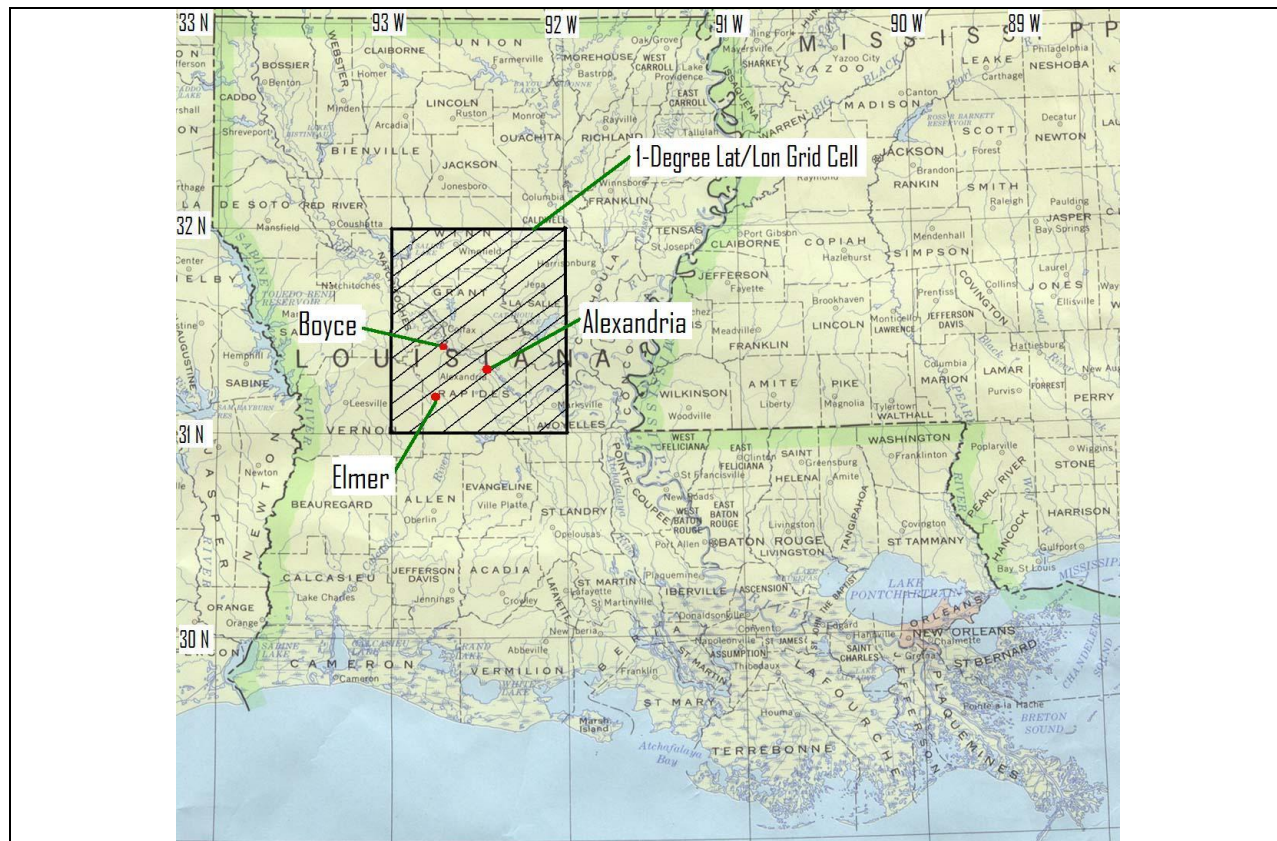
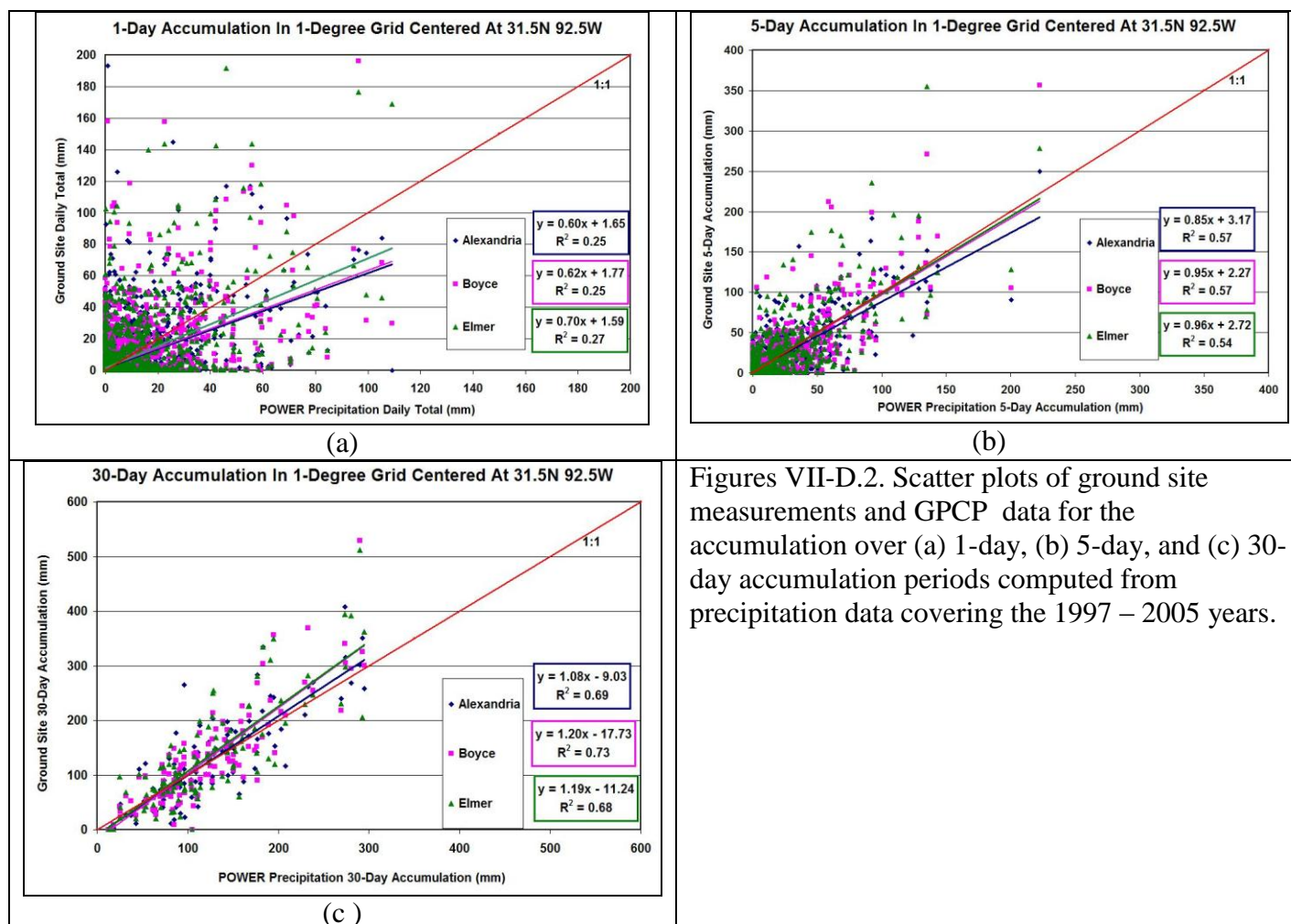


Figure VII-D.1 Location of the three ground sites in Louisiana used in the precipitation comparative study and the 1-degree grid cell over which the GPCP precipitation is averaged.

We first show results comparing GPCP – 1DD data and ground site observations from the single 1-degree cell shown in Figure VII-D.1. Figure VII-D.1 shows the location of three ground sites in Louisiana all within a 1-degree grid cell bounded by on the North and South by 32N and 31S latitudes respectively and on the East and West by 92W and 93W longitudes respectively. Daily mean precipitation data measured at these three sites over a 9-year period beginning in 1997 were compared to daily mean values available from the POWER/Building archive. Figures VII-D.2a, b, and c show scatter plots of the POWER values versus ground site measurements for accumulation over 1-day, 5-day and for a 30-day accumulation.



The results of a cell-by-cell comparison of the daily values from POWER/Building and ground observation within the Continental United States (CONUS) is summarized in Figures VII-D.4 and -5. The ground site observations were reported in the NCEI GSOD files for the year 2004, and the GPCP values are from the POWER/Building archive. Figure VII-D.4 shows the distribution of the NCEI sites for 2004, and Figure VII-D.5 shows the cell-by-cell scatter plot of the ground and POWER/Building values for (a) 1-day accumulation and (b) a 30-day accumulation.

The results from the single cell and the CONUS cell-by-cell comparison echo the results, implicit in the methodology used by McPhee and Margulis (2005) where only spatial (regional) and temporally (seasonal) averaged comparisons were reported and by Bolvin, et. al. (2009). Namely, the agreement between the GPCP 1-DD data products and ground observations improves with temporal (and spatial) averaging.

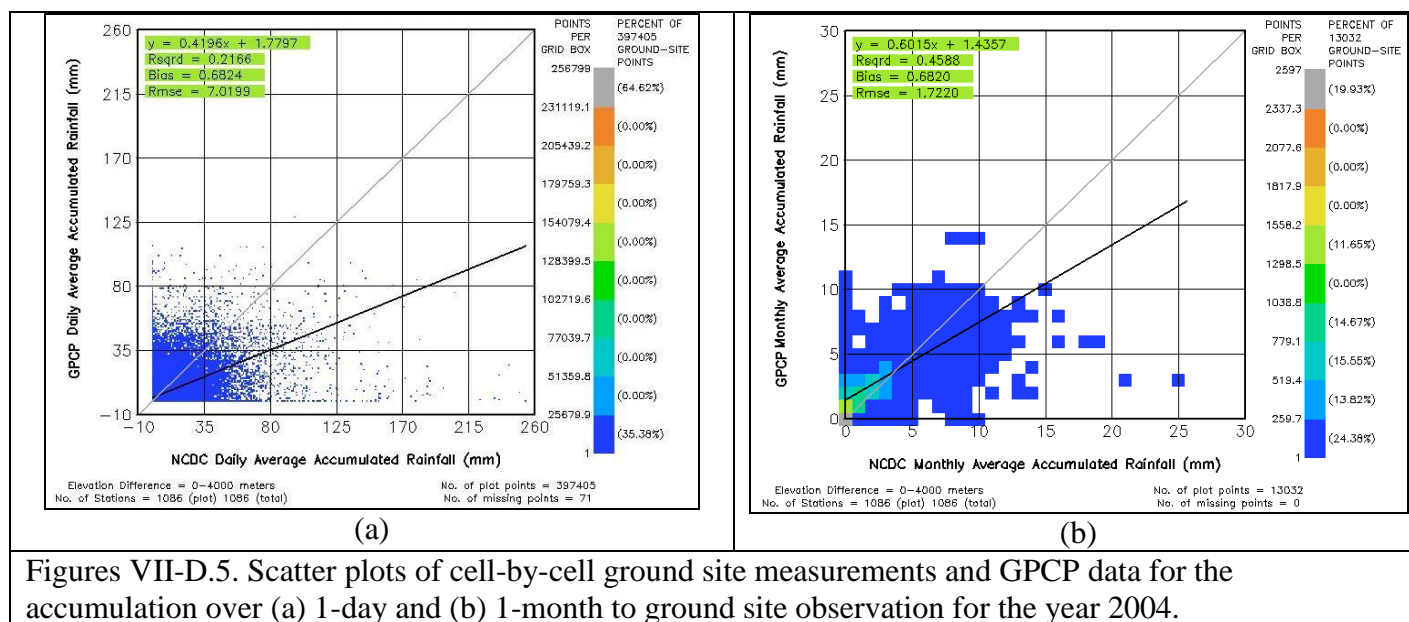
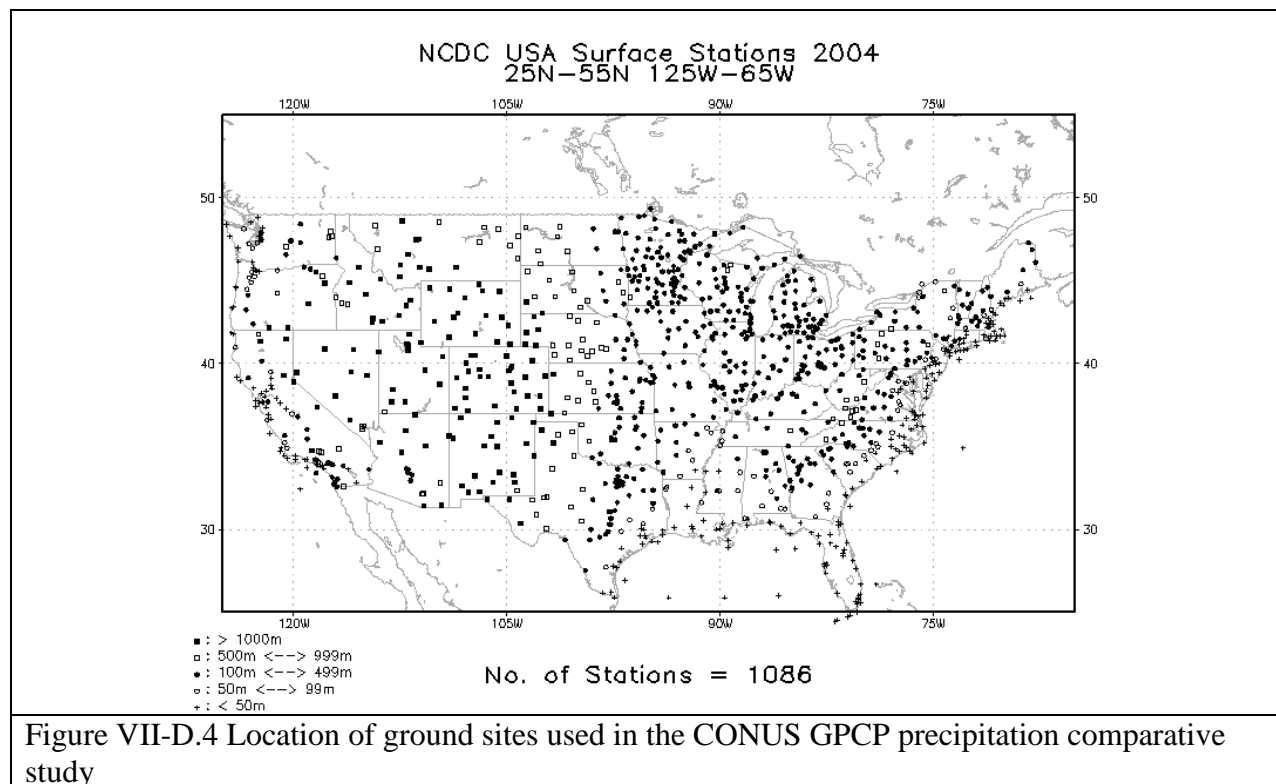


Table VII-D.1. Summary of comparison statistics associated with the scatter plots shown in Figure VII-D.4.		
Parameter	Daily Data	Monthly Data
Slope:	0.42	0.60
Intercept:	1.78 mm	1.44 mm
Rsqr:	0.22	0.46
Bias:	0.68 mm	0.68 mm
Absolute Bias:	2.60 mm	1.14 mm
Rmse:	7.02 mm	1.72 mm
GPCP Mean:	2.57 mm	2.57 mm
GPCP Std Dev:	6.38 mm	1.83 mm
NCEI Mean:	1.89 mm	1.89 mm
NCEI Std Dev:	7.08 mm	2.07 mm

[\(Return to Content\)](#)

VII-E Wind Speed: The POWER/Building archive provides monthly and daily mean winds. The monthly means are based on the Version 1 GEOS (GEOS-1) reanalysis data set described in Takacs, Molod, and Wang (1994). The daily means include GEOS-4 values from January 1, 1983 – December 31, 2007 and GEOS-5 values from January 1, 2008 to within several days of current time.

Monthly Means Winds: The monthly mean winds, given at 50-meter above the earth's surface, were derived from GEOS-1 layer 1 values using equations provided by GEOS project personnel. Adjustments were made in a few regions based on science information from Dorman and Sellers (1989) and recent vegetation maps developed by the International Geosphere and Biosphere Project (IGBP) (Figure VII.E-1). GEOS-1 vegetation maps were compared with IGBP vegetation maps. Significant differences in the geographic distribution of crops, grasslands, and savannas were found in a few regions. In those regions, airport data were converted to new 50-m height velocities based on procedures in Gipe (1999). GEOS-1 50-m values were replaced with the new Gipe-derived estimates in those regions.

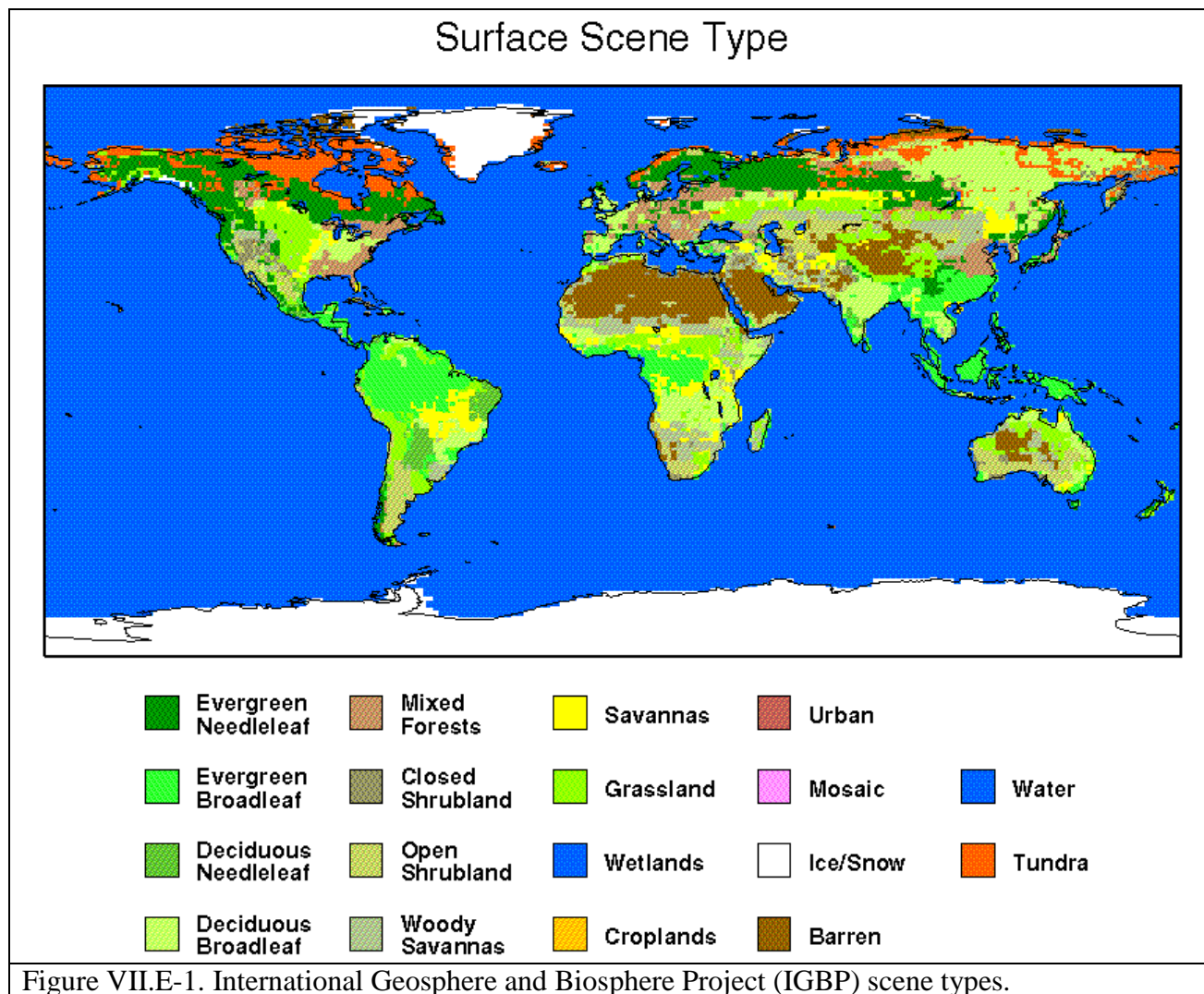


Figure VII.E-1. International Geosphere and Biosphere Project (IGBP) scene types.

Ten-year annual average maps of 50-m and 10-m "airport" wind speeds are shown in Figure VII.E.2. Velocity magnitude changes are now consistent with general vegetation heights that might be expected from the scene types in Figure VII.E.1. Note that heights are above the soil, water, or ice surface and not above the "effective" surface in the upper portion of vegetation canopies.

Ten-year average "airport" estimates were compared with 30-year average airport data sets over the globe furnished by the RETScreen project. In general, monthly bias values varied between ± 0.2 m/s and RMS (including bias) values are approximately 1.3 m/s (Fig. VII.E.3). This represents a 20 to 25 percent level of uncertainty relative to mean monthly values and is about the same level of uncertainty quoted by Schwartz (1999). Gipe (1999) notes that operational wind measurements are sometimes inaccurate for a variety of reasons. Site-by-site comparisons at nearly 790 locations indicate POWER/Building 10-m "airport" winds tend to be higher than airport measurements in remote desert regions in some foreign countries. POWER values are usually lower than measurements in mountain regions where localized accelerated flow may occur at passes, ridge lines or mountain peaks. One-degree resolution wind data is not an

accurate predictor of local conditions in regions with significant topography variation or complex water/land boundaries.

Designers of "small-wind" power sites need to consider the effects of vegetation canopies affecting wind from either some or all directions. Trees and shrub-type vegetation with various heights and canopy-area ratios reduce near-surface velocities by different amounts. GEOS-1 calculates 10-m velocities for a number of different vegetation types. Values are calculated by parameterizations developed from a number of "within-vegetation" experiments in Canada, Scandinavia, Africa, and South America. The ratio of 10-m to 50-m velocities (V_{10}/V_{50}) for 17 vegetation types is provided in Table VII.E.1. All values were taken from GEOS-1 calculations except for the "airport" flat rough grass category that was taken from Gipe.

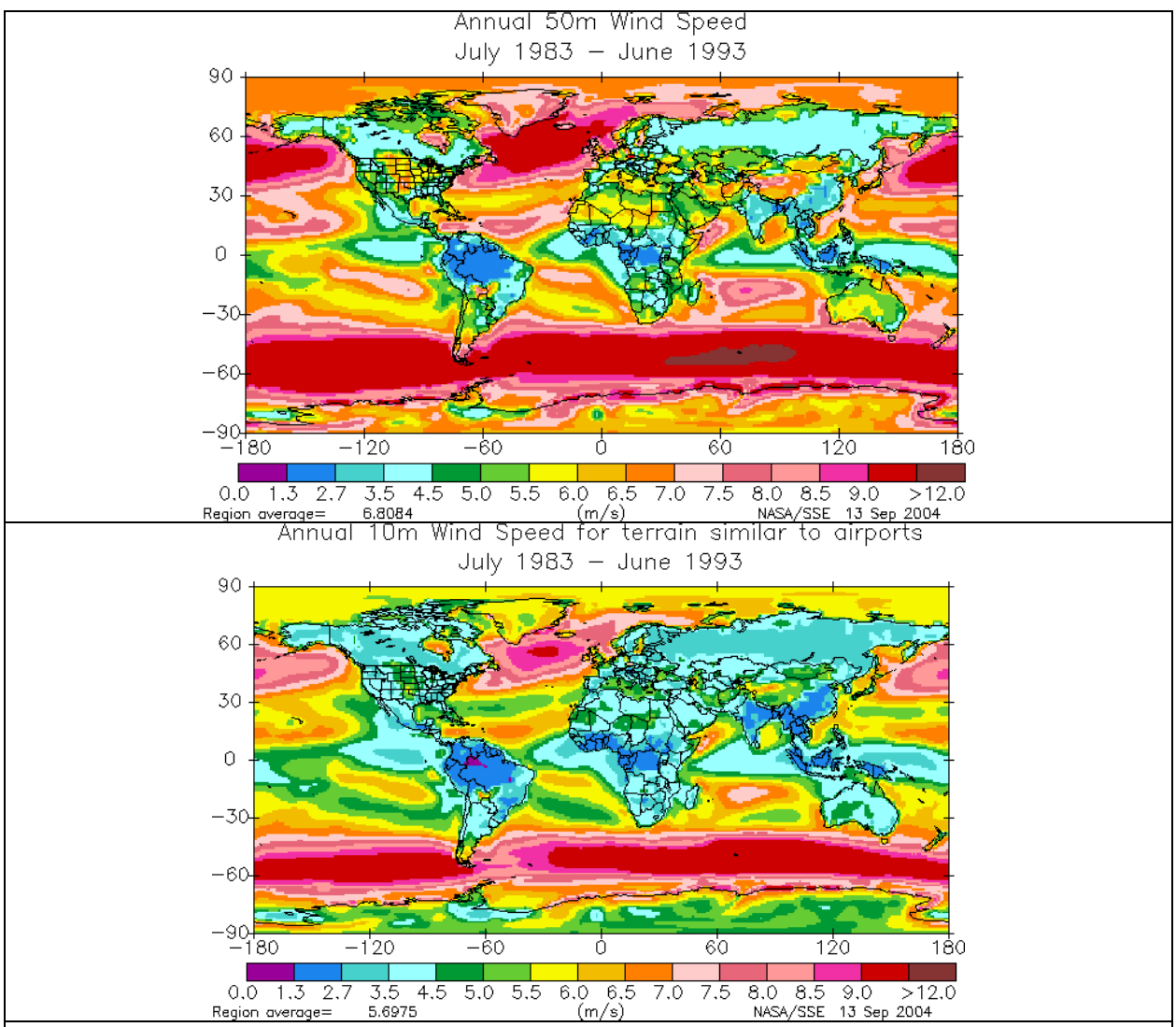


Figure VII.E.2. POWER/Building estimates of wind velocity at 50 and 10 meters above the ground, water, or snow/ice surface.

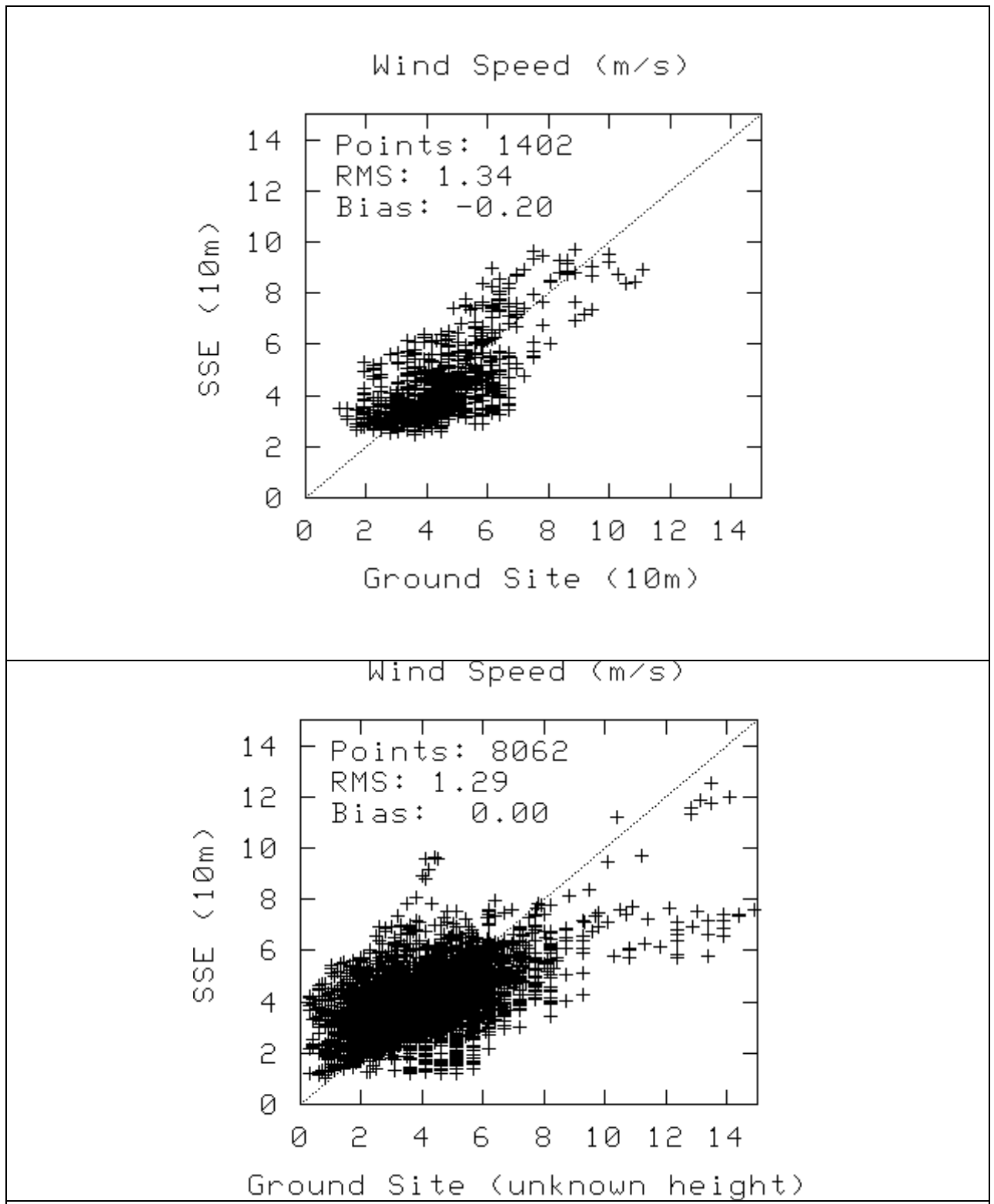


Figure VII.E.3. Comparison of monthly means based upon 10-year POWER/Building 10-m wind speed with monthly means based upon 30-year RETScreen site data. (Note that the SSE and Building values are identical.)

Northern hemisphere month	1	2	3	4	5	6	7	8	9	10	11	12
35-m broadleaf-evergreen trees (70%) small type	0.47	0.47	0.47	0.47	0.47	0.47	0.47	0.47	0.47	0.47	0.47	0.47
20-m broadleaf-deciduous trees (75%)	0.58	0.57	0.56	0.55	0.53	0.51	0.49	0.51	0.53	0.55	0.56	0.57
20-m broadleaf & needleleaf trees (75%)	0.44	0.47	0.50	0.52	0.53	0.54	0.54	0.52	0.50	0.48	0.46	0.45
17-m needleleaf-evergreen trees (75%)	0.50	0.53	0.56	0.58	0.57	0.56	0.55	0.55	0.55	0.54	0.53	0.52
14-m needleleaf-deciduous trees (50%)	0.52	0.53	0.55	0.57	0.57	0.58	0.58	0.54	0.51	0.49	0.49	0.50
18-m broadleaf trees (30%)/groundcover	0.52	0.52	0.52	0.52	0.52	0.52	0.52	0.52	0.52	0.52	0.52	0.52
0.6-m perennial groundcover (100%)	0.65	0.65	0.65	0.65	0.65	0.65	0.65	0.65	0.65	0.65	0.65	0.65
0.5-m broadleaf (variable %)/groundcover	0.65	0.65	0.65	0.65	0.65	0.65	0.65	0.65	0.65	0.65	0.65	0.65
0.5-m broadleaf shrubs (10%)/bare soil	0.65	0.65	0.65	0.65	0.65	0.65	0.65	0.65	0.65	0.65	0.65	0.65
0.6-m shrubs (variable %)/groundcover	0.65	0.65	0.65	0.65	0.65	0.65	0.65	0.65	0.65	0.65	0.65	0.65
Rough bare soil	0.70	0.70	0.70	0.70	0.70	0.70	0.70	0.70	0.70	0.70	0.70	0.70
Crop: 20-m broadleaf-deciduous trees (10%) & wheat	0.64	0.62	0.69	0.57	0.57	0.57	0.57	0.57	0.57	0.59	0.61	0.63
Rough glacial snow/ice	0.57	0.59	0.62	0.64	0.64	0.64	0.64	0.64	0.62	0.59	0.58	0.57
Smooth sea ice	0.75	0.78	0.83	0.86	0.86	0.86	0.86	0.82	0.78	0.74	0.74	0.74
Open water	0.85	0.85	0.85	0.85	0.85	0.85	0.85	0.85	0.85	0.85	0.85	0.85
"Airport": flat ice/snow	0.85	0.85	0.85	0.85	0.85	0.85	0.85	0.85	0.85	0.85	0.85	0.85
"Airport": flat rough grass	0.79	0.79	0.79	0.79	0.79	0.79	0.79	0.79	0.79	0.79	0.79	0.79

Note: 10-m and 50-m heights are above soil, water, or ice surfaces, not above the "effective" surface near the tops of vegetation.

Daily Mean Wind Speed: For the time period January 1, 1983 – December 31, 2007 the daily means winds in the POWER/Sustainable Buildings archive are from the GEOS-4 assimilation model. For the time period January 1, 2008 to within several days of current time the daily means winds are from the GEOS-5 assimilation model. The model winds are at 10m elevation above the Earth's surface. Testing of these winds was performed through comparison with wind measurements reported in the NCEI GSOD files.

GEOS-4 Winds: Comparison of ground site observation reported in the NCEI GSOD files with the 10m GEOS-4 winds for various time periods and regions have typically resulted in the GEOS-4 values being about ½ the ground observations. Table VII-E.2 gives the yearly averaged bias, RMSE, slope, intercept, and R² for a global comparisons of 2007 wind data. The last column in this table gives the total number of daily values in the comparison.

Bias	RMSE	Slope	Intercept	R²	Daily Values
0.011	1.76	0.55	1.62	0.42	1,224,453

GEOS-5 Winds: Table VIII-E.3 gives the bias, rmse, slope, intercept, R², and total number of daily values for a global comparisons of the 2009 GEOS-5 daily mean winds with values reported in the NCEI GSOD files.

Table VII-E.3 Summary of statistics for comparison of GEOS-5 10m daily winds to ground observations during 2009.					
Bias	RMSE	Slope	Intercept	R²	Daily Values
0.38	1.83	0.65	1.62	0.46	956,263

[\(Return to Content\)](#)

VII-F. Heating/Cooling Degree Days:

An important application of the historical temperature data is in the evaluation of heating degree days (HDD) and cooling degree days (CDD). The HDD and CDD are based upon the daily T_{min} and T_{max} with a base temperature, T_{base} = 18⁰C. The HDD and CDD were calculated using the following equations:

Heating Degree Days: For the days of a given time period (e.g. year, month, etc.) sum the quantity

$$[T_{base} - (T_{min} + T_{max}) / 2] \text{ when } (T_{min} + T_{max}) / 2 < T_{base}$$

Cooling Degree Days: For the days of a given time period (e.g. year, month, etc.) sum the quantity

$$[(T_{min} + T_{max}) / 2 - T_{base}] \text{ when } (T_{min} + T_{max}) / 2 > T_{base}.$$

The statistics associated with comparing the HDDs and CDDs based upon the GEOS-4 and observational temperatures are given in Table VII-F.1. The bottom row in Table VII-F.1 provides the mean estimates of the agreement between the HDDs and CDDs based assimilation and observational temperatures for the years 1983 – 2006. Values given in Table VII-F.1 used the uncorrected GEOS-4 temperatures. See Appendix A for a discussion of a methodology for correcting/downscaling assimilation model temperatures and a comparison of the statistics associated with HDDs and CDDc based upon uncorrected vs corrected GEOS-4 temperatures.

Application of the downscaling approach is only available for the SSE monthly mean temperatures over the time period July, 1983 – June, 2005,

Table VII-F.1

Comparison of yearly heating and cooling degree days: Uncorrected GEOS-4 vs ground site observations.															
Year	HDD using uncorrected GEOS-4 Temperatures vs ground site observations reported in NCDC GSOD files							CDD using uncorrected GEOS-4 Temperatures vs ground site observations reported in NCDC GSOD files							No. Stations
	Bias (HDD)	Bias (%)	RMSE (HDD)	RMSE (%)	Slope	Intercept (HDD)	Rsqd	Bias (CDD)	Bias (%)	RMSE (CDD)	RMSE (%)	Slope	Intercept (CDD)	Rsqd	
1983	16.30	6.44	68.59	27.11	1.03	9.85	0.95	-4.78	-8.93	28.53	53.34	0.86	2.68	0.92	1101
1984	16.37	6.34	64.45	24.97	1.03	8.46	0.95	-4.25	-8.35	27.01	53.07	0.86	2.86	0.92	1127
1985	16.13	6.01	64.31	23.97	1.03	9.19	0.96	-5.96	-11.21	27.82	52.33	0.85	1.80	0.92	1102
1986	14.07	5.55	85.41	33.72	0.98	18.25	0.91	-6.60	-12.50	27.73	52.56	0.84	1.91	0.93	1162
1987	14.92	5.91	69.30	27.42	1.02	10.71	0.94	-6.21	-12.01	27.17	52.52	0.85	1.76	0.93	1140
1988	15.20	6.20	65.39	26.68	1.03	6.79	0.95	-5.53	-10.10	27.39	50.05	0.86	2.22	0.93	1155
1989	14.71	5.85	66.75	26.54	1.03	7.55	0.95	-6.29	-11.91	29.02	54.96	0.84	2.35	0.91	1194
1990	16.84	7.09	66.45	27.97	1.04	7.67	0.95	-6.63	-11.92	28.70	51.60	0.83	2.66	0.93	1258
1991	14.69	6.03	78.74	32.33	1.01	11.89	0.92	-6.93	-11.60	30.28	50.71	0.84	2.59	0.92	1223
1992	12.94	5.19	79.58	31.91	1.00	12.11	0.92	-4.94	-10.62	25.52	54.79	0.86	1.80	0.92	1373
1993	17.79	6.94	71.34	27.83	1.03	10.14	0.94	-5.32	-9.97	26.29	49.30	0.88	1.10	0.93	1477
1994	22.88	9.24	72.22	29.17	1.05	11.59	0.95	-6.12	-10.75	27.96	49.09	0.87	1.36	0.93	1508
1995	17.54	7.10	70.60	28.60	1.03	9.83	0.95	-5.38	-9.13	28.04	47.55	0.87	2.28	0.93	1311
1996	10.15	4.64	99.68	45.60	0.93	25.32	0.84	-6.66	-10.70	30.31	48.68	0.86	2.09	0.92	1216
1997	19.61	8.56	62.21	27.16	1.05	7.08	0.95	-6.39	-11.33	28.24	50.06	0.85	2.02	0.92	1497
1998	24.65	11.56	68.35	32.06	1.09	5.74	0.94	-5.19	-8.91	27.48	47.17	0.87	2.30	0.93	1487
1999	18.58	8.53	61.38	28.18	1.06	6.22	0.95	-3.92	-6.53	28.87	48.11	0.88	3.01	0.92	1832
2000	17.61	7.32	66.54	27.67	1.05	6.15	0.95	-3.23	-6.06	27.74	52.00	0.88	3.06	0.92	2324
2001	24.33	9.94	64.77	26.46	1.06	8.60	0.96	-7.08	-12.74	30.00	53.97	0.84	1.75	0.92	1799
2002	16.62	6.92	67.75	28.22	1.03	9.73	0.94	-7.95	-13.80	29.96	52.00	0.83	1.58	0.92	2382
2003	14.75	6.24	66.15	27.96	1.04	6.33	0.94	-5.84	-9.97	30.91	52.77	0.85	3.23	0.91	2676
2004	16.52	6.87	90.29	37.56	1.00	17.33	0.90	-6.14	-11.66	27.97	53.10	0.84	2.19	0.92	2704
2005	20.40	8.32	66.41	27.07	1.05	7.56	0.95	-5.80	-9.96	29.13	49.99	0.86	2.39	0.93	3020
2006	16.56	6.76	126.66	51.69	0.91	39.49	0.81	-4.88	-8.89	29.25	53.28	0.87	2.44	0.92	3077
Mean of individual years	17.09	7.07	73.47	30.33	1.02	11.40	0.93	-5.75	-10.40	28.39	51.37	0.86	2.23	0.92	

[\(Return to Content\)](#)

VII. G. Surface Pressure: Recognizing that improvement in the GEOS-4 temperatures can be achieved through adjustments associated with differences in the average elevation of the GEOS-4 1-degree cell and that of the ground site of interest suggest that other altitude dependent parameters, such as pressure, might also benefit in similar altitude related adjustments. Figures VII-G.1 (a-c) illustrate significant improvements in the GEOS-4 surface pressure values (p) by using the hypsometric equation (VII-G.1), relating the thickness (h) between two isobaric surfaces to the mean temperature (T) of the layer.

$$(VII-G.1) \quad h = z_1 - z_2 = (RT/g)\ln(p_1/p_2) \text{ where:}$$

z_1 and z_2 are the geometric heights at p_1 and p_2 ,
 R = gas constant for dry air, and
 g = gravitational constant.

Figure VII-G.1a shows the scatter plot of the GEOS-4 pressure at 2-meters versus the observations reported in the NCEI archive for 2004. Figure VII-G.1b shows the agreement with the application of equation 1, using the 2m daily mean temperature with no correction to the GEOS-4 temperatures (e.g. no lapse rate or offset correction). Figure VII-G.1c shows the scatter plot where the GEOS-4 surface pressure and temperature have been corrected for elevation

differences. Clearly, adjustment to the GEOS-4 surface pressures using equation 1 results in significant improvements to the estimates of the NCEI station pressures.

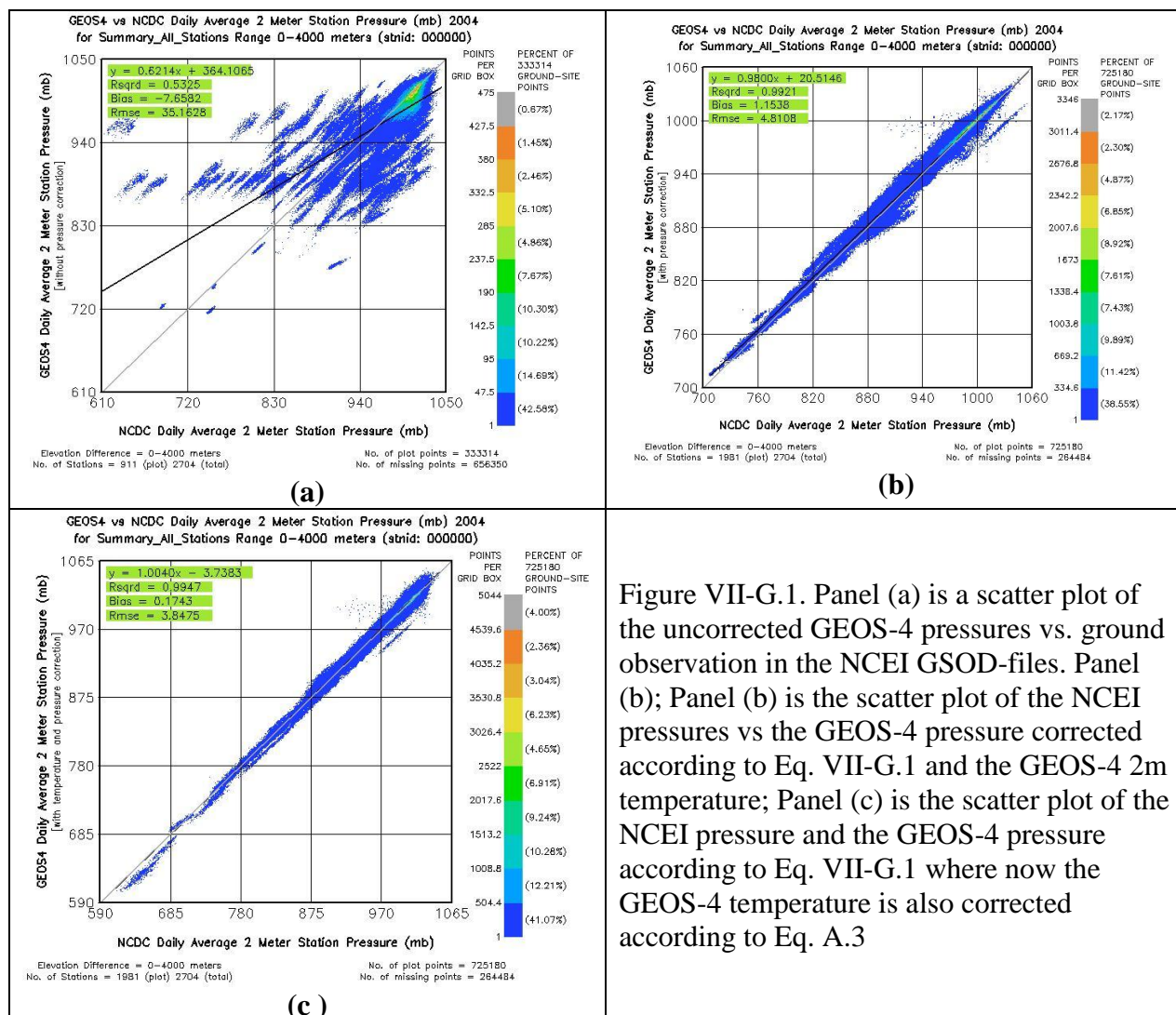


Figure VII-G.1. Panel (a) is a scatter plot of the uncorrected GEOS-4 pressures vs. ground observation in the NCEI GSOD-files. Panel (b); Panel (b) is the scatter plot of the NCEI pressures vs the GEOS-4 pressure corrected according to Eq. VII-G.1 and the GEOS-4 2m temperature; Panel (c) is the scatter plot of the NCEI pressure and the GEOS-4 pressure corrected according to Eq. VII-G.1 where now the GEOS-4 temperature is also corrected according to Eq. A.3

[\(Return to Content\)](#)

VIII. References

- Adler, R.F., G.J. Huffman, A. Chang, R. Ferraro, P. Xie, J. Janowiak, B. Rudolf, U. Schneider, S. Curtis, D. Bolvin, A. Gruber, J. Susskind, P. Arkin, E. Nelkin 2003: The Version 2 Global Precipitation Climatology Project (GPCP) Monthly Precipitation Analysis (1979-Present). *J. Hydrometeor.*, **4**, 1147-1167.
- Bai, J., X. Chen, A. Dobermann, H. Yang, K.G. Cassman, and F. Zhang. 2010. Evaluation of NASA satellite- and model-derived weather data for simulation of maize yield potential in China. *Agron. J.* 102:9–16. doi:10.2134/agronj2009.0085
- Barry, R. G. and R. J. Chorley, 1987: *Atmosphere, Weather, and Climate*. 5th ed. Methuen, 460
- Blandford, Troy R., Karen S. Blandford, Bruan J. Harshburger, Brandon C. Moore, and Von P. Walden. Seasonal and Synoptic Variations in near-Surface Air Temperature Lapse Rates in a Mountainous Basin. *J. Applied Meteorology and Climatology*. 2008, Vol. 47, 249 – 261.
- Bloom, S., A. da Silva, D. Dee, M. Bosilovich, J.-D. Chern, S. Pawson, S. Schubert, M. Sienkiewicz, I. Stajner, W.-W. Tan, M.-L. Wu, Documentation and Validation of the Goddard Earth Observing System (GEOS) Data Assimilation System - Version 4, Technical Report Series on Global Modeling and Data Assimilation, NASA/TM—2005–104606, Vol. 26, 2005
- Bolvin, David T., Robert F. Adler, George J. Huffman, Eric J. Nelkin, Jani P. Poutiainen, 2009: Comparison of GPCP Monthly and Daily Precipitation Estimates with High-Latitude Gauge Observations. *J. Appl. Meteor. Climatol.*, **48**, 1843–1857. doi: 10.1175/2009JAMC2147.1
- Braun, J. E. and J. C. Mitchell, 1983: Solar Geometry for Fixed and Tracking Surfaces. *Solar Energy*, Vol. 31, No. 5, pp. 439-444.
- Briggs, Robert S., R. G. Lucas, Z. T. Taylor, 2003: Climate Classification for Building Energy Codes and Standards. Technical Paper, Pacific NW National Laboratory, March 26, 2002. Continue to use original climate zone definitions.
- Collares-Pereira, M. and A. Rabl, 1979: The Average Distribution of Solar Radiation- Correlations Between Diffuse and Hemispherical and Between Daily and Hourly Insolation Values. *Solar Energy*, Vol. 22, No. 1, pp. 155-164.
- Dorman, J. L. and P. J. Sellers, 1989: A Global Climatology of Albedo, Roughness Length and Stomatal Resistance for Atmospheric General Circulation Models as Represented by the Simple Biosphere Model (SiB). *Journal of Atmospheric Science*, Vol. 28, pp. 833-855.
- Encyclopedia of Agricultural, Food, and Biological Engineering edited by Dennis R. Heldman
Page 189

Erbs, D. G., S. A. Klein, and J. A. Duffie, 1982: Estimation of the Diffuse Radiation Fraction for Hourly, Daily and Monthly average Global Radiation. *Solar Energy*, Vol. 28, No. 4, pp. 293-302.

Flatau, J. Piotr, Robert L. Walko, and William R. Cotton, 1992: *Polynomial Fits to Saturation Vapor Pressure*. Notes and Correspondence, *Journal of Applied Meteorology*. 1507-1513.

Gipe, Paul, 1999: *Wind Energy Basics*, Chelsea Green Publishing, 122 pp.

Gupta, S. K., D. P. Kratz, P. W. Stackhouse, Jr., and A. C. Wilber, 2001: The Langley Parameterized Shortwave Algorithm (LPSA) for Surface Radiation Budget Studies. NASA/TP-2001-211272, 31 pp. Available on-line at: <http://ntrs.nasa.gov/search.jsp>

Harlow, R. C., E. J. Burke, R. L. Scott, W. J. Shuttleworth, C. M. Brown, and J. R. Petti. Derivation of temperature lapse rates in semi-arid south-eastern Arizona, (2004) *Hydrol. and Earth Systems Sci*, 8(6) 1179-1185.

Iribarne, J.V. and W.L. Godson, 1981: *Atmospheric Thermodynamics*. Geophysics and Astrophysics Monographs, D. Riedel Publishing Company, Dordrecht, Netherlands.

Jupp, D. L. B.; 2003, Calculating and converting between common water vapour measures in meteorological data and their use in support of earth observation validation, CSIRO Earth Observation Centre Technical Report, 2003/01.

Klein, S.A., 1977: Calculation of monthly average insolation on tilted surfaces. *Solar Energy*, Vol. 19, pp. 325-329.

Liu, B. Y. H. and R. C. Jordan, 1960: The Interrelationship and Characteristic Distribution of Direct, Diffuse, and Total Solar Radiation. *Solar Energy*, Vol. 4, No. 3, pp. 1-19.

Lookingbill, Todd R. and Dean L. Urban, Spatial estimation of air temperature differences for landscape-scale studies in mountain environments, (2003) *Agri. and Forst. Meteor*, 114(3-4) 141-151.

McPhee, James, Steven A. Margulis, 2005: Validation and Error Characterization of the GPCP-1DD Precipitation Product over the Contiguous United States. *J. Hydrometeor*, **6**, 441-459. doi: 10.1175/JHM429.1

Ohmura, Atsumu, Ellsworth G. Dutton, Bruce Forgan Claus Fröhlich Hans Gilgen, Herman Hegner, Alain Heimo, Gert König-Langlo, Bruce McArthur, Guido Mueller, Rolf Philipona, Rachel Pinker, Charlie H. Whitlock, Klaus Dehne, and Martin Wild, 1998: Baseline Surface

Ohmura, A., E. Dutton, B. Forgan, C. Frohlich, H. Gilgen, H. Hegne, A. Heimo, G. König-Langlo, B. McArthur, G. Muller, R. Philipona, C. Whitlock, K. Dehne, and M. Wild, 1998: Baseline Surface Radiation Network (BSRN/WCRP): New precision radiometry for climate change research. *Bull. Amer. Meteor. Soc.* 79 No. 10, 2115-2136

Pinker, R., and I. Laszlo, 1992: Modeling Surface Solar Irradiance for Satellite Applications on a Global Scale. *J. Appl. Meteor.*, 31, 194–211.

Radiation Network (BSRN/WCRP): New Precision Radiometry for Climate Research, *Bull. Of American Meteor. Soc.*, **79**, 10, p 2115-2136.

RETScreen: Clean Energy Project Analysis: RETScreen® Engineering & Cases Textbook, Third Edition, Minister of Natural Resources Canada, September 2005.

(<http://www.retscreen.net/ang/12.php>, Engineering e-Textbook, Version 4, RETScreen Photovoltaic Project Analysis Chapter, pp. PV.15-PV.21, ISBN: 0-662-35672-1, Catalogue no.: M39-99/2003E-PDF).

Rossow, W.B., and R.A. Schiffer, 1999: Advances in understanding clouds from ISCCP. *Bull. Amer. Meteorol. Soc.*, **80**, 2261-2288, doi:10.1175/1520-0477(1999)080<2261:AIUCFI>2.0.CO;2.

Schwartz, Marc, 1999: Wind Energy Resource Estimation and Mapping at the National Renewable Energy Laboratory. NREL Conf. Pub. NREL/CP-500-26245.

Smith, G.L., R. N. Green, E. Raschke, L. M. Avis, J. T. Suttles, B. A. Wielicki, and R. Davies, 1986: Inversion methods for satellite studies of the Earth's radiation budget: Development of algorithms for the ERBE mission. *Rev. Geophys.*, 24, 407-421.

Surface Weather Observations and Reports, Federal Meteorological Handbook No. 1, FCM-H1-2005, Washington, D.C., 2005

Rasch, P. J., N. M. Mahowald, and B. E. Eaton (1997), Representations of transport, convection, and the hydrologic cycle in chemical transport models: Implications for the modeling of short-lived and soluble species, *J. Geophys. Res.*, 102(D23), 28, 127-128, 138.

Takacs, L. L., A. Molod, and T. Wang, 1994: Volume 1: Documentation of the Goddard Earth Observing System (GEOS) general circulation model - version 1, NASA Technical Memorandum 104606, Vol. 1, 100 pp.

White, Jeffrey W. , Gerrit Hoogenboom, Paul W. Stackhouse Jr., and James M. Hoell, Evaluation of NASA satellite- and assimilation model-derived long-term daily temperature data over the continental US, *Agric. Forest Meteorol.* (2008), doi:10.1016/j.agrformet.2008.05.017

White, Jeffrey W. , Gerrit Hoogenboom, Paul W. Wilkens, Paul W. Stackhouse Jr., and James M. Hoell, Evaluation of Satellite-Based, Modeled-Derived Daily Solar Radiation Data for the Continental United States. *Agron. J.* 103:1242-1251(2011)

[\(Return to Content\)](#)

Appendix A

Downscaling Assimilation Modeled Temperatures

Introduction: In section VII temperature estimates from the GEOS-4 assimilation model were found to exhibit a globally and yearly (1983 – 2006) averaged bias for Tmax of -1.82°C , for Tmin about $+0.27^{\circ}$, for Tave about -0.55°C relative to ground site observations. In this Appendix factors contributions to these biases are noted with the main focus being the description of a methodology that can reduce the biases for local ground site.

The spatial resolution of the GEOS-4 assimilation model's output is initially on a global 1° by 1.25° grid and then re-gridded to a spatial 1° by 1° grid to be spatially compatible with the solar insolation values available through the POWER archive. The elevation of original and re-gridded cell represents the average elevation of the earth's surface enclosed by the dimensions of the grid cell. Figure A.1 illustrates the spatial features associated with a reanalysis cell and a local ground site. In mountainous regions, in particular, the elevation of the grid cell can be substantially different from that of the underlying ground site.

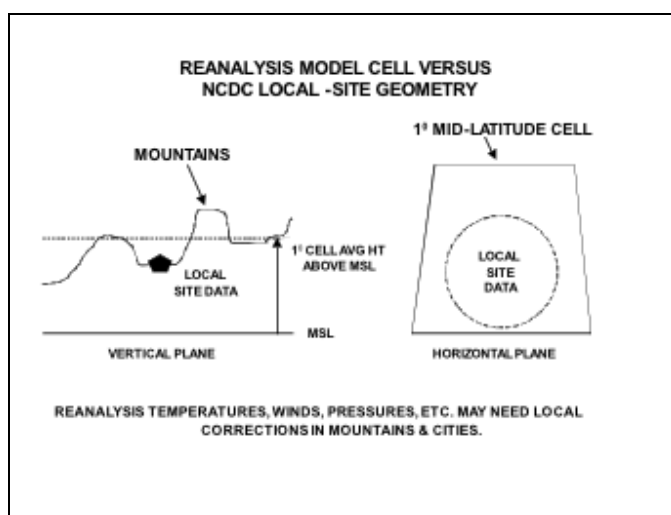


Figure A.1: Relative height and horizontal features associated with a nominal 1-degree cell and a local ground site in the mountains.

The inverse dependence of the air temperature on elevation is well known and suggests that the elevation differences between the re-analysis grid cell and the actual ground site may be a factor contributing to the biases between the modeled and observed temperatures. In figure A-2, the yearly averaged differences between ground site measurements and reanalysis modeled values (i.e. bias) are plotted against the difference in the elevation of the ground site and the reanalysis grid for the ensemble of years 1983 – 2006. The stations have been grouped into 50m elevation difference bins (e.g. 0 to 50m; >50m to 100m; >100m to 150m; etc.) and plotted against the mean yearly bias for the respective elevation bin.

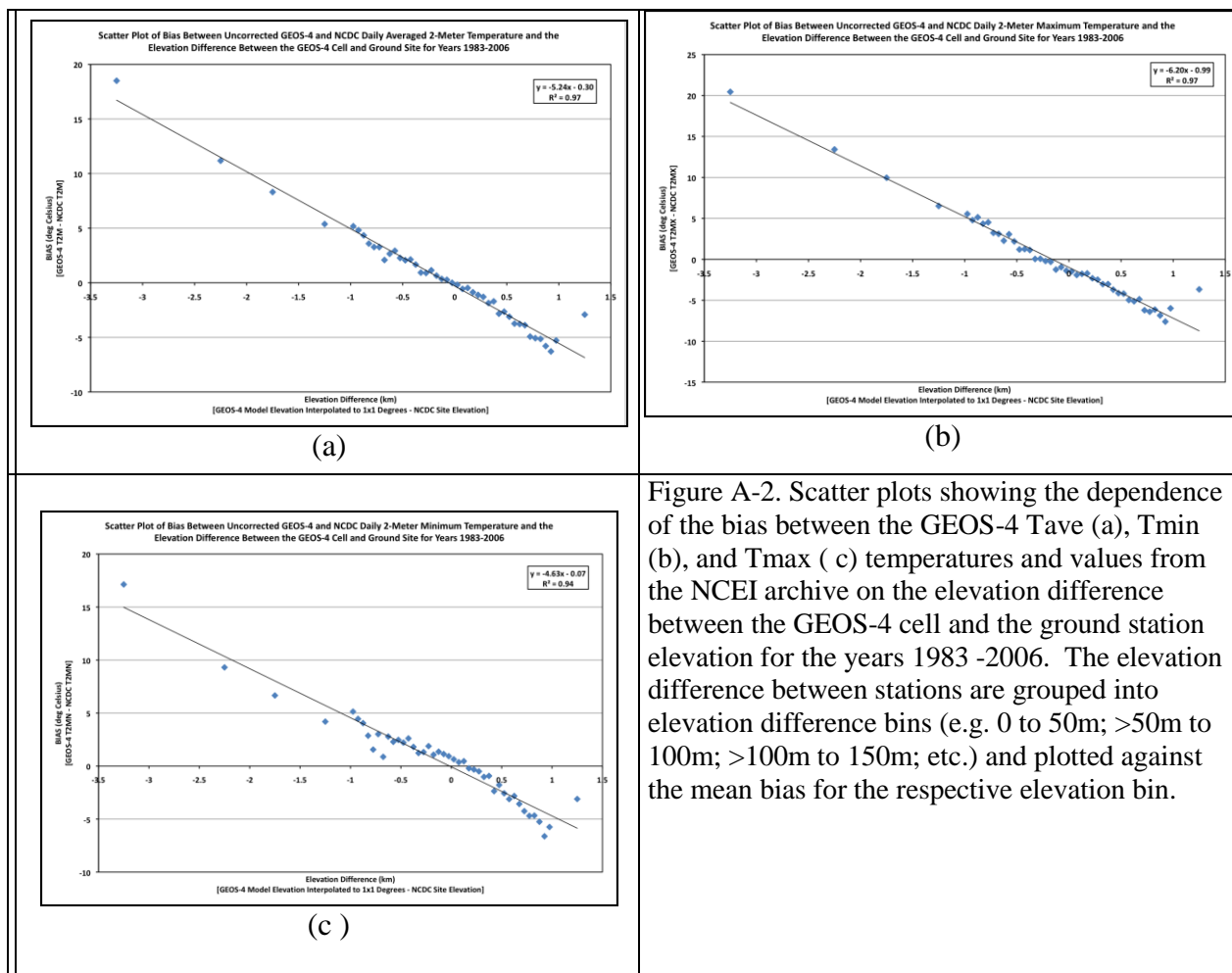


Figure A-2. Scatter plots showing the dependence of the bias between the GEOS-4 Tave (a), Tmin (b), and Tmax (c) temperatures and values from the NCEI archive on the elevation difference between the GEOS-4 cell and the ground station elevation for the years 1983 -2006. The elevation difference between stations are grouped into elevation difference bins (e.g. 0 to 50m; >50m to 100m; >100m to 150m; etc.) and plotted against the mean bias for the respective elevation bin.

The solid line is the linear least squares fit to the scatter plot and the parameters for the fit are given in the upper right hand portion of each plot. Table A-1 gives the parameters associated with linear regression fits to similar scatter plots for individual years and is included here to illustrate the year-to-year consistency in these parameters. The linear dependence of the bias between the GEOS-4 and NCEI temperature values on the elevation difference between the GEOS-4 cell and ground elevation is clearly evident in Figure A-2 and Table A-1. The mean of the slope, intercept, and R^2 for the individual years is given in the row labeled "Average". The bottom row of Table A-1 lists the fit parameters of Figure A-2.

Table A.1. Linear regression parameters associated with scatter plots of GEOS-4 yearly mean bias relative to ground site observations for individual years from 1983 - 2006. The bottom row gives the parameters for the scatter plots of Figure A.2.

Year	Tmax			Tmin			Tave		
	Slope	Intercept	R ²	Slope	Intercept	R ²	Slope	Intercept	R ²
	(C/km)	(C)		(C/km)	(C)		(C/km)	(C)	
1983	-6.2	-0.5	0.74	-4.4	0.4	0.87	-5.2	0.1	0.83
1984	-6.2	-0.6	0.72	-4.3	0.3	0.75	-5.2	0.0	0.79
1985	-6.8	-0.9	0.94	-4.7	0.1	0.77	-5.9	-0.1	0.95
1986	-6.6	-0.7	0.88	-4.3	0.3	0.82	-5.5	0.1	0.91
1987	-6.3	-1.0	0.92	-4.9	0.4	0.83	-5.5	0.0	0.95
1988	-6.2	-0.7	0.76	-4.0	0.5	0.68	-5.0	0.2	0.75
1989	-6.0	-1.0	0.77	-3.4	0.1	0.55	-4.5	-0.2	0.72
1990	-6.6	-0.8	0.9	-4.4	0.2	0.83	-5.4	0.1	0.88
1991	-6.1	-0.8	0.9	-4.4	0.3	0.88	-5.2	0.1	0.9
1992	-6.2	-0.8	0.93	-4.6	0.4	0.88	-5.2	0.0	0.93
1993	-6.1	-0.9	0.92	-5.0	0.2	0.93	-5.4	0.0	0.95
1994	-6.2	-1.0	0.92	-5.4	-0.1	0.92	-5.6	-0.2	0.95
1995	-5.9	-1.3	0.91	-5.4	0.6	0.94	-5.5	-0.1	0.95
1996	-5.3	-0.6	0.79	-4.8	0.7	0.89	-4.9	0.3	0.86
1997	-6.2	-0.8	0.94	-5.2	0.2	0.95	-5.5	-0.1	0.96
1998	-6.0	-0.9	0.9	-4.9	0.3	0.93	-5.2	-0.1	0.94
1999	-6.2	-0.9	0.94	-4.9	0.5	0.95	-5.3	0.0	0.96
2000	-6.2	-1.1	0.97	-5.0	-0.1	0.93	-5.4	-0.4	0.97
2001	-5.7	-1.4	0.9	-5.0	0.0	0.85	-5.3	-0.5	0.93
2002	-6.2	-1.1	0.97	-4.6	-0.1	0.92	-5.2	-0.4	0.97
2003	-6.1	-1.0	0.97	-4.4	-0.2	0.91	-5.1	-0.4	0.97
2004	-6.3	-0.9	0.98	-4.6	-0.2	0.94	-5.3	-0.4	0.98
2005	-6.1	-1.3	0.97	-4.6	-0.1	0.93	-5.2	-0.5	0.97
2006	-5.7	-1.3	0.95	-4.6	-0.4	0.92	-5.0	-0.6	0.96
Average	-6.1	-0.9	0.90	-4.6	0.2	0.87	-5.3	-0.1	0.91
STDEV	0.3	0.2	0.08	0.4	0.3	0.10	0.3	0.2	0.07
All Years Regression Analysis	-6.2	-1.0	0.97	-4.6	-0.1	0.94	-5.2	-0.3	0.97

As already noted, the inverse dependence of the air temperature on elevation is well known with $-6.5^{\circ}\text{C}/\text{km}$ typically accepted as a nominal global environmentally averaged lapse rate value (Barry and Chorley 1987). Moreover, numerous studies have been published (Blandford et al., 2008; Lookingbill et al., 2003; Harlow et al., 2004) that highlight the need to use seasonal and regionally dependent lapse rates for the daily Tmin and Tmax values to adjust ground site observations to un-sampled sites at different elevations. In the remaining sections an approach to statistically calibrate the assimilation model and downscale the reanalysis temperatures to a specific site within the reanalysis grid box is described.

[\(Return to Content\)](#)

A-1. Downscaling Methodology : Figure A-2 illustrates the linear dependence of the bias between the GEOS-4 temperatures and elevation differences between reanalysis grid cell and the ground site elevation. In this section a mathematical procedure is developed for statistically calibrating the GEOS-4 model relative to ground site observations resulting parameters that allow downscaled estimates of the reanalysis temperatures at localized ground sites site values. In subsequent sections the validity of the downscaling approach will demonstrated. The downscaling discussed in this and subsequent sections is only available through the POWER/Building archive with application to the monthly mean temperatures over the time period January 1, 1983 – December 31, 2007.

If we assume that the reanalysis modeled temperatures estimates can in fact be downscaled based upon a lapse rate correction, then we can express the downscaled temperatures at a local ground site as

$$\text{Eq. A-1.} \quad (T^{\text{grd}})_{\text{RA}} = (T^{\text{nat}})_{\text{RA}} + \lambda*(H_{\text{grd}} - H_{\text{RA}}) + \beta$$

Where $(T^{\text{grd}})_{\text{RA}}$ is the downscaled reanalysis temperature, $(T^{\text{nat}})_{\text{RA}}$ is the native reanalysis value averaged over the reanalysis grid cell, λ is the seasonal/regional lapse rate (C/km) appropriate for the given ground site, H_{grd} and H_{RA} are the elevation for ground site and reanalysis grid cell respectively, and β is included to account for possible biases between the reanalysis model estimates and ground observations. Assuming that Eq. A-1 provides an accurate estimate of the air temperature we have

$$\text{Eq. A-2.} \quad (T^{\text{grd}}) = (T^{\text{grd}})_{\text{RA}},$$

where (T^{grd}) is the air temperature at the desired ground site.

Equation Eq. A-1 and Eq. A-2 can be combined to yield

$$\text{Eq. A-3.} \quad (T^{\text{grd}}) = (T^{\text{nat}})_{\text{RA}} + \lambda*(H_{\text{grd}} - H_{\text{RA}}) + \beta$$

or

$$\text{Eq. A-4.} \quad \Delta T = \lambda*\Delta H + \beta$$

where ΔT is the differences between the air temperature at desired ground site and reanalysis cell temperature or Bias, and ΔH is the difference between the elevation of the ground site and the model cell. Equation Eq. A-4 gives a linear relation between ΔT and ΔH with the slope given by λ , the lapse rate, and an intercept value given by β . A linear least squares fit to a scatter plot of ΔT vs ΔH (i.e. Figure A-2) yields λ , the lapse rate, and β , the model bias. These parameters can then be used to downscale the reanalysis temperature values to any ground site within a region that the λ and β values are valid. Note that this methodology lends itself to generating λ and β

values averaged over any arbitrary time period and/or investigating other environmental factors such as the influence of the vegetation type on the downscaling methodology.

The scatter plots shown in Figure A-2 are constructed using the yearly mean bias between GEOS-4 and NCEI temperatures (i.e. ΔT) vs the difference in the elevation between the GEOS-4 grid cell and the ground site (i.e. ΔH). Consequently, from Eq. A-4 the slope and intercept associated with the linear fit to the scatter plot give a set of globally averaged λ and β parameters for downscaling the reanalysis temperatures T_{ave} , T_{min} , and T_{max} to any geographical site. Table A-2 summarizes the values for λ (e.g. lapse rate) and β (e.g. offset) based upon the use of the NCEI GSOD meteorological data as the “calibration” source. The values given in Table A.2 are based upon the globally distributed ground sites in the NCEI GSOD data base, and are based upon yearly mean ground and GEOS-4 data.

Table A-2. Globally and yearly and averaged lapse rate and offset values for adjusting GEOS-4 temperatures to local ground site values (based upon 1983 – 2006 NCEI and GEOS-4 global data).		
	Lapse Rate ($^{\circ}\text{C}/\text{km}$)	Off Set ($^{\circ}\text{C}$)
Tmax	-6.20	-0.99
Tmin	-4.63	-0.07
Tave	-5.24	-0.30

Figure A-3 illustrates that bias between the ground observations and the GEOS-4 values after applying the lapse rate correction and offset values given in Table A-2 is independent of the elevation difference between the ground site and the GEOS-4 1-degree cell and that the average bias is also near zero.

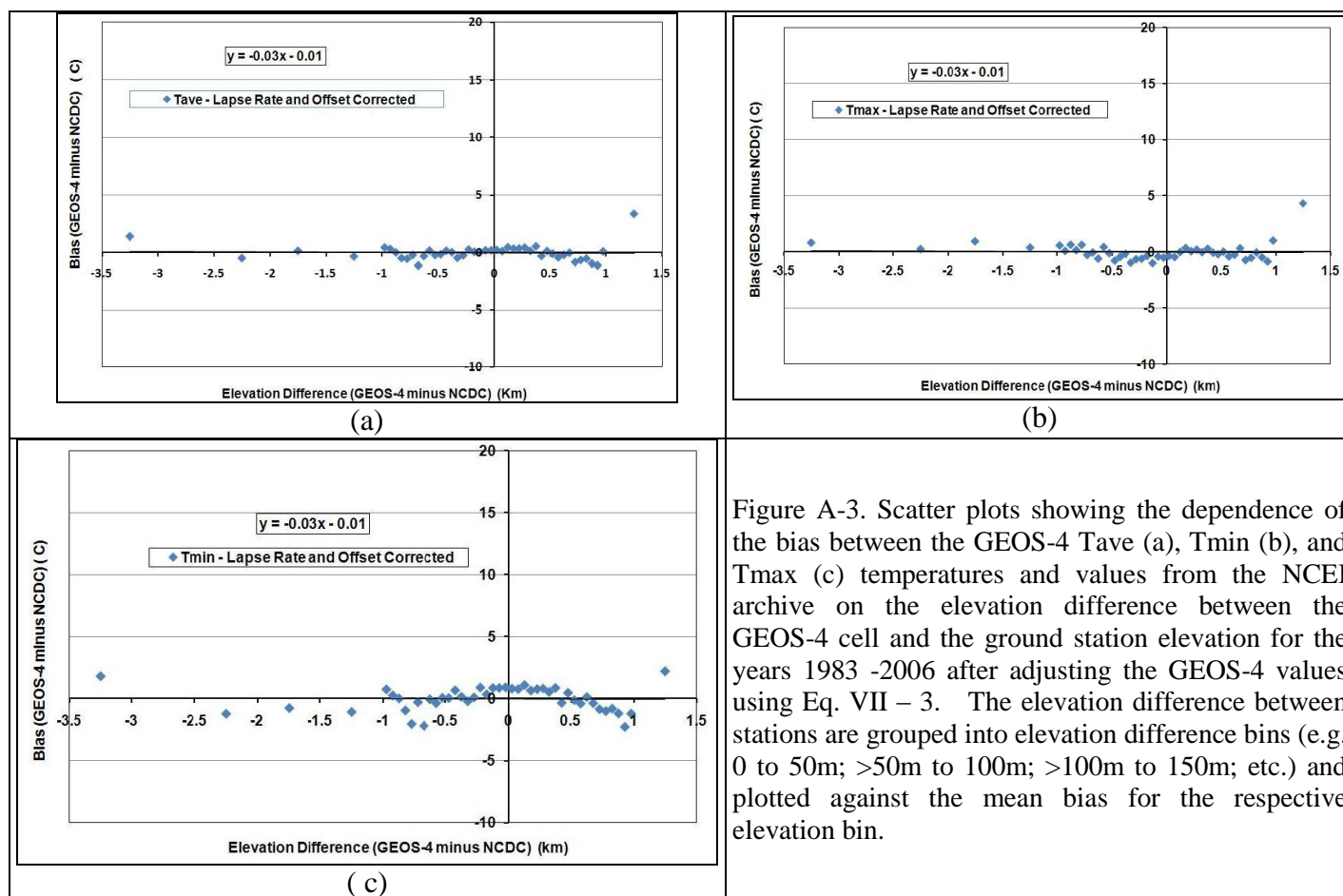


Figure A-3. Scatter plots showing the dependence of the bias between the GEOS-4 Tave (a), Tmax (b), and Tmin (c) temperatures and values from the NCEI archive on the elevation difference between the GEOS-4 cell and the ground station elevation for the years 1983 -2006 after adjusting the GEOS-4 values using Eq. VII – 3. The elevation difference between stations are grouped into elevation difference bins (e.g. 0 to 50m; >50m to 100m; >100m to 150m; etc.) and plotted against the mean bias for the respective elevation bin.

[\(Return to Content\)](#)

Global Downscaling: Table A-3 gives the yearly mean global MBE and RMSE of the native (i.e. un-corrected) and downscaled GEOS-4 temperature values relative to NCEI values for the year 2007. The 2007 GEOS-4 values were downscaled via Eq. A-3 using the lapse rate and offset parameters given in Table A-2. Since the λ and β parameters for downscaling were developed using NCEI data over the years 1983 – 2006, the use of data from 2007 serves as an independent data set for this test.

Table A-3. Globally and yearly averaged Mean Bias Error (MBE) and Root Mean Square Error (RMSE) for 2007 un-corrected and downscaled GEOS-4 temperatures relative to NCEI temperatures. The downscaled GEOS-4 values are based upon the downscaling parameters given in Table A-2 .			
		Un-corrected GEOS-4	Downscaled GEOS-4
Tmax	MBE	-1.58	-0.10
	RMSE	3.79	3.17
Tmin	MBE	0.27	0.71
	RMSE	3.57	3.42

Tave	MBE	-0.50	0.22
	RMSE	2.82	2.47

Note that the lapse rates and offset values given in Table A-2 are yearly averaged values based upon globally distributed ground sites in the NCEI data base. Results from a number of studies have indicated that tropospheric lapse rates can be seasonally and regionally dependent. Table A-4 gives the globally and monthly averaged lapse rate and offset downscaling parameters for GEOS-4 temperatures. These parameters were developed from eq. Eq. A-4 using the monthly averaged temperature data over the years 1983 – 2006 in global distribution of GEOS-4 and NCEI. Tables A-5 and A-6 give respectively the globally and monthly averaged MBE and RMSE of the 2007 GEOS-4 temperatures relative to NCDC ground site values for the unadjusted and downscaled respectively.

Table A-4. Globally and monthly averaged lapse rates and offset values for adjusting GEOS-4 temperatures to local ground site values. Based upon 1983 – 2006 NCEI and GEOS-4 global data.													
	JAN	FEB	MAR	APR	MAY	JUN	JUL	AUG	SEP	OCT	NOV	DEC	YR
Tmx λ	-5.12	-5.97	-6.73	-7.2	-7.14	-6.78	-6.52	-6.44	-6.31	-5.91	-5.44	-4.85	-6.22
Tmx β	-1.61	-1.57	-1.4	-1.01	-0.56	-0.29	-0.24	-0.46	-0.67	-1.08	-1.44	-1.55	-0.99
Tmn λ	-4.34	-4.89	-5.17	-5.16	-4.93	-4.67	-4.46	-4.33	-4.28	-4.31	-4.6	-4.44	-4.63
Tmn β	-0.96	-0.95	-0.69	-0.14	0.22	0.34	0.43	0.5	0.58	0.42	-0.06	-0.61	-0.07
Tm λ	-4.49	-5.19	-5.73	-6.06	-5.91	-5.59	-5.35	-5.27	-5.14	-4.9	-4.8	-4.45	-5.24
Tm β	-1.16	-1.09	-0.9	-0.34	0.17	0.42	0.51	0.35	0.13	-0.18	-0.61	-0.97	-0.3

Table A-5. Globally and monthly averaged MBE and RMSE values associated with unadjusted 2007 GEOS-4 temperatures relative to 2007 NCEI GSOD temperatures.													
	JAN	FEB	MAR	APR	MAY	JUN	JUL	AUG	SEP	OCT	NOV	DEC	YR
Tmax MBE	-2.00	-2.11	-2.00	-1.64	-1.13	-1.15	-0.84	-1.27	-1.49	-1.85	-1.73	-1.90	-1.89
Tmax RMSE	4.04	4.00	4.01	3.75	3.73	3.64	3.57	3.64	3.66	3.72	3.71	4.02	3.79
Tmin MBE	-0.24	-0.49	-0.23	0.19	0.56	0.49	0.66	0.61	0.81	0.76	0.50	-0.41	0.27
Tmin RMSE	4.13	4.02	3.70	3.32	3.25	3.09	3.10	3.13	3.30	3.50	3.84	4.26	3.55
Tave MBE	-1.0	-1.15	-0.88	-0.54	-0.03	-0.06	-0.13	-0.18	-0.15	-0.43	-0.59	-1.08	-0.50
Tave RMSE	3.20	3.18	2.92	2.62	2.66	2.54	2.55	2.50	2.51	2.56	2.91	3.41	2.80

Table A-6. Globally averaged monthly MBE and RMSE associated with downscaled 2007 temperatures relative to 2007 NCEI GSOD temperatures. The GEOS-4 temperatures were downscaled using the globally and monthly averaged λ and β values given in Table A-4.

	JAN	FEB	MAR	APR	MAY	JUN	JUL	AUG	SEP	OCT	NOV	DEC	YR
Tmax MBE	0.04	-0.07	-0.04	-0.06	0.00	-0.32	-0.08	-0.30	-0.32	-0.29	0.14	0.04	-0.10
Tmax RMSE	3.35	3.11	3.17	2.97	3.18	3.16	3.18	3.13	3.02	2.98	3.06	3.40	3.14
Tmin MBE	1.06	0.85	0.87	0.74	0.74	0.52	0.59	0.45	0.57	0.69	0.92	0.56	0.71
Tmin RMSE	4.11	3.87	3.54	3.13	2.99	2.83	2.86	2.87	3.01	3.26	3.71	4.12	3.36
Tave MBE	0.52	0.33	0.48	0.28	0.27	-0.04	0.04	-0.11	0.13	0.14	0.41	0.25	0.22
Tave RMSE	2.94	2.69	2.44	2.11	2.22	2.18	2.24	2.16	2.12	2.20	2.61	3.06	2.41

[\(Return to Content\)](#)

Regional Downscaling: Eq. A-4 can also be used to develop regional specific λ and β values which, for some applications, may be more appropriate than the yearly (Table A-3) or monthly and globally averaged (Table A-4) values. As an example, Table A-7 gives the regionally and monthly averaged λ and β values for Tmax, Tmin, and Tave along with the regionally yearly averaged values for the Pacific Northwest region (40 - 50N, 125 - 110W). These values were developed via Eq. 4 for the US Pacific Northwest using GEOS-4 and NCEI GSOD temperatures over the years from 1983 through 2006.

Table A-7. Regional and monthly averaged lapse rate and offset values for adjusting GEOS-4 temperatures to local ground site values Based upon 1983 - 2006 NCEI and GEOS-4 temperatures in the US Pacific Northwest region.

	JAN	FEB	MAR	APR	MAY	JUN	JUL	AUG	SEP	OCT	NOV	DEC	YR
Tmx λ	-5.13	-6.22	-7.54	-7.88	-7.09	-6.61	-6.29	-5.87	-6.09	-5.83	-5.56	-4.69	-6.23
Tmx β	-1.47	-1.69	-1.63	-1.55	-1.23	-1.12	-1.03	-1.64	-1.82	-2.15	-1.74	-1.09	-1.51
Tmn λ	-5.55	-6.46	-6.68	-6.06	-5.53	-5.64	-5.25	-4.77	-4.7	-4.64	-5.54	-5.37	-5.51
Tmn β	-0.9	-0.69	-0.12	0.31	0.48	0.78	1.36	1.43	1.31	0.81	0.31	-0.68	0.37
Tm λ	-5.35	-6.38	-7.11	-7.26	-6.55	-6.27	-5.87	-5.54	-5.58	-5.39	-5.55	-5.02	-5.98
Tm β	-0.81	-0.7	-0.48	-0.06	0.4	0.7	0.97	0.58	0.2	-0.19	-0.32	-0.61	-0.02

The MBE and RMSE of the unadjusted 2007 GEOS-4 temperatures in the US Pacific Region relative to the ground observations are given in Table A-8, and for comparison the MBE and RMSE associated with the downscaled 2007 GEOS-4 temperatures are given in Table A-9. The

downscaled temperatures are based upon Eq. 3 using the regional λ and β values given in Table 7.

Table A-8. Regional monthly MBE and RMSE values associated with unadjusted 2007 GEOS-4 temperatures in the US Pacific region relative to 2007 NCEI GSOD temperatures													
	JAN	FEB	MAR	APR	MAY	JUN	JUL	AUG	SEP	OCT	NOV	DEC	YR
Tmax MBE	-3.05	-3.41	-4.47	-3.96	-3.10	-3.47	-2.74	-3.23	-3.58	-3.77	-3.25	-3.18	-3.43
Tmax RMSE	5.06	5.11	5.78	5.34	5.06	5.18	4.85	5.28	5.63	5.36	4.99	4.76	5.20
Tmin MBE	-2.59	-2.90	-2.85	-2.30	-1.51	-1.50	-0.34	-0.12	-0.39	-1.19	-1.40	-2.94	-1.67
Tmin RMSE	5.58	5.32	5.03	4.45	4.18	4.36	4.25	4.22	4.33	3.95	4.71	5.53	4.66
Tave MBE	-2.40	-2.56	-3.12	-2.59	-1.52	-1.65	-0.83	-1.15	-1.54	-1.99	-2.11	-2.79	-2.02
Tave RMSE	4.36	4.12	4.33	3.92	3.33	3.38	3.16	3.21	3.41	3.48	3.92	4.52	3.76

Table A-9. Regional monthly MBE and RMSE values associated with downscaled 2007 GEOS-4 temperatures in the US Pacific region relative to 2007 NCEI GSOD temperatures. The GEOS-4 temperatures were downscaled using the regionally and monthly averaged λ and β values for the US Pacific Region given in Table A-7.													
	JAN	FEB	MAR	APR	MAY	JUN	JUL	AUG	SEP	OCT	NOV	DEC	YR
Tmax MBE	0.28	0.54	-0.11	0.45	0.70	0.05	0.58	0.54	0.45	0.50	0.51	-0.39	0.34
Tmax RMSE	4.00	3.63	3.45	3.11	3.77	3.55	3.90	4.05	4.21	3.70	3.71	3.30	3.70
Tmin MBE	0.32	0.14	-0.32	-0.41	0.01	-0.23	0.20	0.18	0.00	-0.31	0.30	-0.32	-0.04
Tmin RMSE	4.58	3.96	3.62	3.25	3.38	3.49	3.70	3.71	3.88	3.41	4.05	4.31	3.78
Tave MBE	0.35	0.46	-0.07	0.10	0.46	-0.08	0.33	0.28	0.28	0.15	0.22	-0.36	0.18
Tave RMSE	3.41	2.81	2.42	2.09	2.36	2.32	2.58	2.47	2.49	2.45	2.91	3.25	2.63

As an additional point of comparison Table A-10 gives the MBE and RMSE values associated with downscaled 2007 GEOS-4 temperatures in the US Pacific Northwest relative to 2007 NCEI

GSOD temperatures where the globally and monthly averaged (Table 4) downscaling parameters (i.e. λ and β) have used.

Table A-10. MBE and RMSE associated with downscaled 2007 temperatures relative to 2007 NCEI GSOD temperatures in the US Pacific Northwest region (40 – 50N, 125 – 110W). The GEOS-4 temperatures were downscaled using the globally and monthly averaged λ and β values given in Table A.6													
	JAN	FEB	MAR	APR	MAY	JUN	JUL	AUG	SEP	OCT	NOV	DEC	YR
Tmax MBE	0.42	0.33	-0.63	-0.33	0.05	-0.72	-0.13	-0.43	-0.63	-0.54	0.16	0.13	-0.19
Tmax RMSE	4.02	3.60	3.48	3.08	3.71	3.62	3.86	4.05	4.24	3.71	3.67	3.28	3.69
Tmin MBE	-0.06	-0.17	-0.29	-0.29	0.05	-0.15	0.85	0.95	0.58	-0.04	0.33	-0.72	0.09
Tmin RMSE	4.61	4.02	3.67	3.28	3.41	3.55	3.85	3.85	3.95	3.41	4.10	4.40	3.84
Tave MBE	0.39	0.42	-0.15	-0.05	0.45	-0.05	0.60	0.41	0.20	-0.03	0.24	-0.20	0.18
Tave RMSE	3.42	2.82	2.44	2.13	2.37	2.34	2.64	2.50	2.50	2.45	2.93	3.25	2.65

The monthly time series of MBE and RMSE values for GEOS-4 2007 temperatures relative to NCEI ground site values provide a summary for the un-scaled and downscaled temperatures in the US Pacific Northwest region. The 2007 downscaled GEOS-4 temperatures are based upon the monthly averaged λ and β values developed from 1983 – 2006 GEOS-4 and NCEI data in this region. The MBE and RMSE monthly time series values are plotted for the uncorrected GEOS-4 and GEOS-4 downscaled using (1) yearly and global mean lapse rate and offset values, (2) monthly mean global lapse rate and offset values, (3) yearly mean regional lapse rate and offset values, and (4) monthly mean regional lapse rate and offset values.

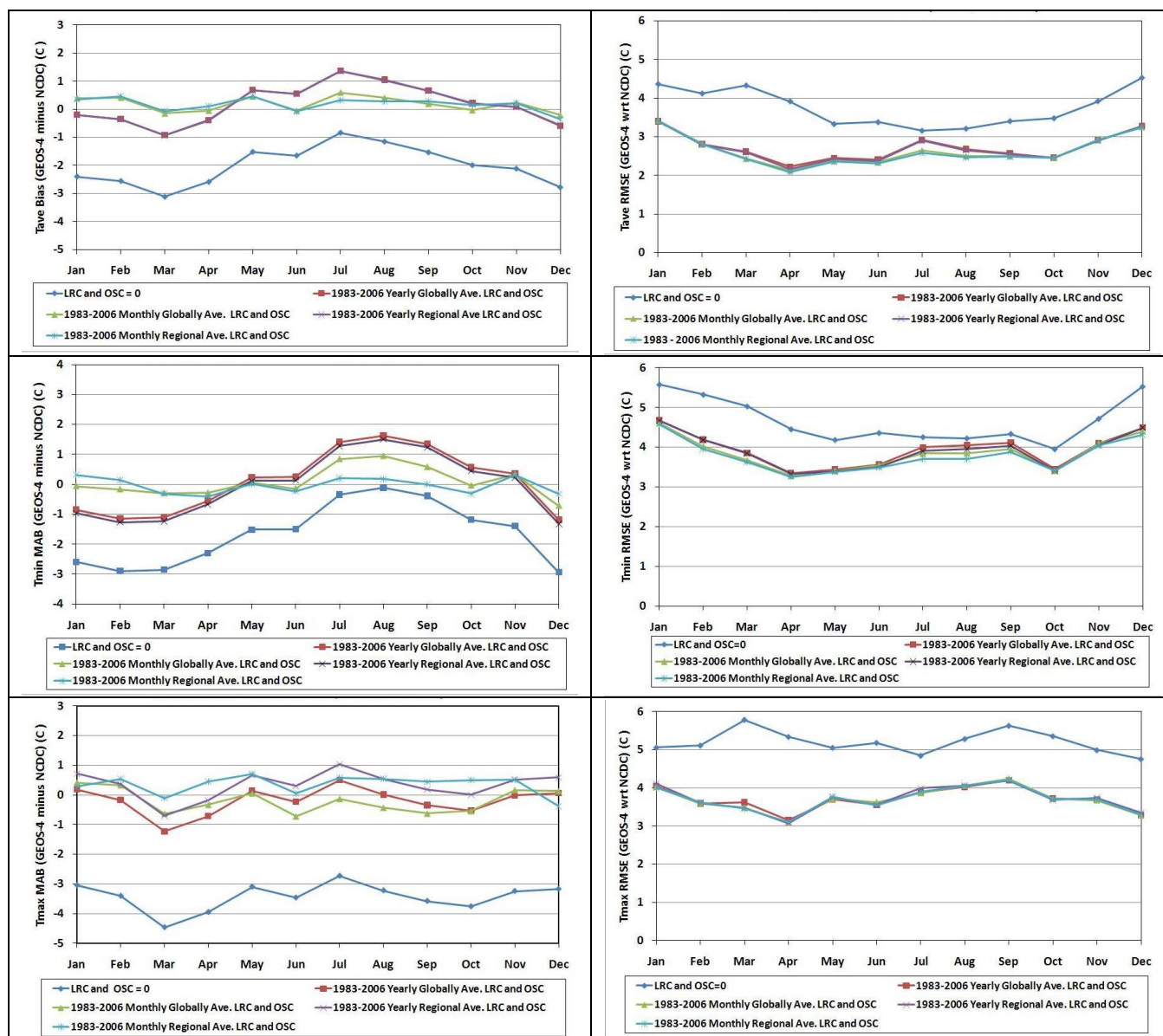


Figure A-4. Monthly time series of the MBE (left column) and RMSE (right column) between 2007 un-scaled and downscaled GEOS-4 and NCEI ground sites observations in the Pacific Northwest region (40 - 50N, 125 - 110W). The MBE and RMSE monthly time series values are plotted for the (1) uncorrected GEOS-4 (i.e. LRC and OSC = 0) and GEOS-4 corrected using (2) yearly and global mean lapse rate and offset values, (3) monthly mean global lapse rate and offset values, (4) yearly mean regional lapse rate and offset values, and (5) monthly mean regional lapse rate and offset values. The downscaling parameters are based upon GEOS-4 and NCEI station temperatures over the years 1983 - 2006.

For each set of downscaling parameters (i.e. lapse rate and offset) there is a substantial reduction in the RMSE relative to the un-adjusted GEOS-4 values; however, there is little difference in the RMSE values relative to the temporal averaging period (i.e. yearly vs. monthly average) or geographical region (global vs. regional) used to generate the downscaling parameters. The MBE is, however somewhat more dependent on the set of downscaling parameters, with the monthly mean regional values yielding the lowest MBE error particularly in the MBE for T_{min}.

The downscaling discussed above is not currently available through the POWER/Building archive, and is discussed here only to give users guidance in its application.

[\(Return to Content\)](#)

Heating/Cooling Degree Days: Tables A-11 and A-12 give the year-by-year statistics associated with comparing the heating degree days (HDD) and the cooling degree days (CDD) based upon the uncorrected GEOS-4 assimilation model temperatures and the downscaled or adjusted temperatures with observational data. In each table the bottom row gives the mean over the years. The GEOS-4 values used in Table A-12 were downscaled using the globally averaged λ and β values given in Table A-3. Note that the use of the downscaled GEOS-4 temperatures result in a significant improvement in the agreements between the GEOS-4 and NCEI based HDD and CDD, particularly in the bias values.

Table A.11

Yearly Mean Heating Degree Days (HDD)															
Year	Uncorrected GEOS-4 Temperatures vs ground site observations reported in NCDC GSOD files							Corrected (i.e. downscaled) GEOS-4 Temperatures vs ground site observations reported in NCDC GSOD files							No. Stations
	Bias (HDD)	Bias (%)	RMSE (HDD)	RMSE (%)	Slope	Intercept (HDD)	Rsqr	Bias (HDD)	Bias (%)	RMSE (HDD)	RMSE (%)	Slope	Intercept (HDD)	Rsqr	
1983	16.30	6.44	68.59	27.11	1.03	9.85	0.95	0.48	0.19	57.56	22.75	1.01	-1.06	0.96	1101
1984	16.37	6.34	64.45	24.97	1.03	8.46	0.95	0.06	0.02	52.69	20.41	1.01	-1.96	0.96	1127
1985	16.13	6.01	64.31	23.97	1.03	9.19	0.96	-0.68	-0.25	54.86	20.45	1.00	-1.97	0.96	1102
1986	14.07	5.55	85.41	33.72	0.98	18.25	0.91	-2.55	-1.01	78.34	30.93	0.96	6.42	0.92	1162
1987	14.92	5.91	69.30	27.42	1.02	10.71	0.94	-0.79	-0.31	60.04	23.76	1.00	-0.16	0.95	1140
1988	15.20	6.20	65.39	26.68	1.03	6.79	0.95	-0.35	-0.14	55.38	22.59	1.01	-3.68	0.96	1155
1989	14.71	5.85	66.75	26.54	1.03	7.55	0.95	-0.58	-0.23	57.80	22.98	1.01	-3.33	0.96	1194
1990	16.84	7.09	66.45	27.97	1.04	7.67	0.95	2.04	0.86	53.42	22.49	1.02	-2.71	0.96	1258
1991	14.69	6.03	78.74	32.33	1.01	11.89	0.92	0.00	0.00	67.86	27.86	0.99	1.30	0.94	1223
1992	12.94	5.19	79.58	31.91	1.00	12.11	0.92	-2.55	-1.02	69.80	27.99	0.99	0.69	0.93	1373
1993	17.79	6.94	71.34	27.83	1.03	10.14	0.94	0.92	0.36	61.86	24.13	1.01	-1.93	0.95	1477
1994	22.88	9.24	72.22	29.17	1.05	11.59	0.95	4.72	1.91	59.03	23.84	1.03	-1.85	0.96	1508
1995	17.54	7.10	70.60	28.60	1.03	9.83	0.95	0.92	0.37	59.47	24.09	1.01	-2.25	0.96	1311
1996	10.15	4.64	99.68	45.60	0.93	25.32	0.84	-5.88	-2.69	93.53	42.78	0.91	13.74	0.85	1216
1997	19.61	8.56	62.21	27.16	1.05	7.08	0.95	2.86	1.25	47.93	20.92	1.03	-4.71	0.97	1497
1998	24.65	11.56	68.35	32.06	1.09	5.74	0.94	7.41	3.48	53.79	25.23	1.06	-5.63	0.96	1487
1999	18.58	8.53	61.38	28.18	1.06	6.22	0.95	2.32	1.06	47.22	21.68	1.03	-4.64	0.97	1832
2000	17.61	7.32	66.54	27.67	1.05	6.15	0.95	0.45	0.19	51.64	21.48	1.03	-6.58	0.96	2324
2001	24.33	9.94	64.77	26.46	1.06	8.60	0.96	6.89	2.82	49.99	20.42	1.04	-3.02	0.97	1799
2002	16.62	6.92	67.75	28.22	1.03	9.73	0.94	0.25	0.11	55.07	22.94	1.01	-2.59	0.95	2382
2003	14.75	6.24	66.15	27.96	1.04	6.33	0.94	-0.66	-0.28	53.93	22.80	1.02	-5.05	0.96	2676
2004	16.52	6.87	90.29	37.56	1.00	17.33	0.90	-0.27	-0.11	81.18	33.77	0.98	4.36	0.91	2704
2005	20.40	8.32	66.41	27.07	1.05	7.56	0.95	3.43	1.40	53.04	21.62	1.03	-4.88	0.96	3020
2006	16.56	6.76	126.66	51.69	0.91	39.49	0.81	0.25	0.10	120.46	49.15	0.89	27.04	0.82	3077
Mean of individual years	17.09	7.07	73.47	30.33	1.02	11.40	0.93	0.78	0.34	62.33	25.71	1.00	-0.19	0.94	

Table A.12

Yearly Mean Cooling Degree Days (CDD)															
Year	Uncorrected GEOS-4 Temperatures vs ground site observations reported in NCDC GSOD files							Corrected (i.e. downscaled) GEOS-4 Temperatures vs ground site observations reported in NCDC GSOD files							No. Stations
	Bias (CDD)	Bias (%)	RMSE (CDD)	RMSE (%)	Slope	Intercept (CDD)	Rsqr	Bias (CDD)	Bias (%)	RMSE (CDD)	RMSE (%)	Slope	Intercept (CDD)	Rsqr	
1983	-4.78	-8.93	28.53	53.34	0.86	2.68	0.92	2.29	4.28	28.59	53.45	0.94	5.27	0.91	1101
1984	-4.25	-8.35	27.01	53.07	0.86	2.86	0.92	2.27	4.46	27.52	54.05	0.94	5.21	0.91	1127
1985	-5.96	-11.21	27.82	52.33	0.85	1.80	0.92	0.94	1.77	26.66	50.18	0.94	4.35	0.92	1102
1986	-6.60	-12.50	27.73	52.56	0.84	1.91	0.93	0.38	0.72	25.87	49.01	0.92	4.61	0.93	1162
1987	-6.21	-12.01	27.17	52.52	0.85	1.76	0.93	0.42	0.81	25.74	49.74	0.93	4.11	0.93	1140
1988	-5.53	-10.10	27.39	50.05	0.86	2.22	0.93	1.14	2.08	26.62	48.64	0.94	4.62	0.93	1155
1989	-6.29	-11.91	29.02	54.96	0.84	2.35	0.91	0.37	0.70	27.79	52.63	0.91	4.93	0.91	1194
1990	-6.63	-11.92	28.70	51.60	0.83	2.66	0.93	0.16	0.29	26.45	47.55	0.91	5.09	0.93	1258
1991	-6.93	-11.60	30.28	50.71	0.84	2.59	0.92	0.74	1.24	28.36	47.49	0.93	4.84	0.92	1223
1992	-4.94	-10.62	25.52	54.79	0.86	1.80	0.92	1.83	3.93	23.87	51.24	0.95	4.13	0.93	1373
1993	-5.32	-9.97	26.29	49.30	0.88	1.10	0.93	1.84	3.46	25.96	48.68	0.96	4.07	0.93	1477
1994	-6.12	-10.75	27.96	49.09	0.87	1.36	0.93	1.97	3.46	28.10	49.32	0.96	4.41	0.92	1508
1995	-5.38	-9.13	28.04	47.55	0.87	2.28	0.93	2.27	3.85	27.28	46.27	0.95	5.31	0.93	1311
1996	-6.66	-10.70	30.31	48.68	0.86	2.09	0.92	2.73	4.38	30.52	49.01	0.95	6.07	0.91	1216
1997	-6.39	-11.33	28.24	50.06	0.85	2.02	0.92	1.97	3.48	26.52	47.00	0.94	5.17	0.92	1497
1998	-5.19	-8.91	27.48	47.17	0.87	2.30	0.93	3.34	5.74	27.21	46.70	0.96	5.56	0.93	1487
1999	-3.92	-6.53	28.87	48.11	0.88	3.01	0.92	4.49	7.48	29.46	49.07	0.97	6.49	0.92	1832
2000	-3.23	-6.06	27.74	52.00	0.88	3.06	0.92	4.51	8.45	28.40	53.22	0.97	6.33	0.92	2324
2001	-7.08	-12.74	30.00	53.97	0.84	1.75	0.92	0.51	0.91	29.40	52.89	0.92	4.70	0.91	1799
2002	-7.95	-13.80	29.96	52.00	0.83	1.58	0.92	-0.24	-0.42	28.45	49.35	0.92	4.65	0.92	2382
2003	-5.84	-9.97	30.91	52.77	0.85	3.23	0.91	2.55	4.35	29.83	50.90	0.94	6.34	0.91	2676
2004	-6.14	-11.66	27.97	53.10	0.84	2.19	0.92	1.82	3.45	26.77	50.80	0.93	5.33	0.92	2704
2005	-5.80	-9.96	29.13	49.99	0.86	2.39	0.93	1.85	3.17	28.47	48.84	0.94	5.40	0.92	3020
2006	-4.88	-8.89	29.25	53.28	0.87	2.44	0.92	2.63	4.79	28.94	52.70	0.95	5.37	0.91	3077
Mean of individual years	-5.75	-10.40	28.39	51.37	0.86	2.23	0.92	1.78	3.20	27.61	49.95	0.94	5.10	0.92	

[\(Return to Content\)](#)